

**Determination of Selected Hydrocarbon Concentrations
in Reformate Using Near Infrared Spectroscopy**

A Thesis Presented to the Department of Chemistry
at Marshall University in Partial Fulfillment of the Requirements for the
Degree of Master of Science

By

Roy Roger Bledsoe, Jr.

Marshall University

August, 1997

© 1997 Ashland Petroleum Company

MARSHALL UNIVERSITY
DEPARTMENT OF CHEMISTRY

THIS THESIS WAS ACCEPTED ON August 8, 1997
AS MEETING THE RESEARCH REQUIREMENT FOR THE DEGREE
OF MASTER OF SCIENCE

J. Graham Rankin

Dr. J. Graham Rankin

Advisor, Department of Chemistry

Lawrence R. Schmitz

Dr. Lawrence R. Schmitz

Member, Department of Chemistry

Michael L. Norton

Dr. Michael L. Norton

Member, Department of Chemistry

Leonard J. Deutsch

Dr. Leonard J. Deutsch

Dean, Graduate School

To My Wife and Children

Acknowledgments

I would like to thank Dr. J. Graham Rankin, my research advisor, for his guidance and extreme patience through the course of writing my thesis, and for permitting me to do this research as my thesis. I would also like to thank Bill Welch, the Patent Law department, and the rest of Ashland Petroleum for permitting me to do this research as my thesis, and supporting my pursuit of higher education. I thank my parents for always encouraging me to do well in school. Also, very special thanks goes out to my wife, who has put up with the many days I have been away from home in pursuit of my Master of Science Degree.

TABLE OF CONTENTS

Abstract	ii
Chapter 1. Introduction	1
Background	2
I. Theory of Near Infrared Absorbance	3
II. Sample and Process	8
III. Regression Techniques	10
Chapter 2. Experimental	16
I. Sampling	17
II. Near Infrared Instrumentation	18
III. Near Infrared Instrument Setup	22
IV. Data Collection and Treatment	24
Chapter 3. Results and Discussion	28
I. PIANO Results	29
II. Instrument Test Results	29
III. Band Assignments	29
IV. Areas of Variance	32
V. Regression Analyses	37
VI. Application for On-line Analysis	79
VII. Conclusion	81
REFERENCES	82
APPENDIX I	89
APPENDIX II	91
APPENDIX III	100
APPENDIX IV	102
APPENDIX V	103

ABSTRACT

Near infrared spectroscopy was used as a quantitative technique employing multiple linear regression and partial least squares regression for determining the concentration of hydrocarbon groups and individual hydrocarbons present in reformat, a refinery process stream. Models were generated for total aromatics, benzene, toluene, total xylenes and individual xylene isomers, ethylbenzene, total paraffins, *n*-hexane, *n*-heptane, total isoparaffins, isopentane, 2-methylhexane, total naphthenes, methylcyclopentane, and total olefins. Some models are being used with an on-line instrument to constantly monitor a reformat stream as it leaves the reforming unit, with a standard error of performance of 0.118 volume percent for the prediction of the benzene concentration for a six month period. This technique serves as a faster method which takes less than a minute to perform the operation, whereas the primary methods of gas chromatography can take in excess of three hours to perform. By providing reliable data, this faster analysis can lead to enhanced economics concerning analysis time and can be used on-line for better control of a refinery process.

CHAPTER 1
INTRODUCTION

I. BACKGROUND

Near infrared spectroscopy (near-IR) has gained popularity as a technique for quantitative and qualitative analysis. The samples may be of various compositions, ranging from pure compounds to very complex mixtures of compounds that may give rise to difficulties with other methods of analysis. Near-IR has been used as a qualitative and/or quantitative tool in many different fields of chemistry,¹⁻⁴ including the agricultural and food industries,⁵⁻⁹ the pharmaceutical industry,^{10,11} the cosmetics industry, the chemical industry,¹²⁻¹⁵ the petroleum and fuels industries,¹⁶⁻⁴⁴ environmental studies,⁴⁵ biological studies,^{46,47} research in astronomy and diverse areas of academic research.⁴⁸⁻⁵¹

Although earlier industrial applications of near-IR pertained primarily to the agriculture and pharmaceutical industries, near-IR is finding a definite foothold in the analysis of hydrocarbons. It is of great interest, industrially and economically, to be able to determine parameters of hydrocarbons, with only a small amount of time elapsing. This could prevent damage to part of a processing unit and/or ensure that the quality of the product meets a desired specification. In the petroleum industry, near-IR has been used to control finished gasoline blending.^{34,35,40} In many of these latter applications, near-IR is generally used to determine octane numbers (research :r, motor :m, $(r+m)/2$). Others have utilized more of the spectral information in determining the concentration of certain chemical groups present in gasoline (e.g. paraffins, isoparaffins, aromatics, naphthenes, olefins, weight percent oxygen).^{37,44}

As computers became more readily accessible and faster, near-IR saw a resurgence. A combination of instruments with detectors which are very sensitive and improved data reduction algorithms can be used for qualitative and quantitative applications. The use of algorithms in conjunction with spectroscopic data to determine physical or compositional characteristics is referred to as multivariate analysis. With near-IR, the overlapping bands in the spectrum create limitations on quantification on the order of parts per million, but, as shown in this paper, these can be overcome when the

concentration is on the order of hundredths of a percent and greater.

This research involved using near-IR spectroscopy to determine the concentration of chemical groups and individual hydrocarbon compounds present in a product (reformat) from an oil refinery process unit. This method of analysis can then be utilized for feedback control of the unit itself. The analysis time is greater than two hundred times faster than traditional gas chromatography methods (including the processing of the chromatogram). The utilization of this technique for advanced control allows for the optimization of the economics surrounding the operation of the unit.

I. THEORY OF NEAR INFRARED ABSORBANCE

The electromagnetic spectrum is divided into several spectral regions. At wavelengths just beyond the visible region (700 nm), is the infrared (IR) region, subdivided into three regions. These regions are the near infrared (near-IR) region which encompasses radiation having wavelengths from 780 nm to 2500 nm (wavenumbers from $12,800\text{ cm}^{-1}$ to 4000 cm^{-1}), the middle infrared (mid-IR) region which encompasses radiation having wavelengths from $2.5\text{ }\mu\text{m}$ to $50\text{ }\mu\text{m}$ (wavenumbers from 4000 cm^{-1} to 200 cm^{-1}), and the far infrared (far-IR) region which encompasses radiation having wavelengths from $50\text{ }\mu\text{m}$ to $1000\text{ }\mu\text{m}$ (wavenumbers from 200 cm^{-1} to 10 cm^{-1}).⁵² Mid-IR has received the most attention, since most organic compounds have unique spectra in this region. The near-IR region, until recently, has received less attention because it was thought less suitable for identification and lacked the ease of interpretation.^{1,4,53} In the past several years, there has been a steady growth in the area of near-IR spectroscopy and it is quickly accumulating a patronage. An advantage that near-IR has over mid-IR is that the signal to noise ratio is much greater in the near-IR region. This is because a higher energy radiation is being utilized which contributes to minimizing the noise and leads to maximizing the signal.⁵⁴ The lower noise in near-IR allows for the use of less sensitive detectors, meaning less sensitive to thermal noise. For detectors that are comprised of a

semiconductor, such as lead sulfide, there exists a band gap that a valence electron must be excited beyond in order for the detector to conduct electricity. This gap is wider for some detectors, whereas it is small for others. Thus, a wider gap results in the detector being less sensitive to thermal noise.⁵²

Infrared radiation of specific wavelengths can interact with a molecule and induce rotational and vibrational energy level transitions within the molecule. An absorption of energy (photon) results in this shifting of energy levels, meaning a mode of vibration undergoes a transition from the ground state of $v=0$ to the excited state of $v=1$.⁵⁵ The absorption of infrared radiation can only occur if there is a change in the dipole moment of the molecule during the vibration.⁵² The strength of the dipole moment is proportional to the strength of the absorbance.⁵⁶ This selection rule for infrared spectroscopy refers to one end of a bond being slightly positive, and one end being slightly negative. When the distance (bond length) between the two atoms involved in the bond increases, a larger dipole is created. The wavelength of absorbance is dependent on the reduced mass of the atoms and the strength of the bond.⁵⁶

The well-defined bands in the mid-IR region arise from characteristic absorptions of infrared wavelengths of radiation by vibrations of specific chemical bonds and bond groups. The bands between 2700 cm^{-1} to 3300 cm^{-1} make up the fundamental C-H stretching vibrational frequency bands.^{52,57} As seen in the mid-IR spectrum of toluene (Figure 1, top), individual bands have been assigned to characteristic vibrations of parts of the molecule.

However, the near-IR region of the spectrum does not look as interesting upon first glance (Figure 1, bottom). The bands are not as well defined, and fewer bands appear to be present. This is because we are no longer looking at fundamental frequency bands, but rather overtones and combinations that arise from the fundamental frequency bands. An overtone is a result of molecular vibrations that occur when a mode of vibration is excited from the ground state of $v=0$ to excited states greater than $v=1$. The mode

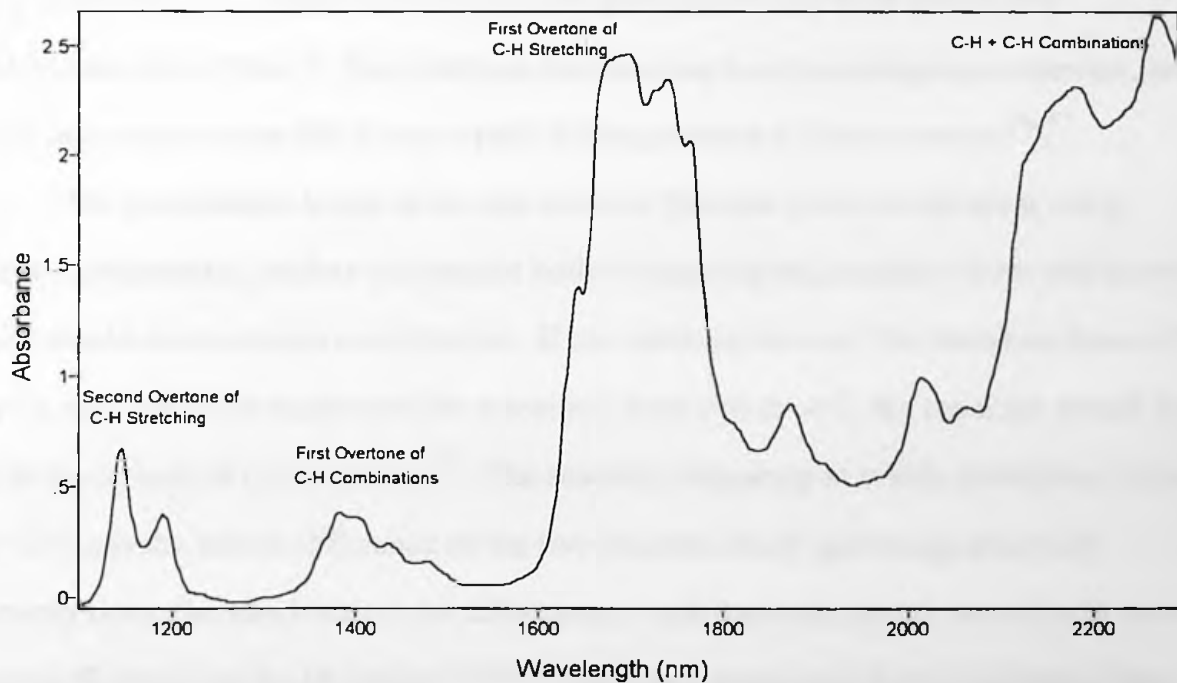
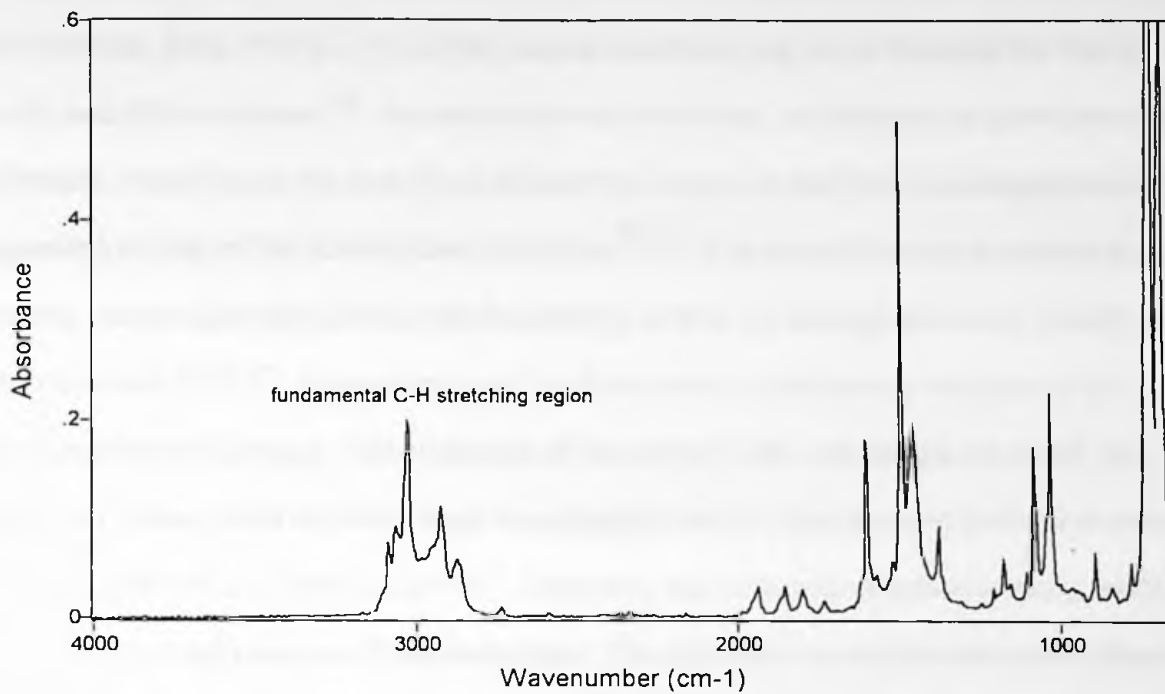


Figure 1. (Top) Middle infrared spectrum of toluene. The fundamental C-H stretching region is indicated. (Bottom) Near infrared spectrum of toluene. The C-H stretching combination and overtone regions are indicated.

undergoes the transition from the ground state of $v=0$ to the excited state of $v=2$ for the first overtone, from $v=0$ to $v=3$ for the second overtone, and so on through the third, fourth, and fifth overtones.⁵⁵ An assessment of overtones, in reference to pure harmonic oscillation, would be to say that the first overtone occurs at half the wavelength (twice the frequency) of that of the fundamental vibration.^{56,57} The second overtone occurs at one-third the wavelength (three times the frequency), and so on through the third, fourth, and fifth overtones.^{55,56,57} An analogy used to allow one to visualize an overtone is the vibration of a violin string. The vibration of the string is not one distinctive wave, but rather two waves, both of which have wavelengths half of what the one distinctive wave would be, and twice its frequency.^{56,57} However, the presence of anharmonicity tends to create a shift in the position of the overtones. The anharmonic oscillations create these deviations from the normal harmonic functions because the energy levels are not evenly spaced due to the types of atoms and bonds present.^{52,58} Bands do not appear to be as sharp in the near-IR because several overtone absorptions may arise from a few fundamental absorptions.¹ This results in the overtone bands overlapping somewhat, and hence these absorptions fail to retain their individualism and distinctiveness.^{56,57}

The combination bands occur due to more than one mode of vibration being excited concurrently, such as two modes both undergoing the transition from $v=0$ to $v=1$, which results in an original combination. If one mode underwent the transition from $v=0$ to $v=1$, and one mode underwent the transition from $v=0$ to $v=2$, the resultant would be the first overtone of combinations.⁵⁵ The resultant frequency at which absorption occurs due to this is the sum or difference of the two frequencies of light being absorbed, primarily being the sum because the differences would be in the longer wavelength area of the mid-IR region or far-IR region.^{52,55,56} The two frequencies that are involved here need not be both fundamentals, because combinations from fundamentals and overtones have also been observed.⁵⁶

The near-IR region is dominated by overtones and combinations of C-H, O-H, and

N-H stretching vibrations.^{1,56} The fundamentals of these vibrations lie in the mid-IR at $\sim 2700 - 3500 \text{ cm}^{-1}$. The first, second, and third overtones of these vibrations occur in the near-IR region at $\sim 1560 - 1800 \text{ nm}$, $\sim 1120 - 1260 \text{ nm}$, and $\sim 850 - 965 \text{ nm}$, respectively. In contrast, stretching and bending vibrations of C-C, C=C, C=O, etc. that may be expected in organic compounds occur at substantially lower wavenumbers ($< 1800 \text{ cm}^{-1}$). Only the second or higher overtones would fall into the near-IR region. Due to the much higher probability of these modes of vibration going from $v=0$ to $v=1$ than from $v=0$ to $v=2$, these higher overtones are substantially weaker than the first overtones of C-H stretching bands, they may be omitted from consideration. There is very little overlap among symmetrical and asymmetrical stretches between the hydrogen atom and the principal atom to which it is bonded. However, only anharmonic oscillation of molecules is observed in reality as revealed by the Morse potential, and only asymmetric vibrations are observed in the different C-H stretches because the anharmonicity constant for asymmetric stretching is substantially larger than the constant for symmetric stretching.⁵⁹

The purpose of the research presented here was to utilize near-IR to determine chemical properties of reformat, a refinery process stream. This involved examining near-IR spectra over the range of 1100 nm to 2300 nm for a closer look at the composition of a sample, and not only to determine the concentration of the chemical groups, but take it a step further and determine the concentration of individual compounds present (e.g. benzene, toluene). These concentrations could then be utilized to control the operating parameters of a catalytic reformer.

Due to the largely overlapping bands, it has been suggested that the use of near-IR for the determination of individual compounds would be difficult.⁶⁰ Swarin and Drumm attempted the prediction of the benzene concentration in gasoline using near-IR.²⁹ They reported being able to do so if they used a partial least squares calibration of the spectrum, but were unsuccessful with multiple linear regression. No mention is made of specific ranges of the spectrum that could be utilized for the prediction of benzene concentration.

Likewise, in a United States patent, Hieftje et al. claims determination of benzene in a mixture of hydrocarbons, but indicates that the sample and prediction sets were comprised of only four known hydrocarbons.²¹ Heiftje revealed the wavelengths used in making the calibration, but those wavelengths differ from the wavelengths shown in this work.

This research reveals the specific spectral regions for the quantification of selected hydrocarbons. The data clearly reflects the novelty of the research and the usefulness of such a method in industries involving petroleum and petrochemicals. The results of an on-line study for the quantification of benzene in a petroleum refining stream are also presented.

II. SAMPLE AND PROCESS

The sample used in this research is referred to as reformat (sometimes whole reformat) or platformate. It is the product of a catalytic reformer process unit. In this research, the particular unit is a low pressure continuous catalyst regenerating reformer (LPCCR). Reformat is a complex mixture of hydrocarbons (often greater than 250 compounds), predominately aromatics. The stream is typically of high octane, and the composition is important to petrochemical operations as well as to gasoline blending operations.

Petrochemical operations (the section of a refinery involved in the production of petrochemicals) views this product as many valuable commodities mixed together, out of which numerous petrochemicals can be isolated. These include, but are not limited to, benzene, toluene, ethylbenzene, and xylenes (as a mixture and as individual isomers). These isolated chemicals can then be sold on the chemical market or can serve as the feed for another process (e.g. benzene serves as the feed for the production of cumene).

Gasoline blending operations (the section of a refinery involved in the production of gasoline) is also very interested in reformat, because reformat is a high octane component for gasoline blending, and comprises approximately 40 percent of the United

States' finished gasoline product.⁶¹ There is a greater interest in the unit's operation if a refinery's octane pool is based on reformer severity (changing the operating conditions of the unit to provide a product possessing the desired properties) rather than the operation severity for other units in the refinery. On the other hand, reformate is also the primary source of aromatics and benzene present in gasoline. Due to new regulations that are currently being implemented (e.g. reformulated fuels), finished gasolines will be required to meet new requirements.⁶² The reformulated fuels gasoline (RFG) requirements include a maximum volume concentration of total aromatics, total olefins, and benzene. The best way to assure that the gasoline will meet the requirements is to have the blending components at the desired property values. The utilization of near-IR for feedback control of a unit to yield a product with a targeted lower benzene concentration of 2.5 percent by volume, rather than the 5.0 percent typical of reformate, would greatly benefit a refinery. Welch et al. and Zilberman et al. explain advantages of using near-IR to determine properties of blending components and process streams.^{35,63}

The feed for a catalytic reformer is ordinarily, but not limited to, naphtha. Naphtha characteristically has a paraffin and isoparaffin composition of 45-55 percent, olefins 0-2 percent, naphthenes 30-40 percent, and aromatics 5-10 percent.⁶¹ The octane number of the feed varies, but typically lies in the range of 30-60. This octane number is greatly increased in the product from the reformer process, which increases its value to gasoline blending. The feed passes through a heater, where some of the lighter compounds are removed by distillation. The feed, along with a hydrogen supply, is then directed into a reactor. In the reactor, the feed passes through a bed of catalyst. The primary reaction occurring in the reactor is the formation of aromatics. Several types of catalytic reactions occur during the reforming process, including: (1) dehydrogenation and cyclization of paraffins and isoparaffins to naphthenes (cycloparaffins), with further dehydrogenation of the naphthenes to aromatic compounds; (2) isomerization of paraffins; (3) hydrocracking of paraffins and olefins; (4) hydrogenation of olefins to form paraffins; and (5) dealkylation

of naphthenes and aromatics.^{61,64} The principal, and desired, process that occurs is dehydrogenation of naphthenes.

During the reforming process, some coke will collect on the catalyst causing the catalyst to lose activity. The hydrogen produced in reforming is split into two streams. One stream is recycled through the unit to help keep coke accumulation on the catalyst at a minimum, and for the hydrogenation of olefins to form paraffins.⁶⁵ If enough coke builds up on the catalyst to allow the performance of the catalyst to degrade below the desired level, the catalyst can be put through a regeneration process in which the coke is removed by oxidation and the activity of the catalyst increased to an optimum level.

The product from the unit then passes through a debutanizer heater where much of the butane and lighter compounds which formed during reforming are removed. The heavier stream, also referred to as debutanized bottoms because of its sample site, is given the name whole reformat. Whole reformat is then used by petrochemical operations and gasoline blending operations as mentioned above. The analyzer probe is located in a fast loop, which is a sample line that provides a route for a representative portion of the stream to the analyzer and then back to the stream line.

III. REGRESSION TECHNIQUES

The application of statistical techniques such as regression analysis to chemical or spectroscopic analysis is often referred to as chemometrics, but this term is too broad.⁶⁶ When more than one wavelength is involved, a better label for the regression of spectroscopic data is multivariate analysis. Because near-IR spectra are comprised of overlapping bands, there may be only subtle differences between spectra. However, these subtleties can be exploited through multivariate analysis. The use of an algorithm (equation, model) in conjunction with spectroscopic data for the purpose of doing quantification is not new. Beer's law states the absorbance is equal to the product of the molar extinction coefficient, the pathlength, and the concentration.⁵²

$$A = \epsilon b c \quad (1)$$

The molar extinction coefficient is specifically dependent upon the individual wavelengths of light and the temperature of the sample. Theoretically, the curve generated by Beer's law goes through the origin, but in practice it rarely does.⁵⁴ Because the reformat is a complex mixture of compounds, a multicomponent system, Beer's law must be expanded for each individual compound present, as is shown below where ϵ_1 , ϵ_2 , and ϵ_3 are the molar extinction coefficients at a given wavelength and c_1 , c_2 , and c_3 are the concentrations of each respective compound present.⁶⁷

$$A = (\epsilon_1 c_1 + \epsilon_2 c_2 + \epsilon_3 c_3 + \dots)b \quad (2)$$

However, the disadvantage is that the concentration of every component present in the sample must be used in the calibration. Inverse Beer's law is better suited because only the concentration of the component of interest is all that need be known.^{68,69} One type of regression analysis, used with inverse Beer's law, is multiple linear regression (MLR).

MLR is an expanded form of inverse Beer's law that is suitable for use with multicomponent systems, and has been used in earlier studies involving chromatography and spectroscopies.^{17,23,50,69,70} This involves using a combination of two or more wavelengths to generate a least squares equation. At each wavelength, a constant (weighting factor) is assigned for each wavelength based upon all of the correlating variables involved in the equation. These serve as multiplication factors for the absorbance values at specified wavelengths. An additional constant is added to correct for the intercept of the line being created. This type of equation corresponds to the form shown in Equation 3.⁵⁸

$$[X] = k(0) + k(1)A_1 + k(2)A_2 + k(3)A_3 + e \quad (3)$$

In this operation, $k(0)$ is the correction for the intercept which is referred to as the bias coefficient, and $k(n)$ represents the coefficient for wavelength, λ_n . The values for the constants should not be extremely large, otherwise noise could give rise to bad predictions. For example, one milliabsorbance unit being multiplied by a constant value of

10,000 in an equation will yield a percentage change of 10. The object of this operation is to determine the optimum wavelengths (bands) which correspond to the minimization of the sum of squares of the residuals for the property of interest. However, the data to be used will be in the second derivative form, so the equations created will take on the form shown in Equation 4.⁷¹

$$[X] = k(0) + k(1)(d^2A/d\lambda^2)_{\lambda_1} + k(2)(d^2A/d\lambda^2)_{\lambda_2} + k(3)(d^2A/d\lambda^2)_{\lambda_3} + e \quad (4)$$

In this form, the term $(d^2A/d\lambda^2)_{\lambda_n}$ represents the second derivative of absorbance at wavelength n.

A second type of regression analysis is partial least squares regression (PLSR, sometimes referred to as just PLS). PLS is a type of the iteration estimation techniques that were first introduced by Wold in 1966.⁷²⁻⁷⁴ At that time, he had revealed his design for "Nonlinear Iterative LEast Square procedures" (NILES), and gave an example of the procedures using horse races.⁷² In 1973, he announced new developments with the iterative estimation techniques, referring specifically to "Nonlinear Iterative Partial Least Squares" (NIPALS).⁷³ The new developments involved a description of how models are built.⁷³ Since that time, PLS has been used with a variety of applications, including psychological testing, chromatography, and spectroscopy.^{9,22,32,37,75-89} The theory of the PLS algorithm has been described in literature and papers presented at conferences.^{68,90,91} In PLS, the concentrations of interest are regressed against the spectra during the decomposition of the spectra. This generates factors which serve as a matrix that corresponds to variables in the spectra and the constituents. The PLS algorithm is listed below, with the symbols defined in Table I and a detailed explanation following.^{56,90}

Note: Taken from Reference 90. With permission. (See Appendix I.)

$$(1) \mathbf{u}_{start} = \mathbf{y}_j$$

$$(2) \mathbf{w}' = \mathbf{u}'\mathbf{X}/\mathbf{u}'\mathbf{u}$$

$$(3) \mathbf{w}'_{new} = \mathbf{w}'_{old} / \|\mathbf{w}'_{old}\|$$

$$(4) \mathbf{t} = \mathbf{X}\mathbf{w}'_{new}$$

$$(5) \mathbf{q} = \mathbf{t}'\mathbf{Y}/\mathbf{t}'\mathbf{t}$$

$$(6) \mathbf{q}'_{new} = \mathbf{q}'_{old} / \|\mathbf{q}'_{old}\|$$

$$(7) \mathbf{u} = \mathbf{Y}\mathbf{q}'_{new}$$

$$(8) \text{if } \|\mathbf{t} - \mathbf{t}_{old}\| > 10^{-6} \text{ go to step (2)}$$

$$(9) \mathbf{p}' = \mathbf{t}'\mathbf{X}/\mathbf{t}'\mathbf{t}$$

$$(10) \mathbf{p}'_{new} = \mathbf{p}'_{old} / \|\mathbf{p}'_{old}\|$$

$$(11) \mathbf{t}'_{new} = \mathbf{t}'_{old} / \|\mathbf{p}'_{old}\|$$

$$(12) \mathbf{w}'_{new} = \mathbf{w}'_{old} / \|\mathbf{p}'_{old}\|$$

$$(13) \mathbf{b} = \mathbf{u}'\mathbf{t}'_{new}$$

Calculation of Residuals: $\mathbf{E}_h = \mathbf{E}_h - 1 - \mathbf{t}_h\mathbf{p}'_h$

$$\mathbf{F}_h = \mathbf{F}_h - 1 - \mathbf{b}\mathbf{t}_h\mathbf{q}'_h$$

The PLS algorithm begins by setting the column vector of scores for the Y block equal to the column vector of scores for the X block.^{68,90} The spectra are then weighted with the concentration of the component.⁶⁸ In step 2, \mathbf{w}' represents the weighting of the spectral signal, \mathbf{u}' , with the concentration of the component, X. In step 3, a normalized weighted average spectrum is then derived from the weighting. In steps 4 and 5, the normalized weighted average spectrum is used to generate a scores matrix. In step 6, the spectra are regressed onto the scores, generating a loading vector.⁶⁸ In step 7, the scores for factor 1 are generated from the loading vectors. Step 8 relays that if the scores value in step 4 is equal to the original scores value, the scores generation process can stop.⁹⁰ If they are not equal, the process is repeated (factor 2, factor 3, etc.) using the residuals from the individual spectra being subtracted from the weighted average spectrum as the loading matrix for the X block and the residual concentrations from the factor 1 equation in place of the original concentrations, because they serve some function for the continuance of the

Table I. Explanation of symbols used in PLS algorithm.⁹⁰

$\ \ $	the Fröbenius or Euclidian norm
i	a dummy index for counting samples (objects)
j	a dummy index for counting independent (x) variables
k	a dummy index for counting dependent (y) variables
h	a dummy index for counting components or factors
n	the number of samples in the calibration (training) set
m	the number of independent (x) variables
p	the number of dependent (y) variables
a	the number of factors used ($<$ rank of X)
r	the number of samples in a prediction (test) set
x	a column vector of features for the independent variables (size $m \times 1$)
y	a column vector of features for the dependent variables (size $p \times 1$)
X	a matrix of features for the independent variables (size $n \times m$)
Y	a matrix of features for the dependent variables (size $n \times p$)
b	a column vector of sensitivities for the MLR method (size $m \times 1$)
B	a matrix of sensitivities for the MLR method (size $m \times p$)
t_h	a column vector of scores for the X block, factor h (size $n \times 1$)
p'_h	a row vector of loadings for the X block, factor h (size $1 \times m$)
w'_h	a row vector of weights for the X block, factor h (size $1 \times m$)
T	the matrix of X scores (size $n \times a$)
P'	the matrix of X loadings (size $a \times m$)
u_h	a column vector of scores for the Y block, factor h (size $n \times 1$)
q'_h	a row vector of loadings for the Y block, factor h (size $n \times 1$)
U	the matrix of Y scores (size $n \times a$)
Q'	the matrix of Y loadings (size $a \times p$)
M_h	a rank 1 matrix, outer product of t_h and p'_h (size $n \times m$)
E_h	the residual of X after subtraction of h components (size $n \times m$)
F_h	the residual of Y after subtraction of h components (size $n \times p$)
b_h	the regression coefficient for one PLS component
I_n	the identity matrix of size $n \times n$
I_m	the identity matrix of size $m \times m$

Note: Taken from Table 1 in Reference 90. With permission. (See Appendix I.)

operation.^{68,90} The scores in step 4 for the X block are not orthogonal in the algorithm.⁹⁰ Therefore, steps 9, 10, 11, and 12 replaces the loading matrix with a weighting matrix to achieve orthogonal X scores, allowing for the prediction to be made without error.⁹⁰ In step 13, the concentrations are regressed onto the scores, with the regression coefficient,

b, being generated.^{68,90} In step 14, the residual concentrations are being calculated by removing the product of the scores and the loading vector from each spectrum.^{68,90}

The object of this operation is to determine the optimum wavelengths (bands) which correspond to the minimization of the sum of squares of the residuals for the property of interest. When such a point is reached where the continuing regression of the residuals does not improve the model, due to the residual data becoming random, this juncture before iteration occurs is the point at which the regression model should be ended. If the number of factors is extended beyond the optimum number, overfitting occurs in the regression model. This results in a regression equation too specific to the calibration samples used to generate the model. The observed coefficient of correlation and standard error of cross validation usually improves as the number of factors is extended beyond the optimum number, but this makes it highly probable to have greatly increased errors in the prediction of samples not in the original set of calibration samples. This operation differs from other regression techniques because it is not focussed on the point, or points, of highest correlation, with the primary goal of achieving a coefficient of correlation of 1.00.⁵⁸ In the NSAS software, this correct number of factors to use is determined at the point where the ratio of the current mean standard error of cross validation to the minimum standard error of validation becomes less than 1.25.⁵⁸

CHAPTER 2

EXPERIMENTAL

I. SAMPLING

In October of 1993, the low pressure continuous catalyst regeneration reformer (LPCCR) at Ashland Petroleum's Catlettsburg, Kentucky #1 refinery was commissioned. The desired temperature of the unit's reactors was 980°F (~527°C). According to refinery operations personnel, this was believed to be the temperature at which the product from the unit would have a desired research octane number of approximately 98. Until recently, a reformer at the Catlettsburg refinery was controlled by sampling from the process stream for a research octane determination once or twice per day and making adjustments to the operation of the unit based upon the results, or using combustion measurement devices on-line. In the published literature, others have determined properties of reformate using gas chromatography, mid-IR, density correlation, or as in conjunction with the work presented here, using an on-line NIR to predict the octane numbers of the reformate sample.^{20,26,37,92-94} Much of the literature available relates primarily to work done in the laboratory or pilot plant.

After the unit's reactors reached a temperature of 700°F (~371°C), 5-gallon (~19 liters) samples were collected every fifteen minutes for a period of three hours. At this time, the period of time between sampling increased as the unit was being brought up to its desired level. After the first night, the samples were collected by the operators every morning, Monday through Friday, until the first week of February 1994. The sample set was selected primarily on octane number. One gallon (~3.8L) of randomly selected samples was submitted to Ashland Petroleum's Catlettsburg, Ky refinery control lab for research and motor octane analysis by knock engine (ASTM D 2699 and D 2700). A total of fifty-two samples were collected in the desired research octane number range for product from the unit. This set of fifty-two samples served as the calibration set for the original research project. The research was then repeated after eighteen additional samples were collected in April and May of 1994. Ten of these additional samples were combined with the original set of fifty-two samples and served as the second calibration

set. Most of these samples were collected at such a time when the unit was at, or near, full scale operation producing product at, or near, the desired research octane number. The remaining eight samples served as the prediction set. Four ounces (~118 ml) of every sample in the calibration and prediction sets were transferred to four ounce amber wide-mouth bottles with polyseal caps, which were placed in a freezer at a temperature of $< -25^{\circ}\text{F}$ ($\sim < -32^{\circ}\text{C}$). The amber bottles help prevent ultraviolet light from interacting with the sample. The polyseal caps prevent light ends from escaping. Both the polyseal caps and two PTFE type caps were pre-tested using a hot water bath, and only the polyseal cap did not leak.

The calibration and prediction sets were submitted to Ashland Petroleum's Research and Development gas chromatography laboratory for P.I.A.N.O. analysis. A P.I.A.N.O. analysis involves gas chromatography separation of the sample into the individual compounds present. The concentrations of the individual components (sometimes >250) are then summed into the corresponding hydrocarbon type group, paraffins, isoparaffins, aromatics, naphthenes, and olefins (hence P.I.A.N.O.). Although the method achieves reliable results, the method ordinarily takes over two hours of analysis time in the chromatograph and approximately one hour of processing time by a skilled technician using a computer program. Thus, a faster and more efficient method of analysis would be desirable for on-line and laboratory analysis. A Hewlett-Packard 5890 gas chromatograph with a 100 meter Supelco Petrocol DH fused silica column with an inside diameter of 0.25 mm and a wall coating phase of bonded poly(dimethylsiloxane), a flame ionization detector (FID), and P.I.A.N.O. Software by Analytical Automation Specialists, Inc. was used to perform the analysis. Helium was used as the carrier gas. A complete P.I.A.N.O. report is attached as Appendix II.

II. NEAR INFRARED INSTRUMENTATION

The instrument utilized for this research was a NIRSystems on-line 5000. A

schematic diagram of the instrument is shown in Figure 2. The radiation source was a General Electric tungsten halogen lamp, ANSI code EPT, 42 watts, 10.8 volts, with an operating temperature of 2900°K, of which the intensity is controlled. The wavelength range of the source is 350 nm to 2500 nm.⁵² There is a noticeable drop off in intensity at the longer wavelengths in the range. The scanning range of the instrument is 1100 nm to 2500 nm, but there is a considerable decrease in signal/noise observed in the range of 2300 nm to 2500 nm due to lower source intensity and high sample absorbance.

The instrument is equipped with two sets of fiber optic bundles, an internal reference fiber bundle and a sample fiber bundle. A solenoid and shutter are used to switch the path of the light between sample and reference. The fibers are silica fibers with a characteristic low hydroxyl concentration to reduce interference in the spectra due to -OH stretching in the fibers. The reference fiber is eighteen inches (~46 cm) in length, comprised of 420 fibers, and runs a path directly from the source to where it is radiated onto an

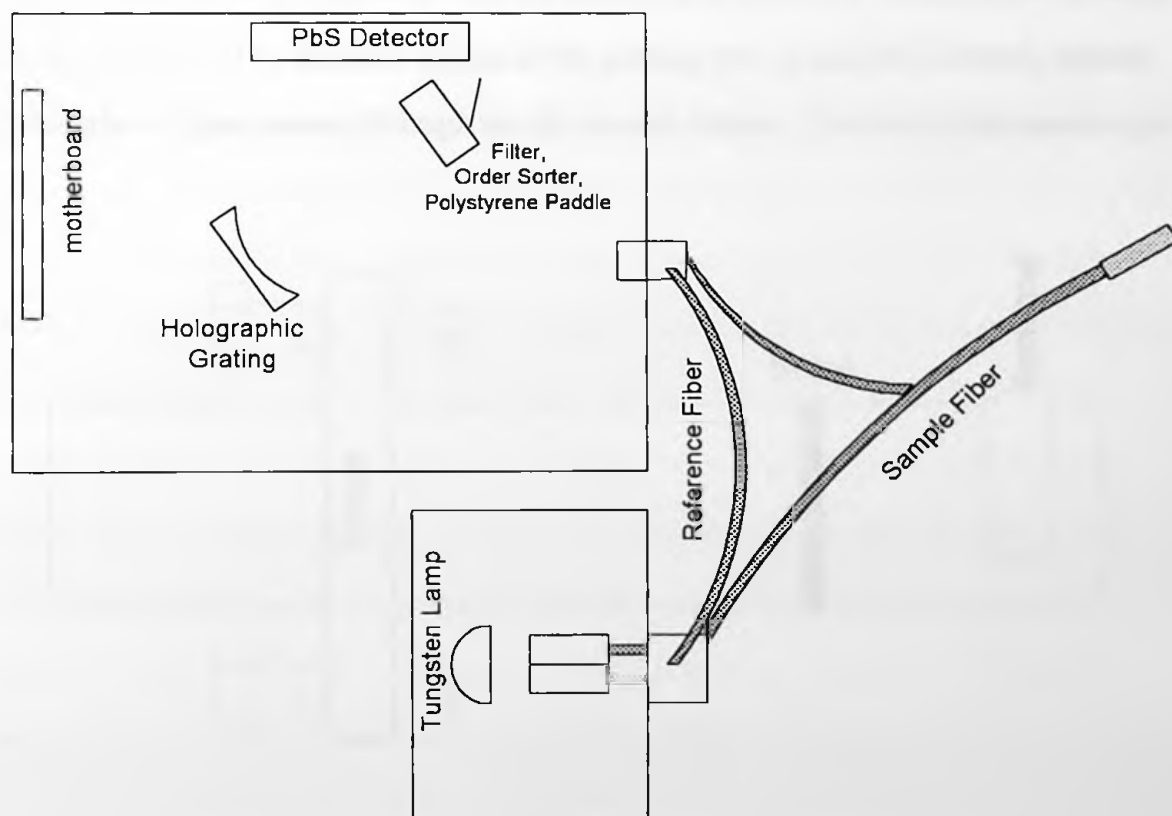


Figure 2. Schematic diagram of the near infrared instrument.

oscillating holographic grating.⁹⁵ The sample fiber is three feet (~90 cm) in length and is divided into two sections within, an outer bundle of 840 fibers and an inner bundle of 420 fibers.⁹⁶ The outer bundle conducts light from the source to the sample. The inner bundle conducts light from the sample to the point where it is radiated onto a grating. Attached to the sample fiber is a custom designed stainless steel immersion probe with a reflector tip (Figure 3). The probe is affixed over the fibers at the point where the fibers become flush against a sapphire window, on which a drop of immersion oil is placed for refractive index matching. The reflector tip consists of a sapphire window with mirrored backing embedded into stainless steel. The path length between sapphire windows is 8 mm, resulting in an overall path length of 16 mm after the light has passed through the sample once to the reflector tip and back through the sample again to the internal bundle. The light then travels through the fiber and is radiated onto the grating. The scan rate is 1.8 scans/second.⁹⁷

The light is then dispersed from the grating as a spectrum, which passes through an order/sorter filter. The different angles of the grating (via an encoder) identify specific wavelengths of light passing through the slit at each instant. The individual wavelengths

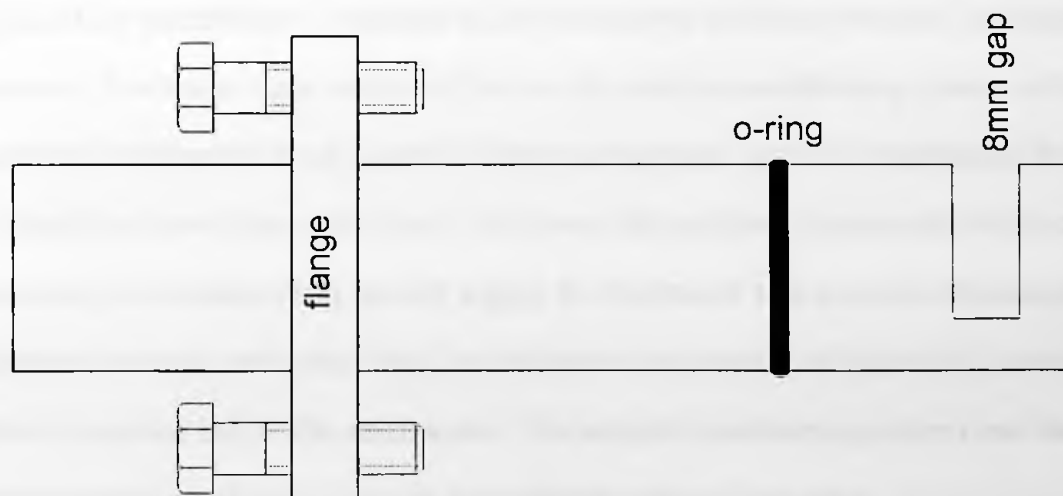


Figure 3. Custom designed stainless steel immersion probe.

of light are then reflected off a mirror and to the detector. The order/sorter filter moves synchronously with the grating to ensure that the wavelengths used in generating the spectrum come from a specific order and not a higher order. The filter is comprised of a series of bandpass filters which are used to allow only the specific order of light to pass and absorbs all higher orders.⁵⁸

The instrument possesses a lead sulfide (PbS) detector and a transmittance amplifier.⁵⁸ This detector, which is very sensitive in the near-IR, is a crystalline semiconductor which serves as a photoconductor. A regulated current is passed through the crystal. When radiation is absorbed by the sample, there is a measured change in the resistance, or conductivity, of the circuit.⁵⁸ These changes are then amplified and converted to percent transmittance, which is then converted to absorbance. The results are then arranged and saved as a spectrum over the range of 1100 nm to 2500 nm at 2.0 nm data intervals. The monochromator wavelength accuracy, based upon instrument to instrument repeatability, is 0.15 nm, with a wavelength repeatability of better than 0.02 nm.⁹⁷

For the industrial environment involved, the instrument is mounted inside a stainless steel enclosure that is purged and temperature controlled to 70°F (~21°C) with an attached air conditioner. Adjacent to the instrument enclosure are two additional enclosures. The lower right enclosure houses the sample conditioning system, of which the primary components are a heater, a cooler, a degasser, and two rotometers for controlling the flow of the reformat. The lower left enclosure houses the electrical connections, termination strip, power supply for the heater and cooler in the sample conditioning system, and controllers for the heater and cooler. A protofuel system manifold is located below the enclosures. The sample conditioning system and the protofuel system are discussed more thoroughly in the next chapter.

III. NEAR INFRARED INSTRUMENT SETUP

A cap was removed from an empty amber bottle. A hole exactly the same diameter as the probe tip was drilled into the cap. The cap was then placed onto the probe and slid all of the way up to the flange. An o-ring was then slid up to the cap. This aided in keeping volatiles from escaping during the acquisition of the spectrum. An empty amber bottle was placed over the probe, and the lid was screwed down onto the bottle. The amber bottle helps to minimize the effects of ultraviolet and unwanted stray light. Ashland's InfraTane® software was utilized to setup the instrument and collect the spectra. The detector measures the intensity of the radiation observed coming from the source, and this is converted to a voltage signal. This voltage signal must be within a given acceptable range to ensure the detector gain and attenuation are properly set. The voltage for the sample fiber was set at 5.167V by adjusting the gain and attenuation of the detector accordingly. The voltage for the reference fiber was set at approximately 5.169V by adjusting a blocker to cover up a portion of reference fibers so that the voltage matches the sample fiber voltage. The instrument parameters were then set to take an average of 16 scans with a detector gain of 1. The encoder was automatically calibrated (linearized) with an internal polystyrene sample (Figure 4). The position of the maxima of four bands was generated, but the fourth band maximum was deleted because it is in the range of 2300-2500 nm where the intensity of the source is too weak. The encoder position is proportional to the corresponding wavelengths. Based on the positions and absorbances of the three band maxima, the linearization program generated an equation that was downloaded to the sensor to assure wavelength accuracy.⁵⁸ The individual linearization constants of the reference fiber and the sample fiber are listed in Table II. If a difference between any of the certified wavelengths and the wavelengths identified by the instrument is greater than 0.5 nm, an error message is displayed and the linearization equation is not downloaded to the sensor.

Upon completion of the linearization of the sensor, a bandwidth test was

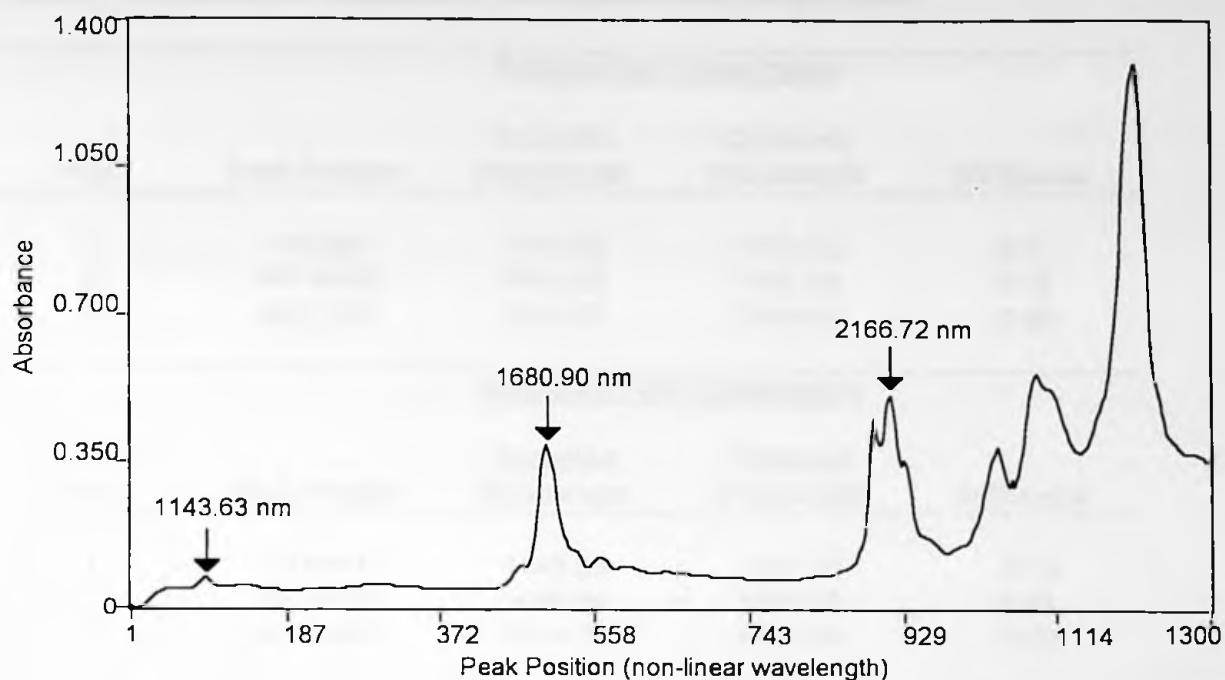


Figure 4. Polystyrene spectrum.

performed on the sample fiber to establish the wavelength accuracy, precision, and bandpass by use of the polystyrene again.⁵⁸ The bandwidth refers to the average width of the bands mentioned previously in conjunction with the polystyrene spectrum at one-half of the maximum absorbance. In this test, each output scan was based upon the instrument being setup for 16 scans per acquisition. The average bandwidth should be within the specified range of 10.00 ± 1.00 nm. A noise test was performed to the photometric noise of the instrument.⁵⁸ This was done by observing the situation where the most noise would be encountered in the sampling system, and comparing the sample fiber to the reference fiber. The program subtracts one from the other to show the noise that is present in the instrument. Again, the instrument was setup for 16 scans per acquisition. NIRSystems' NSAS manual states "that the peak-to-peak value does not exceed 0.500 and the root mean square (RMS) of the noise does not exceed 0.100."⁵⁸

Table II. Linearization constants of the reference and sample fibers.

<u>Sample Fiber Linearization</u>				
Point	Peak Position	Accepted Wavelength	Observed Wavelength	Difference
1	74.3565	1143.63	1143.52	-0.11
2	487.6425	1680.90	1681.08	0.18
3	902.7701	2166.72	2166.63	-0.09
<u>Reference Fiber Linearization</u>				
Point	Peak Position	Accepted Wavelength	Observed Wavelength	Difference
1	79.6944	1143.63	1143.53	-0.10
2	492.4677	1680.90	1681.06	0.16
3	907.5851	2166.72	2166.64	-0.08

IV. DATA COLLECTION AND TREATMENT

The samples were taken out of the freezer eight hours before analysis, so they would have time to warm up to approximately 72°F (~22°C). The samples were then shaken and agitated in a circular motion to assure a homogenous sample, with no stratification of compounds being present in the sample. The empty amber bottle was removed and replaced with a bottle containing a sample. The instrument was set to take 32 scans of the sample. The 32 scans were averaged to produce a spectrum. The most primitive spectrum that the software will collect is a n-point smoothed spectrum, which is a raw absorption spectrum that has been smoothed by averaging n nanometers to yield a data scan of greater precision, n being 2 nm in this case.⁵⁸ Spectra were collected for all of the calibration set and prediction set samples. A reformat sample of known values was poured into each of 13 bottles. Each of these samples was then spiked with 20 percent by volume of one of either benzene, toluene, *o*-xylene, *m*-xylene, *p*-xylene, mixture of xylenes, ethylbenzene, pentane, hexane, heptane, isooctane, 1-octene, or

methylcyclohexane, and spectra of each of these were also collected. By subtracting the original sample from the spiked samples, one can deduce the areas of unique spectral features where the absorbance of the particular group or individual sample is likely to have the greatest variance.

A second derivative conversion of the spectra is used for the calibration. The second derivative transformation of the data eliminates baseline variations due to small changes in density and/or temperature, while maintaining band positions.^{58,98} Some spectral features are improved in the second derivative spectrum.^{58,98} This is made possible by the extremely high signal to noise level of the near infrared instrumentation.⁶⁶

A constituent file was created for each sample spectrum when the spectrum was stored. The constituent file links each sample spectrum with its corresponding constituent data. The constituents in this case are the volume percentages of hydrocarbon groups (aromatics, olefins, etc.) and individual hydrocarbon species (benzene, toluene, etc.) present in the sample. The correct data must be input for each specific spectrum. Otherwise, unexpected and unsolvable errors may be encountered during multivariate analysis. After the constituent data was entered, a search was made for areas of greatest variance for hydrocarbon groups and hydrocarbon species within the groups. After areas of variance were located in the spectrum, regression analysis was applied to the multivariate data.

The spectra were divided into four sample populations for PLS, so as to allow for cross validation using three of the four populations at a time (leaving one out). Upon completing the cross validation, the four intervals were then averaged together to indicate the correct number of factors to use.

During the generation of the equations, the following statistical operations were performed by the software on the residual concentrations.

Coefficient of Correlation, R :⁹⁹

\hat{X} is the predicted value for the analyte from the equation

\bar{X} is the mean laboratory value for the analyte

X is the actual laboratory value for the analyte

$$R = \left[\frac{\sum (\hat{X} - \bar{X})^2}{\sum (X - \bar{X})^2} \right]^{1/2} \quad (5)$$

Standard Error of Calibration, SEC: ⁹⁹

n is the number of samples

k is the number of wavelengths or factors used

$$SEC = \left[\frac{\sum (X - \hat{X})^2}{n - k - 1} \right]^{1/2} \quad (6)$$

The reason for not using more wavelengths in developing the MLR equation is that the model must be very robust, and the data must not be overfitted. Overfitting occurs in MLR when the equations generated with more and more wavelengths appear to give good results, but the equation might not work with a sample not used to generate the model.

The measurement of robustness is referred to as the F of regression.⁹⁹ The F value indicates how robust the model is, and if it will work well with samples not included in the calibration set. A larger F value indicates a better model than one with a lower F value.

The equation for the F of regression is listed below with n being the number of samples in the model and k being the number of wavelengths used.⁹⁹

$$F = \frac{R^2}{(1-R)^2} * \frac{n-k-1}{k} \quad (7)$$

The equations generated for the second calibration set were then used to predict the analyte of interest in the eight samples of the prediction set. From the predicted data, the standard error of prediction (performance) was calculated to give some idea of the performance of the equation.

Standard Error of Prediction, SEP:⁵⁸

$$SEP = \left[\frac{\sum (x - \hat{x})^2}{n - 1} \right]^{1/2} \quad (8)$$

2. 2.4 AND RESULTS

The FLUXIX results for the various parameters of the model are given in Table 2.1. The model is a simple one, and the results are in good agreement with the data. The primary energy of the source is estimated to be 10^{38} erg s⁻¹.

The results of the FLUXIX analysis are given in Table 2.1. The data are in good agreement with the model. The primary energy of the source is estimated to be 10^{38} erg s⁻¹. The results of the analysis are given in Table 2.1. The data are in good agreement with the model. The primary energy of the source is estimated to be 10^{38} erg s⁻¹. The results of the analysis are given in Table 2.1. The data are in good agreement with the model. The primary energy of the source is estimated to be 10^{38} erg s⁻¹.

CHAPTER 3

RESULTS AND DISCUSSION

III. OBSERVATIONAL TEST RESULTS

The results of the observational test are given in Table 3.1. The data are in good agreement with the model. The primary energy of the source is estimated to be 10^{38} erg s⁻¹. The results of the analysis are given in Table 3.1. The data are in good agreement with the model. The primary energy of the source is estimated to be 10^{38} erg s⁻¹.

III. DISCUSSION

The results of the discussion are given in Table 3.2. The data are in good agreement with the model. The primary energy of the source is estimated to be 10^{38} erg s⁻¹. The results of the analysis are given in Table 3.2. The data are in good agreement with the model. The primary energy of the source is estimated to be 10^{38} erg s⁻¹.

I. P.I.A.N.O. RESULTS

The P.I.A.N.O. results for the chemical properties of interest of the original calibration set and the second calibration set are listed in Appendix III. This primary method data was used to create correlations with the NIR spectra.

No repeatability for P.I.A.N.O. analysis has been published. Therefore, a repeatability study was performed. A reformat sample was repeatedly submitted blind for analysis eight times over a period of two months. This time frame allowed for bottles of the carrier gas to be changed, and for different technicians to run the analysis. The repeatability results are listed in Table III. The relative standard deviations were less than 0.210 volume percent for each of the hydrocarbon groups and less than 0.090 volume percent for each of the selected compounds. The relative standard deviation for number of peaks detected in the chromatogram was 6.182 peaks.

II. INSTRUMENT TEST RESULTS

The settings for the bandwidth test and the results are listed in Appendix IV. The average bandwidth observed in this test was 10.45 nm. This is an acceptable bandwidth, since it is within the range of 10 ± 1 nm.⁵⁸ All results for the noise test are listed in Appendix V. The average peak-to-peak value was 0.098, which is less than the 0.500 specified limit.⁵⁸ Also, the RMS observed was 0.017, and this is well within the 0.100 limit that is specified.⁵⁸

III. BAND ASSIGNMENTS

Weyer assigned the band of about 2150 nm as an Ar-H band using a spectrum of benzene.¹⁰⁰ The range of the Ar-H band is being defined as 2100-2160 nm, depending upon shifts due to substitutions on the ring or neighboring molecules. Weyer also mentions an olefin (=CH) band at 2100 nm.¹⁰⁰ There is a larger amount of overlapping amongst the combination bands than in the overtones. This range for the =CH band is

Table III. GC-PIANO Results for Repeatability Study.

Sample #	Vol% Total Aromatics	Vol% Benzene	Vol% Toluene	Vol% Total Xylenes	Vol% <i>m</i> -Xylene	Vol% <i>p</i> -Xylene
1	59.632	3.768	12.853	14.919	7.261	3.045
2	59.482	3.769	12.878	14.962	7.263	3.073
3	59.394	3.779	12.887	14.929	7.274	3.042
4	59.396	3.772	12.855	14.918	7.267	3.040
5	59.641	3.760	12.836	14.925	7.261	3.050
6	59.713	3.751	12.792	14.914	7.259	3.044
7	59.708	3.758	12.857	14.888	7.237	3.047
8	59.230	3.658	12.782	14.873	7.256	3.014
Average	59.525	3.752	12.843	14.916	7.260	3.044
Std. Dev.	0.176	0.039	0.038	0.027	0.011	0.016

Sample #	Vol% <i>o</i> -Xylene	Vol% Ethylbenzene	Vol% Total Olefins	Vol% Total Paraffins	Vol% Hexane	Vol% <i>n</i> -Heptane
1	4.613	3.057	1.098	13.103	3.087	2.584
2	4.626	3.065	1.092	13.096	3.088	2.586
3	4.613	3.060	1.095	13.132	3.094	2.592
4	4.611	3.055	1.100	13.127	3.093	2.589
5	4.614	3.058	1.064	13.059	3.085	2.582
6	4.611	3.052	1.062	13.016	3.076	2.574
7	4.604	3.048	1.064	13.041	3.087	2.574
8	4.603	3.050	1.035	13.049	3.097	2.594
Average	4.612	3.056	1.076	13.078	3.088	2.584
Std. Dev.	0.007	0.006	0.023	0.043	0.007	0.008

Sample #	Vol% Total Isoparaffins	Vol% Isopentane	Vol% 2-methylhexane	Vol% Total Naphthenes	Vol% Methylcyclopentane	# of Peaks
1	24.545	3.820	2.741	0.868	0.175	238
2	24.398	3.814	2.746	1.038	0.175	238
3	24.596	3.824	2.749	0.870	0.176	235
4	24.438	3.823	2.749	1.031	0.176	240
5	24.419	3.809	2.741	1.040	0.175	236
6	24.506	3.799	2.733	0.873	0.175	227
7	24.397	3.816	2.735	1.034	0.176	227
8	25.004	3.801	2.760	0.964	0.176	245
Average	24.538	3.813	2.744	0.965	0.176	235.75
Std. Dev.	0.202	0.010	0.009	0.082	0.001	6.182

being defined as 2050-2110 nm, considering shifts due to neighboring molecules.

Osborne et al. assigned the first overtone wavelength band vibration for Ar-H as 1685 nm.⁷ There could be some shifting of the bands observed in going from an agriculture sample to a sample comprised of only hydrocarbons. NIRSystems' near infrared absorption chart depicts the Ar-H band as ranging from 1610-1650 nm.¹⁰¹ In practice, this range could be extended to include the 1685 nm assignment. However, too

large of an absorbance for the CH₃ band frequently occurs due to the size of the pathlength. This limits the useable vibration band range to 1610-1670 nm. Weyer assigned the first overtone wavelength band vibration for =CH as 1620 nm.¹⁰⁰ There is overlapping of these two different types of bands, but the reference material always indicates that the =CH band occurs at shorter wavelengths than the Ar-H band in the same overtone.¹⁰¹ Therefore, the range for =CH band is defined as 1560-1626 nm.

The bands in the first overtone of C-H combinations are broad with considerable overlapping. The NIRSystems chart gives the CH₃ band an assignment range of 1360-1410 nm, and Osborne et al. assigned CH₃ to a band at 1360 nm.^{7,101} The range for CH₃ band is defined here as 1290-1430 nm. Osborne et al. also assigned a band at 1415 nm to CH₂.⁷ This is in the overlapping region. In Figure 5, it can be seen that the CH₂ band should be extended to about 1530 nm. The *n*-heptane spiked sample, which would have a larger molar ratio of CH₂ than the base sample or the sample spiked with *o*-xylene, clearly has larger absorbance values over this range. Therefore, the range for the CH₂ band is

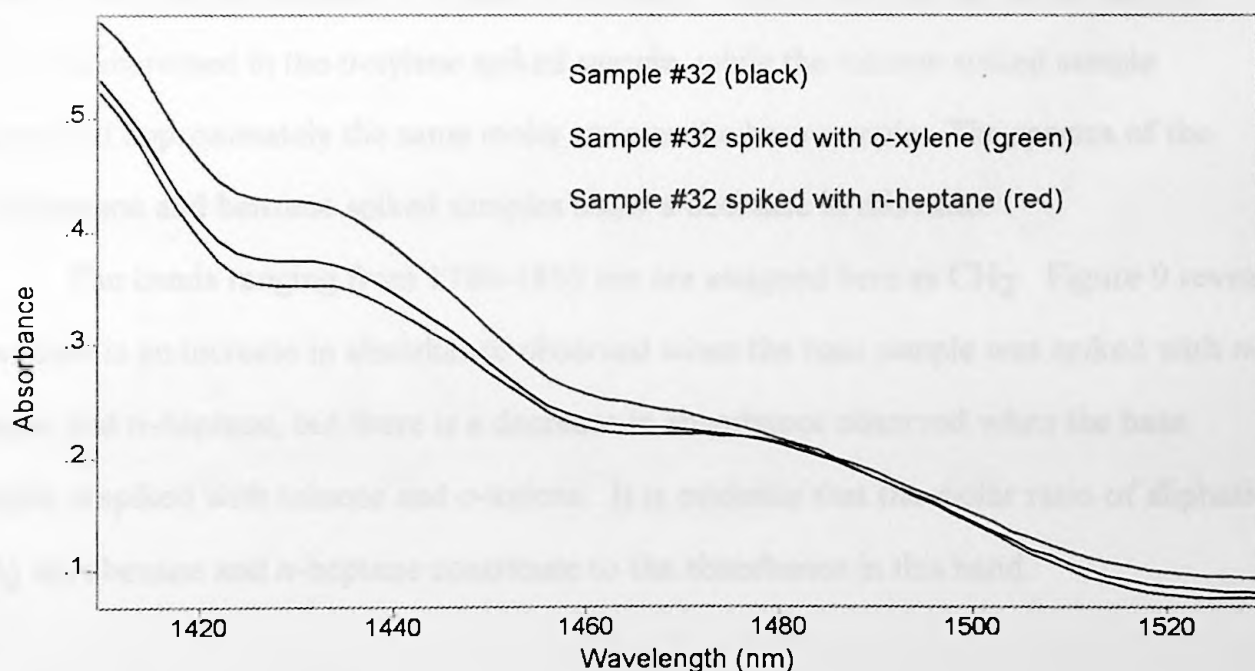


Figure 5. Comparison of spectra of a reformate (sample #32) and that same reformate spiked individually with *o*-xylene and *n*-heptane.

being defined as 1410-1530 nm.

Maggard assigned band ranges for this overtone in his patent.²³ His assignments are a CH₃ band range of 1174-1212 nm, a CH₂ band range of 1228-1268 nm, and a *t*-butyl/methylene band range of 1212-1228 nm. The NIRSystems chart extends the CH₃ band down to about 1120 nm.¹⁰¹ It can clearly be seen in Figures 6 and 7 that there is another band present with a maximum at around 1140 nm. This is the Ar-H band that Weyer makes reference to in his assignment of 1143 nm.¹⁰⁰ The range for the Ar-H band is being defined as 1132 to 1156 nm. There is some overlap with the CH₃ bands observed, so the CH₃ band range is defined as 1156-1214 nm.

There were two other bands which apparently have not been previously assigned. The band showing a maximum absorbance at around 2000 nm is assigned here as CH₃. An increase in absorbance is observed in this region when xylenes were added to the sample, but no significant increase in absorbance was observed in the samples spiked with toluene, ethylbenzene, and benzene (Figure 8, top). This difference is seen more clearly using second derivative spectra (Figure 8, bottom). This is because the molar ratio of CH₃ was increased in the *o*-xylene spiked sample, while the toluene spiked sample maintained approximately the same molar ratio as the base sample. The spectra of the ethylbenzene and benzene spiked samples show a decrease in this ratio.

The bands ranging from 1780-1858 nm are assigned here as CH₂. Figure 9 reveals that there is an increase in absorbance observed when the base sample was spiked with *n*-hexane and *n*-heptane, but there is a decrease in absorbance observed when the base sample is spiked with toluene and *o*-xylene. It is evidence that the molar ratio of aliphatic CH₂ in *n*-hexane and *n*-heptane contribute to the absorbance in this band.

IV. AREAS OF VARIANCE

The spectra of four of the spiked samples and the original sample are shown in

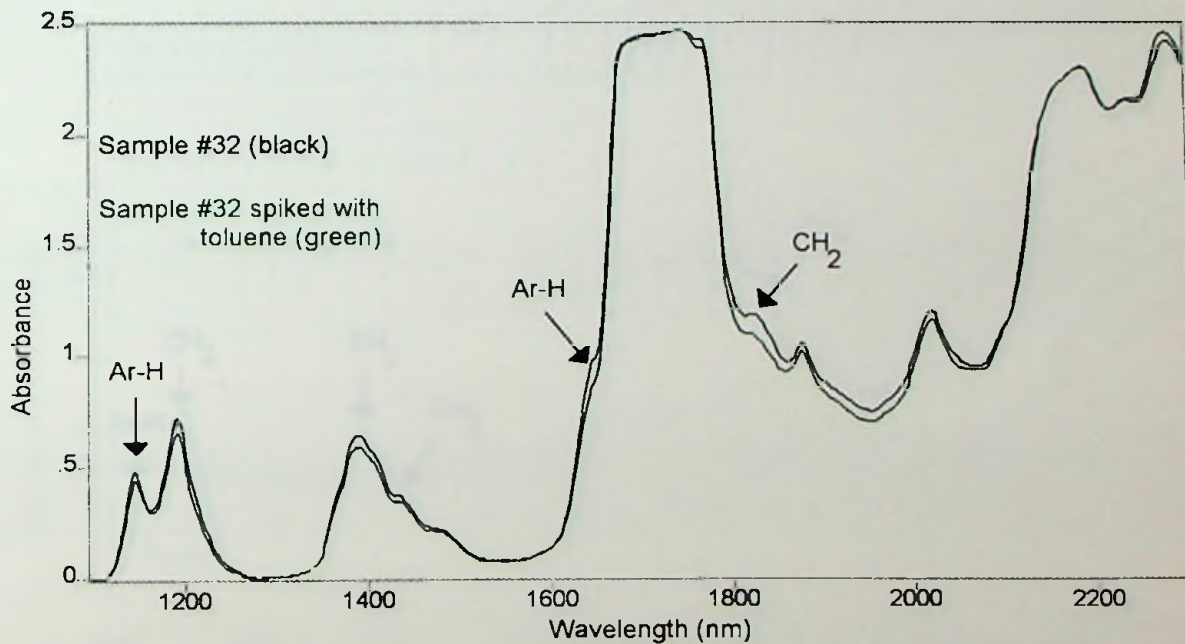
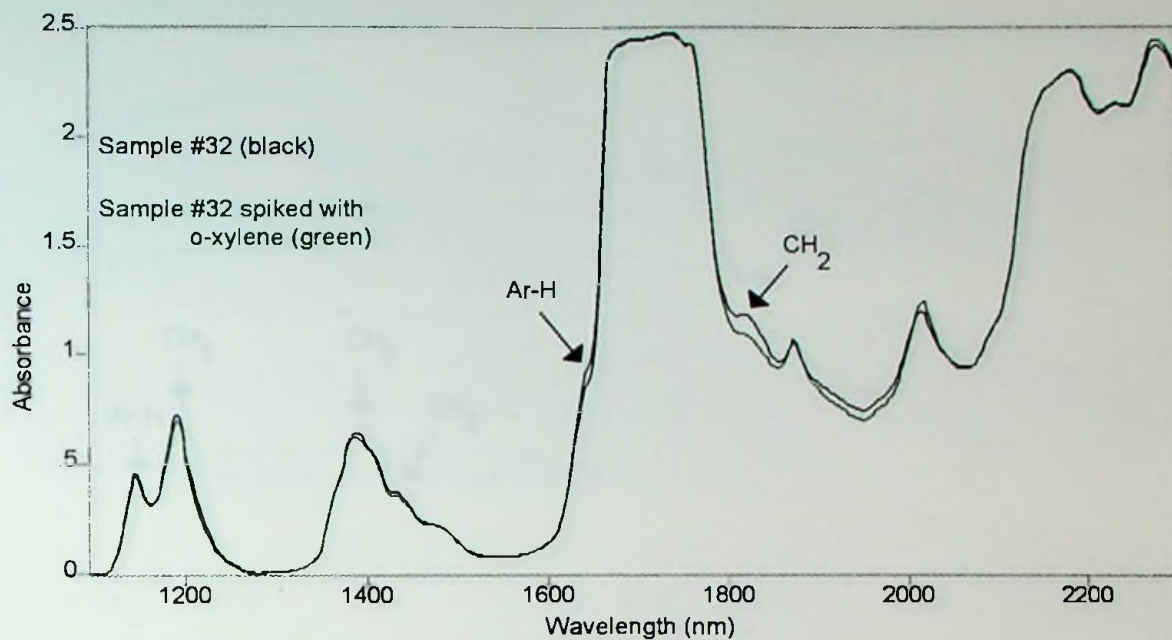


Figure 6. (top) Comparison of a reformate (sample #32) and that same reformate spiked with *o*-xylene. (bottom) Comparison of a reformate (sample #32) and that same reformate spiked with toluene.

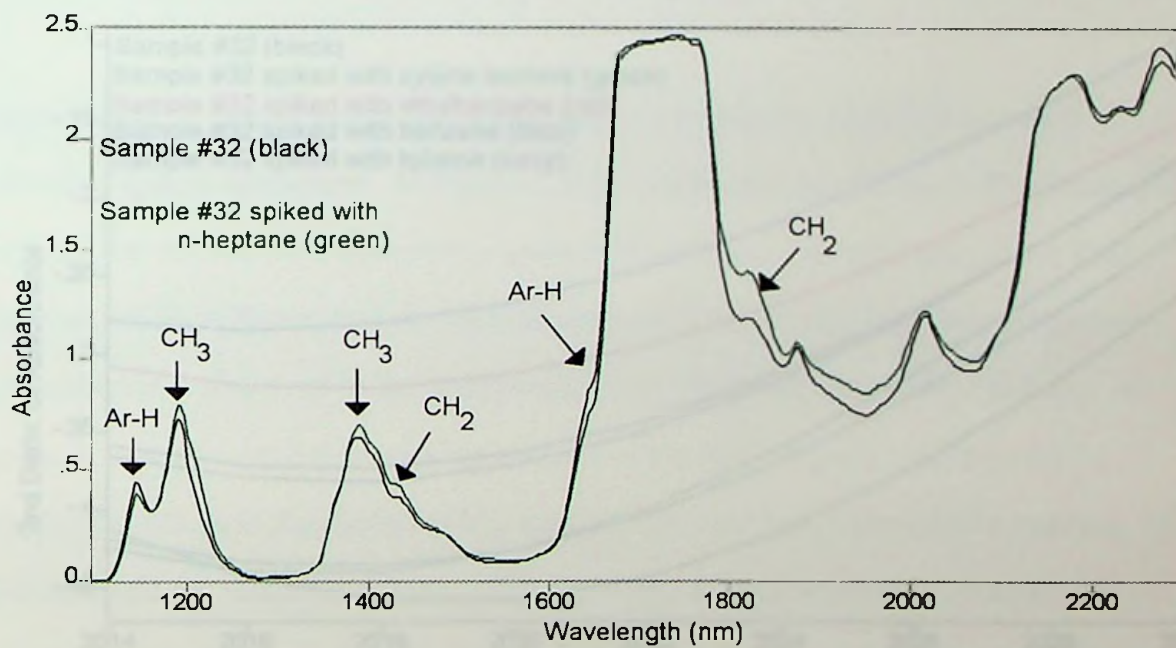
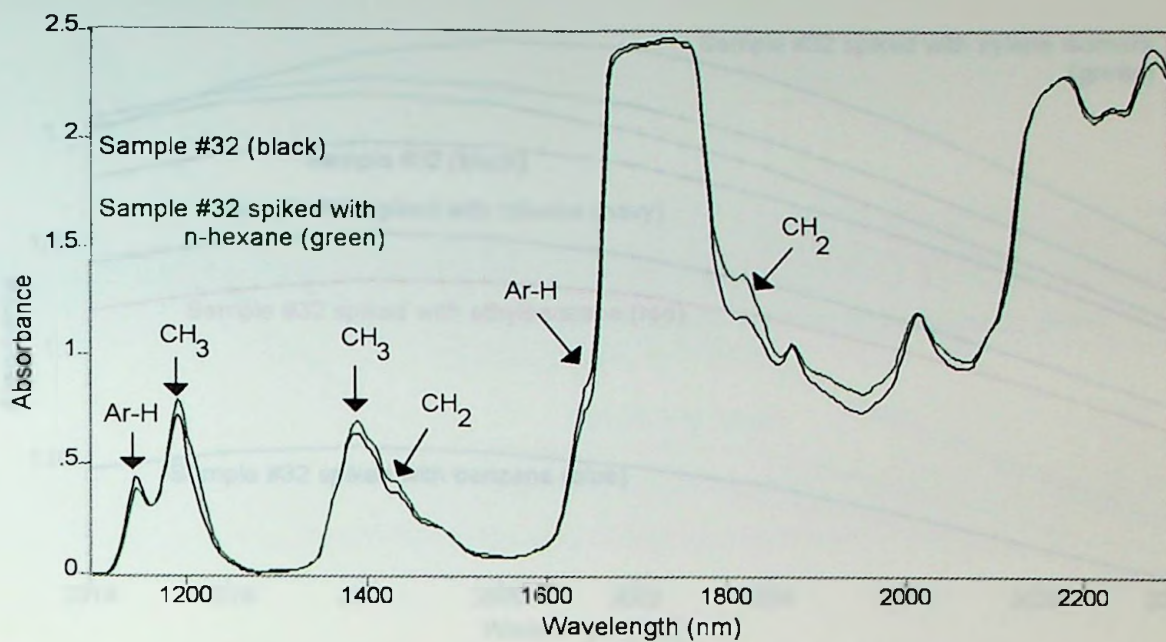


Figure 7. (top) Comparison of a reformate (sample #32) and that same reformate spiked with *n*-hexane. (bottom) Comparison of a reformate (sample #32) and that same reformate spiked with *n*-heptane.

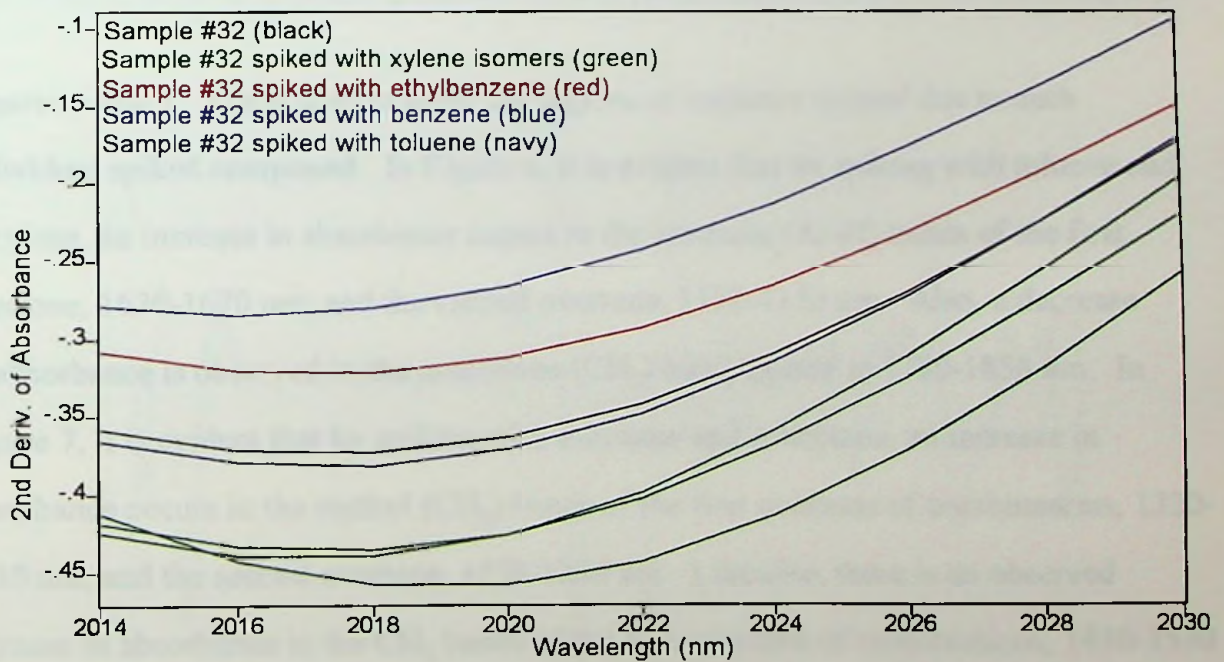
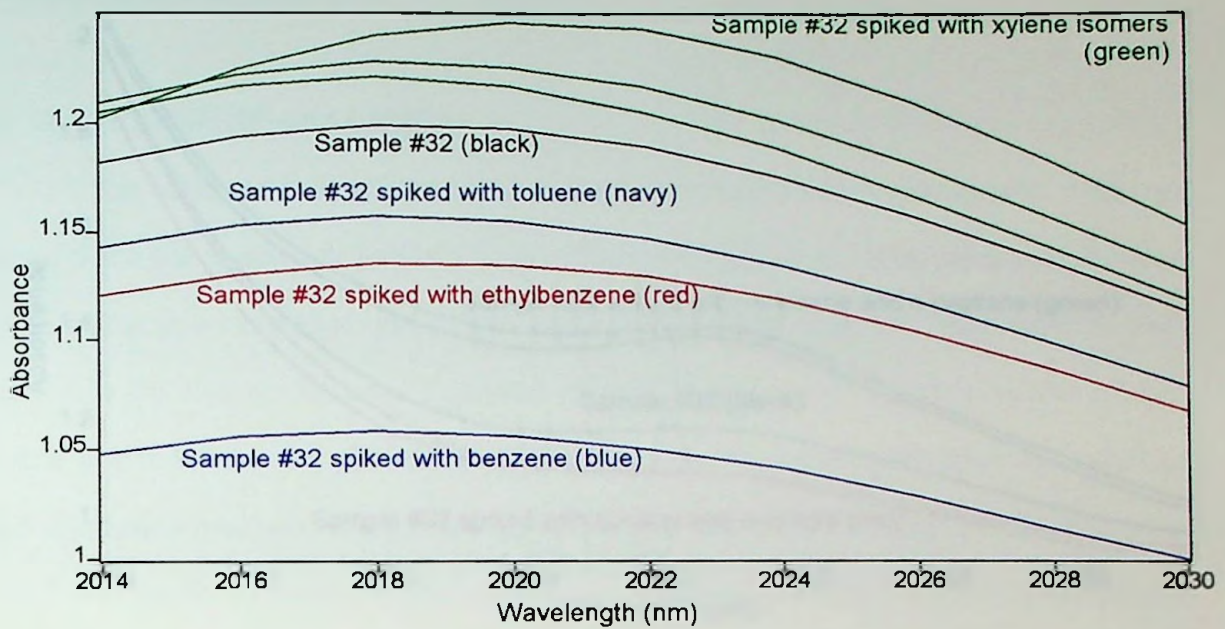


Figure 8. Comparison of absorbance (top) and second derivative (bottom) spectra of a reformat (sample #32) and that same reformat, spiked individually with xylene isomers, toluene, ethylbenzene, and benzene.

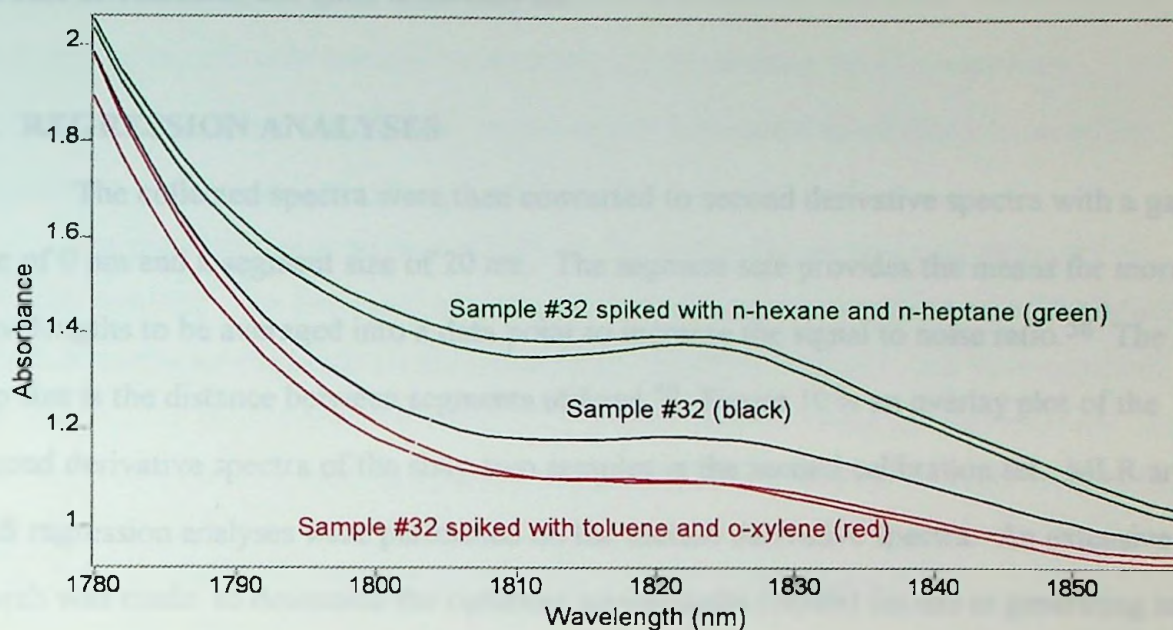


Figure 9. Comparison of spectra of a reformat (sample #32) and that same reformat spiked individually with *n*-hexane, *n*-heptane, toluene, and *o*-xylene.

Figures 6 and 7. These spectra show the regions of variance created due to each individual spiked compound. In Figure 6, it is evident that by spiking with toluene and *o*-xylene, an increase in absorbance occurs in the aromatic (Ar-H) bands of the first overtone, 1620-1670 nm, and the second overtone, 1132-1156 nm. Also, a decrease in absorbance is observed in the methylene (CH₂) band located at 1780-1858 nm. In Figure 7, it is evident that by spiking with *n*-hexane and *n*-heptane, an increase in absorbance occurs in the methyl (CH₃) bands of the first overtone of combinations, 1320-1430 nm, and the second overtone, 1156-1214 nm. Likewise, there is an observed increase in absorbance in the CH₂ bands of the first overtone of combinations, 1430-1530 nm, and the second overtone, 1230-1264, as well as the band located at 1780-1858 nm. Also observed in Figure 7 is the decrease in absorbance in the Ar-H bands of the first and second overtones. By locating the areas of variance, an initial starting point can be reached for the beginning of regression techniques. Not all areas of variance may provide

the best correlations, but quite often they do.

V. REGRESSION ANALYSES

The collected spectra were then converted to second derivative spectra with a gap size of 0 nm and a segment size of 20 nm. The segment size provides the means for more wavelengths to be averaged into a data point to increase the signal to noise ratio.⁵⁸ The gap size is the distance between segments utilized.⁵⁸ Figure 10 is an overlay plot of the second derivative spectra of the sixty-two samples in the second calibration set. MLR and PLS regression analyses were performed on the second derivative spectra. An extensive search was made to determine the optimum wavelengths (bands) for use in generating an equation for the prediction of each desired property. The function of each equation generated was examined closely. In doing this, wavelengths (bands) that have little or no contribution, alone or in combination with other wavelengths (bands), were excluded from

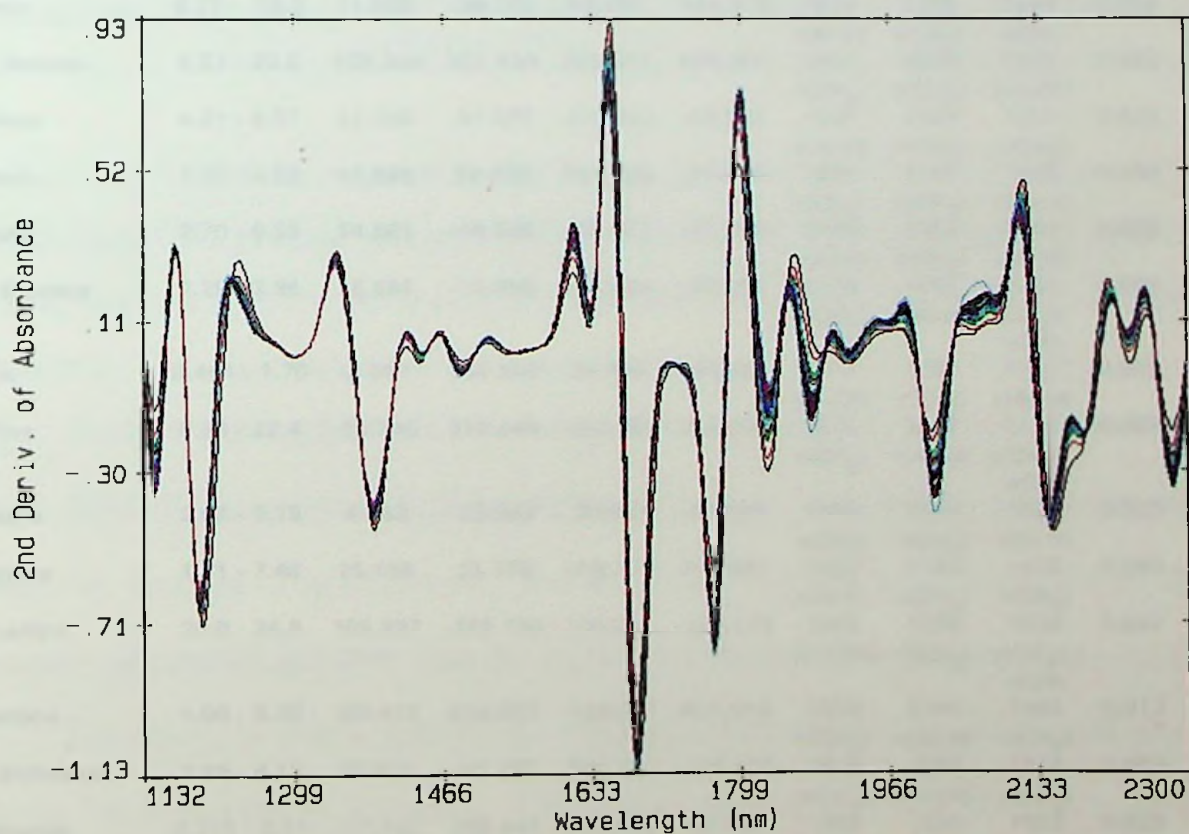


Figure 10. Second derivative spectra of the sixty-two samples in the second calibration set overlaid.

the calibration equation.⁹⁹ Three wavelengths were used in combination to develop the MLR equations, and only selected bands were used to develop the PLS equations.

Regression analyses were performed on an original calibration set of fifty-two samples, and later on the second calibration set of sixty-two samples.

The regression process was initially performed on the original calibration set of fifty-two samples. The generated equations and results were extremely good. The MLR and PLS results for the original calibration set are listed in Tables IV and V, respectively. One goal was to predict benzene within 0.21 volume percent of the primary method. This goal was met with both types of equations. The standard error of calibration for the MLR

Table IV. MLR results for the original calibration set.

Compound	Volume % Range	Constants				Wavelengths (nm)			R	NIR Std Error of Calibration (Vol%)
		k(0)	k(1)	k(2)	k(3)	1	2	3		
Total Aromatics	35.9 - 68.0	79.902	93.863	82.716	-105.131	1834	1624	1232	0.999	0.30
						v(CH ₂)	v(Ar-H)	v(CH ₂), v(CH)		
Benzene	2.70 - 5.73	19.610	-12.233	-75.612	21.631	2128	1624	1834	0.995	0.07
						v(Ar-H)	v(Ar-H)	v(CH ₂)		
Toluene	8.77 - 16.2	11.905	-39.118	86.410	-144.518	1650	1796	1224	0.992	0.22
						v(Ar-H)	v(CH ₂)	v(CH)		
Total Xylenes	8.51 - 20.0	-108.345	901.434	203.014	488.084	1458	2028	1622	0.989	0.42
						v(CH ₂)	v(CH ₃)	v(Ar-H)		
<i>m</i> -Xylene	4.01 - 9.57	51.160	-57.877	-476.542	-53.513	1648	1504	1400	0.978	0.28
						v(Ar-H)	v(CH ₂)	v(CH ₂)		
<i>p</i> -Xylene	1.80 - 4.03	12.589	32.439	111.426	-21.007	1204	1356	1646	0.984	0.10
						v(CH ₃)	v(CH ₃)	v(Ar-H)		
<i>o</i> -Xylene	2.70 - 6.39	24.885	-46.606	-28.127	-47.216	2148	1854	1646	0.986	0.18
						v(Ar-H)	v(CH ₂)	v(Ar-H)		
Ethyl-Benzene	2.29 - 3.96	18.684	-13.859	-18.225	-23.611	1176	1642	1230	0.983	0.09
						v(CH ₃)	v(Ar-H)	v(CH ₂), v(CH)		
Olefins	0.464 - 1.70	-3.051	134.146	24.440	104.801	1612	1200	1140	0.978	0.05
						v(=CH)	v(CH ₃)	v(Ar-H)		
Paraffins	8.36 - 22.4	-50.245	217.444	-147.095	264.005	1976	2062	1232	0.997	0.24
						v(CH ₃)	v(=CH)	v(CH ₂), v(CH)		
<i>n</i> -Hexane	2.67 - 5.19	4.362	-25.343	-30.921	-53.680	1844	2014	1624	0.926	0.18
						v(CH ₂)	v(CH ₃)	v(Ar-H)		
<i>n</i> -Heptane	1.61 - 7.48	25.158	28.376	105.983	235.947	1662	1184	1418	0.990	0.12
						v(Ar-H)	v(CH ₃)	v(CH ₃)		
Isoparaffins	20.0 - 34.6	103.497	-285.180	109.252	-203.116	2084	1938	1230	0.997	0.30
						v(=CH)	v(CH ₃)	v(CH ₂), v(CH)		
Isopentane	1.06 - 8.25	-83.412	444.557	-139.031	404.416	1970	2144	1484	0.917	0.61
						v(CH ₃)	v(Ar-H)	v(CH ₂)		
2-Methylhexane	1.88 - 4.12	73.421	-45.227	-180.792	-128.404	1804	1592	1244	0.907	0.16
						v(CH ₂)	v(=CH)	v(CH ₂)		
Naphthenes	0.811 - 6.51	-17.732	285.844	648.948	67.139	1368	1294	1802	0.986	0.23
						v(CH ₃)	v(CH ₂)	v(CH ₂)		
Methylcyclopentane	0.165 - 1.88	2.228	-53.642	103.606	46.526	1192	1374	1234	0.987	0.06
						v(CH ₃)	v(CH ₃)	v(CH ₂)		

Table V. PLS results for the original calibration set.

Compound	Volume %		Wavelength Range (nm)	Factors	R	NIR Std Error of Calibration (Vol%)
	Range					
Total Aromatics	35.9 - 68.0		1214 - 1260 ; 1600 - 1670 ; 1780 - 1858 v(CH), v(CH ₂); v(=CH), v(Ar-H); v(CH ₃)	7	0.999	0.30
Benzene	2.70 - 5.73		1132 - 1260 ; 1600 - 1670 ; 1780 - 1858 ; 2100 - 2160 v(Ar-H), v(CH ₃), v(CH), v(CH ₂); v(Ar-H); v(CH ₂); v(Ar-H)	12	1.000	0.02
Toluene	8.77 - 16.2		1214 - 1230 ; 1600 - 1670 ; 1780 - 1858 ; 2000 - 2160 v(CH), v(Ar-H), v(CH ₂); v(CH ₃), v(=CH), v(Ar-H)	8	0.997	0.13
Total Xylenes	8.51 - 20.0		1132 - 1214 ; 1320 - 1530 ; 1600 - 1670 ; 2000 - 2040 v(Ar-H), v(CH ₃), v(CH ₂), v(=CH), v(Ar-H), v(CH ₃)	12	0.998	0.22
<i>m</i> -Xylene	4.01 - 9.57		1320 - 1430 ; 1480 - 1530 ; 1600 - 1670 ; 2000 - 2040 v(CH ₃), v(CH ₂), v(=CH), v(Ar-H), v(CH ₃)	7	0.991	0.19
<i>p</i> -Xylene	1.80 - 4.03		1156 - 1214 ; 1320 - 1430 ; 1600 - 1670 ; 2000 - 2040 v(CH ₃), v(CH ₃), v(=CH), v(Ar-H), v(CH ₃)	12	0.997	0.04
<i>o</i> -Xylene	2.70 - 6.39		1600 - 1670 ; 1780 - 1858 ; 2000 - 2040 ; 2100 - 2160 v(=CH), v(Ar-H), v(CH ₂), v(CH ₃), v(Ar-H)	8	0.995	0.11
Ethyl-Benzene	2.29 - 3.96		1156 - 1264 ; 1600 - 1670 v(CH ₃), v(CH), v(CH ₂), v(=CH), v(Ar-H)	5	0.983	0.09
Olefins	0.464 - 1.70		1132 - 1214 ; 1600 - 1670 v(Ar-H), v(CH ₃), v(=CH), v(Ar-H)	6	0.973	0.06
Paraffins	8.36 - 22.4		1214 - 1264 ; 1940 - 2100 v(CH), v(CH ₂), v(CH ₃), v(=CH)	6	0.998	0.19
<i>n</i> -Hexane	2.67 - 5.19		1430 - 1480 ; 1780 - 1858 v(CH ₂), v(CH ₂)	9	0.961	0.14
<i>n</i> -Heptane	1.61 - 7.48		1156 - 1214 ; 1320 - 1480 ; 1600 - 1670 v(CH ₃), v(CH ₃), v(CH ₂), v(=CH), v(Ar-H)	8	0.995	0.09
Isoparaffins	20.04 - 34.57		1214 - 1264 ; 1920 - 2100 v(CH), v(CH ₂), v(CH ₃)	7	0.998	0.27
Isopentane	1.06 - 8.25		1430 - 1500 ; 1940 - 2040 ; 2100 - 2160 v(CH ₂), v(CH ₃), v(Ar-H)	13	0.994	0.19
2-Methylhexane	1.88 - 4.12		1214 - 1260 ; 1560 - 1626 ; 1780 - 1858 v(CH), v(CH ₂), v(=CH), v(CH ₂)	11	0.974	0.09
Naphthenes	0.81 - 6.51		1264 - 1430 ; 1780 - 1858 v(CH ₃), v(CH ₂), v(CH ₂)	12	0.998	0.08
Methylcyclopentane	0.165 - 1.88		1156 - 1260 ; 1320 - 1430 v(CH ₃), v(CH), v(CH ₂), v(CH ₃)	4	0.988	0.06

equation was 0.07 volume percent, and the standard error of cross validation for the PLS equation was 0.02 volume percent. Taking into consideration that the GC-PIANO repeatability was 0.039 volume percent, this demonstrates the high degree of accuracy in the models. This high degree of accuracy is observed for all of the analytes.

Another accomplishment was being able to quantify the individual isomers of xylene. Mid-IR has received high marks for selectivity, whereas the selectivity of near-IR is generally thought of as moderate. The research presented here indicates that the selectivity of near-IR is better than moderate if multivariate analysis is used correctly.

The standard errors of calibration for total aromatics are 0.30 volume percent for both the MLR and the PLS models. This value is extremely small relative to the large range of aromatics in the calibration sample set. This again demonstrates the high degree of accuracy in these models. Traditional methods for determining the concentration of

aromatics in hydrocarbons, fluorescent indicator absorption (ASTM D 1319) and GC/MS (ASTM D 5769), have reproducibilities in excess of 2.00 percent by volume.^{102,103}

Schematic plots of the near-IR predicted versus GC-PIANO values for the calibration models listed in Tables IV and V are shown in Figures 11-27, starting with the aromatics and following with the paraffins, isoparaffins, naphthenes, and olefins, respectively. From these plots, the quality of the correlations can be visualized.

In Figure 11 (top), the correlations between the GC-PIANO values for total aromatics and the near-IR predicted total aromatics by MLR and PLS are given. It is evident that both models are linear, and based upon the residuals of the calibration set (Figure 11, bottom), neither the MLR nor the PLS model is superior over the other. For ethylbenzene, total paraffins, *n*-hexane, *n*-heptane, total isoparaffins, methylcyclopentane, and total olefins (Figures 18, 19, 20, 21, 22, 26, and 27, respectively), there is not a large noticeable difference in residuals of the correlation data for the MLR and PLS models. This is a strong similarity to what is observed with the data for total aromatics.

In Figure 12 (top), the correlations between the GC-PIANO values for benzene and the near-IR predicted benzene by MLR and PLS are given. It is evident that both models are linear, and based upon the residuals of the calibration set (Figure 12, bottom), the MLR data is more variable than the PLS data. This indicates that the PLS model may be better for the samples in the calibration set, but not necessarily a better predictor (see below).

For toluene, total xylenes, *m*-xylene, *p*-xylene, *o*-xylene, isopentane, 2-methylhexane, and naphthenes (Figures 13, 14, 15, 16, 17, 23, 24, and 25, respectively), the correlation data for the calibration samples is tighter for the PLS models than the MLR models. However, the difference in tightness between the models for these constituents is not as great as it is for benzene.

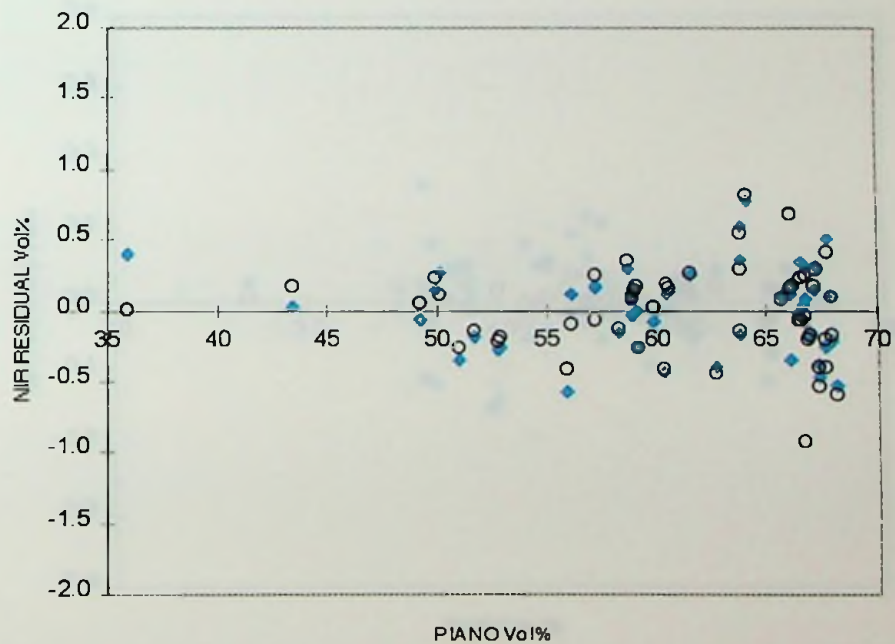
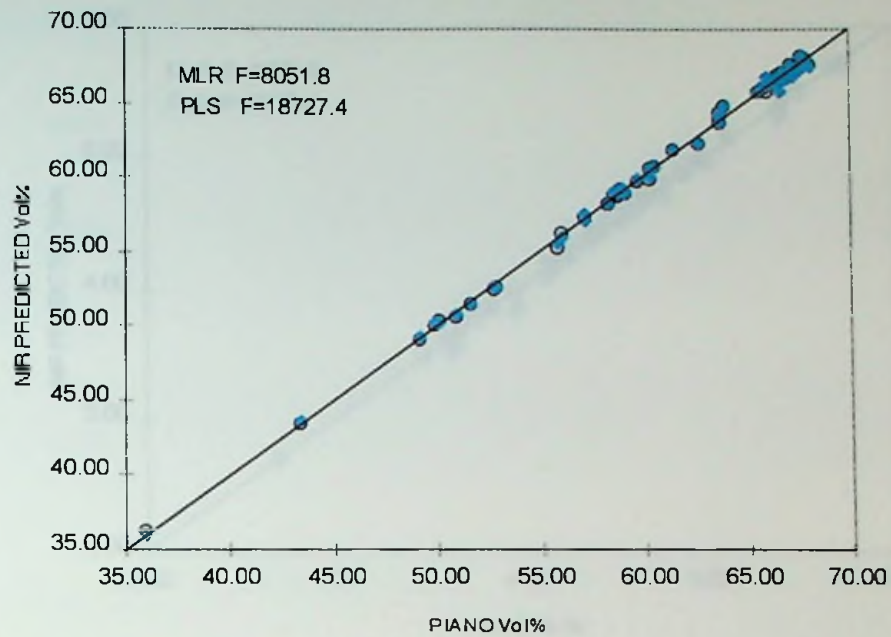


Figure 11. (top) PIANO vs. NIR Predictions for Total Aromatics in the Original Calibration Set by MLR and PLS. (bottom) NIR Residuals for Total Aromatics in the Original Calibration Set by MLR and PLS. The blue diamonds represent the MLR data, and the black circles represent the PLS data.

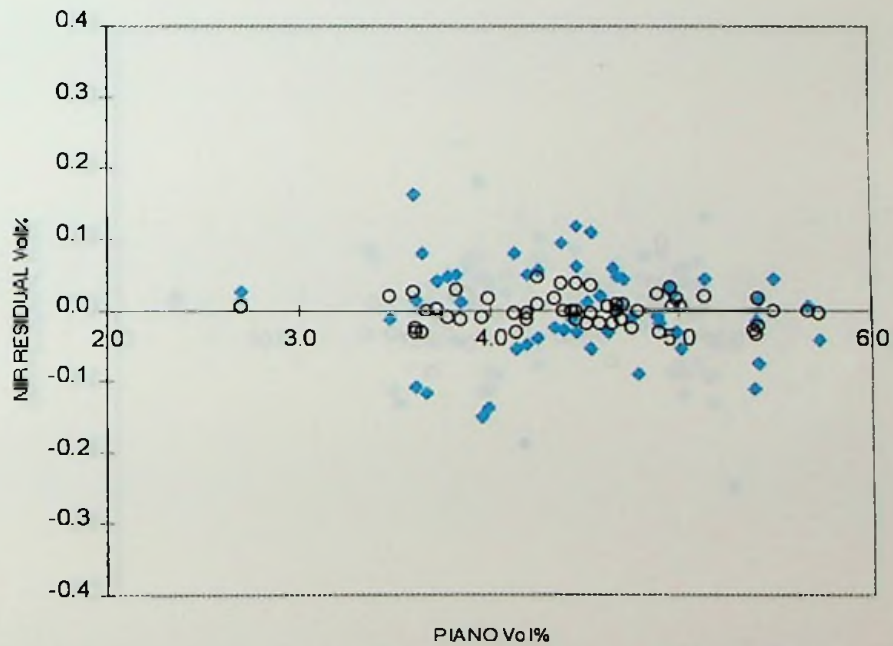
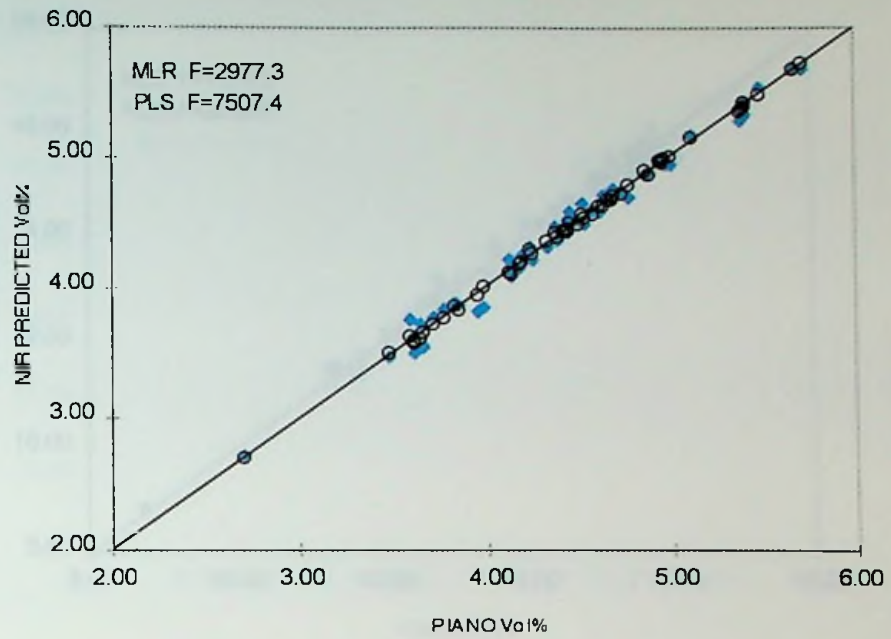


Figure 12. (top) PIANO vs. NIR Predictions for Benzene in the Original Calibration Set by MLR and PLS. (bottom) NIR Residuals for Benzene in the Original Calibration Set by MLR and PLS. The blue diamonds represent the MLR data, and the black circles represent the PLS data.

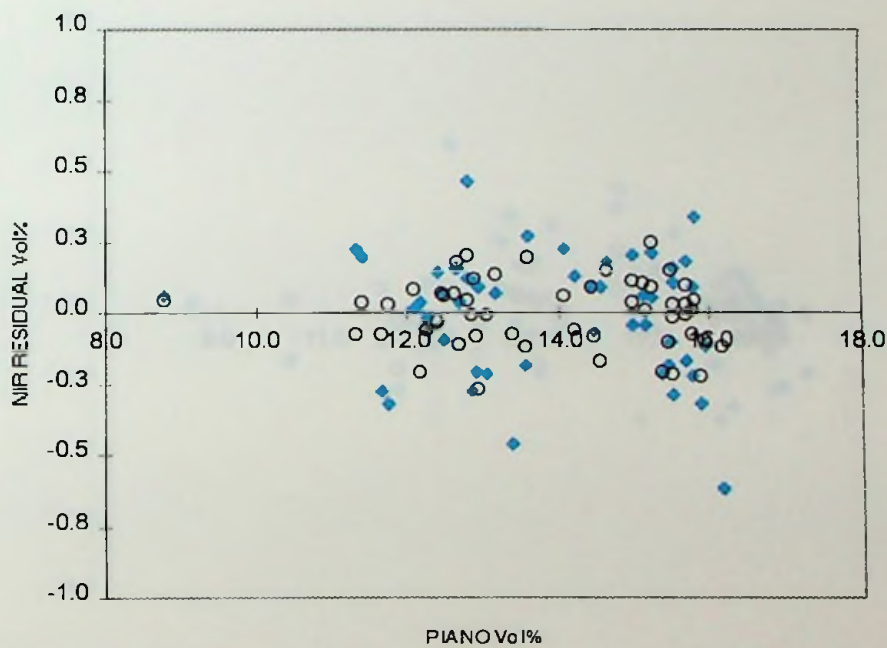
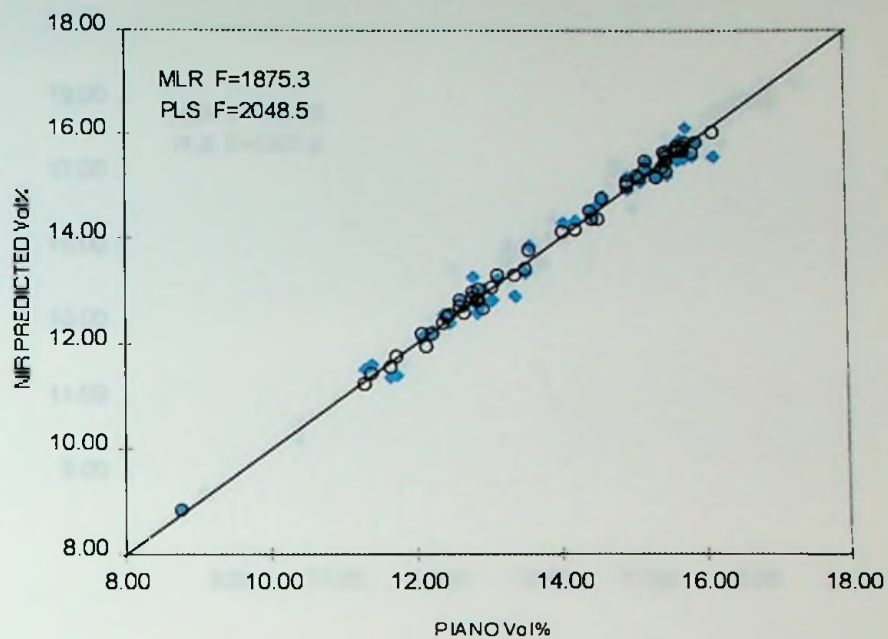


Figure 13. (top) PIANO vs. NIR Predictions for Toluene in the Original Calibration Set by MLR and PLS. (bottom) NIR Residuals for Toluene in the Original Calibration Set by MLR and PLS. The blue diamonds represent the MLR data, and the black circles represent the PLS data.

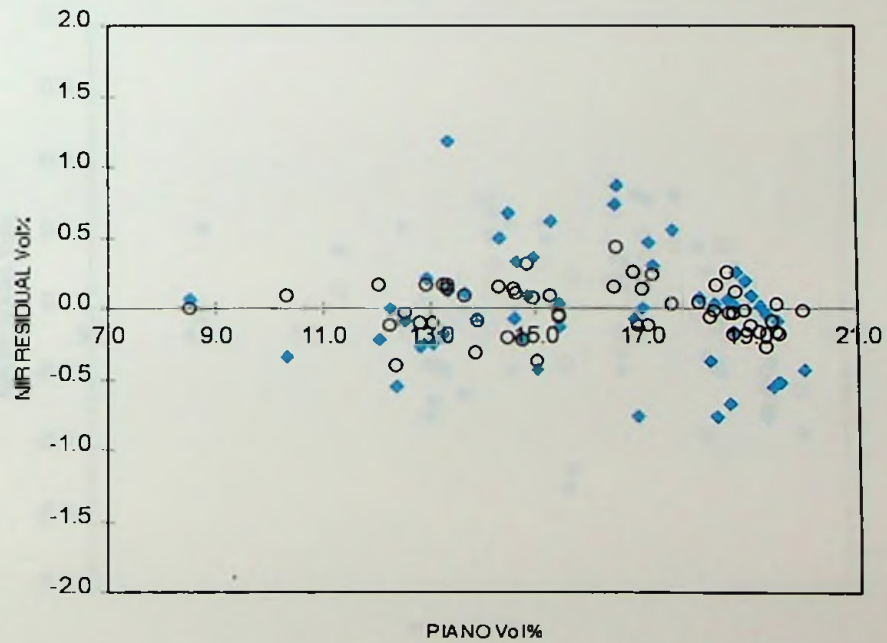
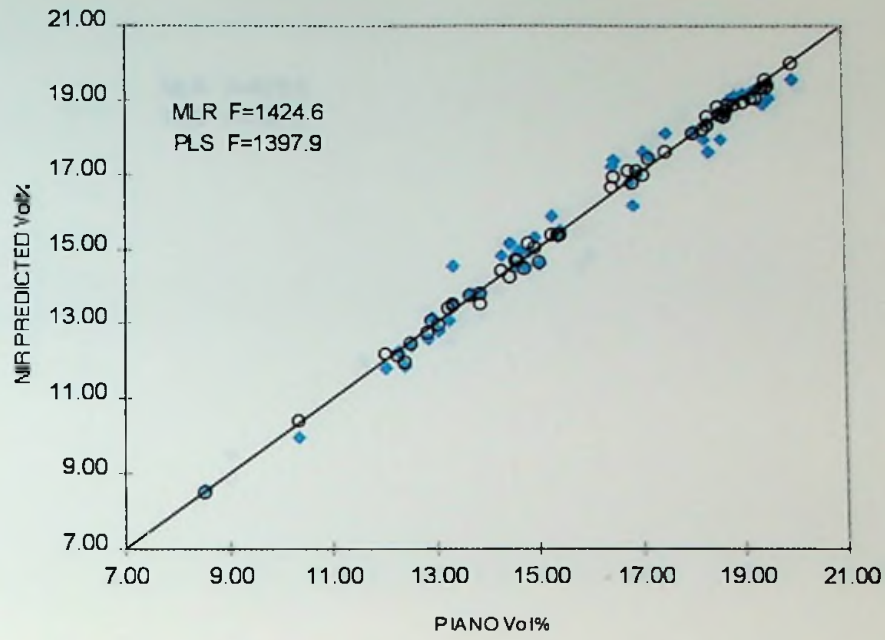


Figure 14. (top) PIANO vs. NIR Predictions for Total Xylenes in the Original Calibration Set by MLR and PLS. (bottom) NIR Residuals for Total Xylenes in the Original Calibration Set by MLR and PLS. The blue diamonds represent the MLR data, and the black circles represent the PLS data.

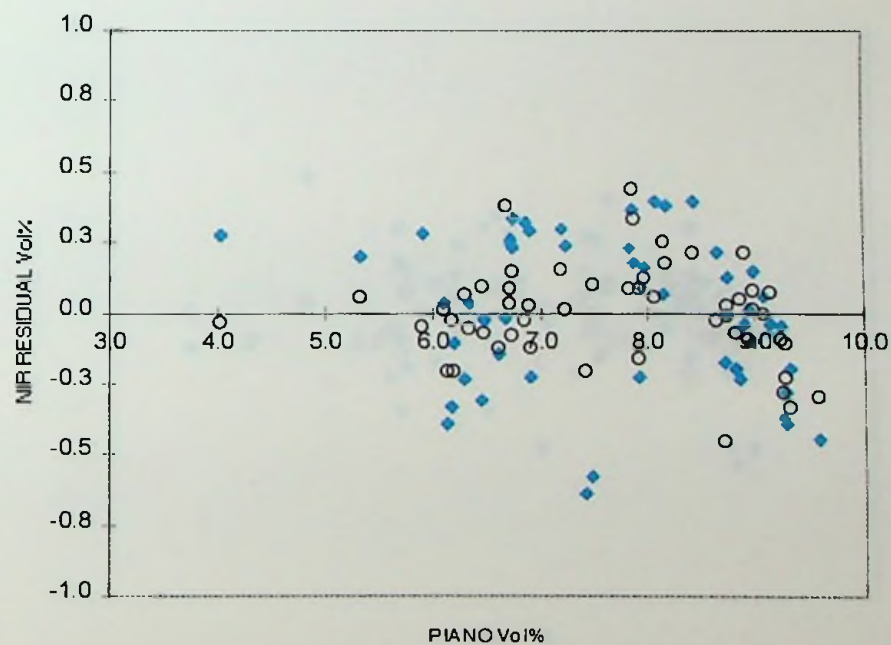
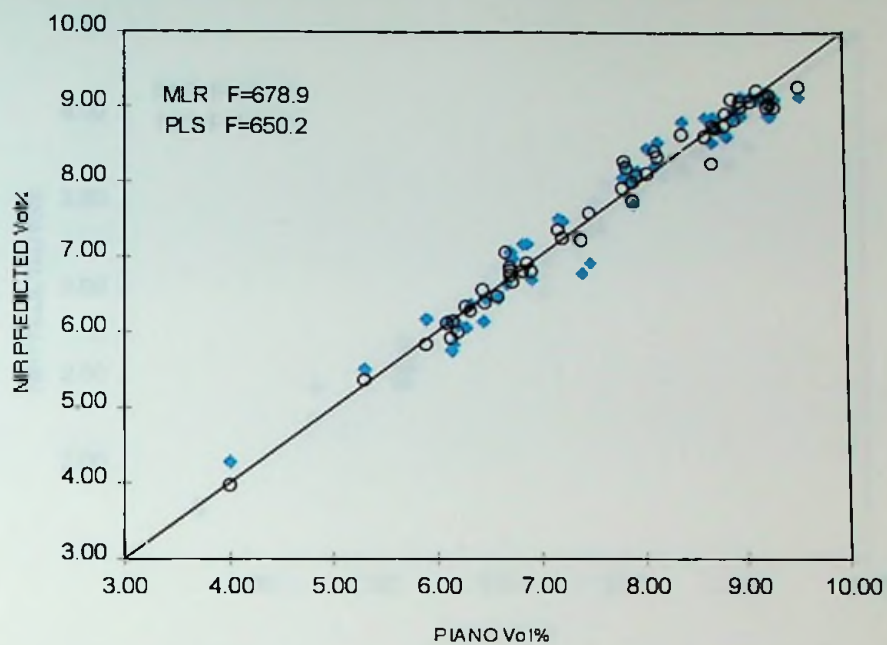


Figure 15. (top) PIANO vs. NIR Predictions for *m*-Xylene in the Original Calibration Set by MLR and PLS. (bottom) NIR Residuals for *m*-Xylene in the Original Calibration Set by MLR and PLS. The blue diamonds represent the MLR data, and the black circles represent the PLS data.

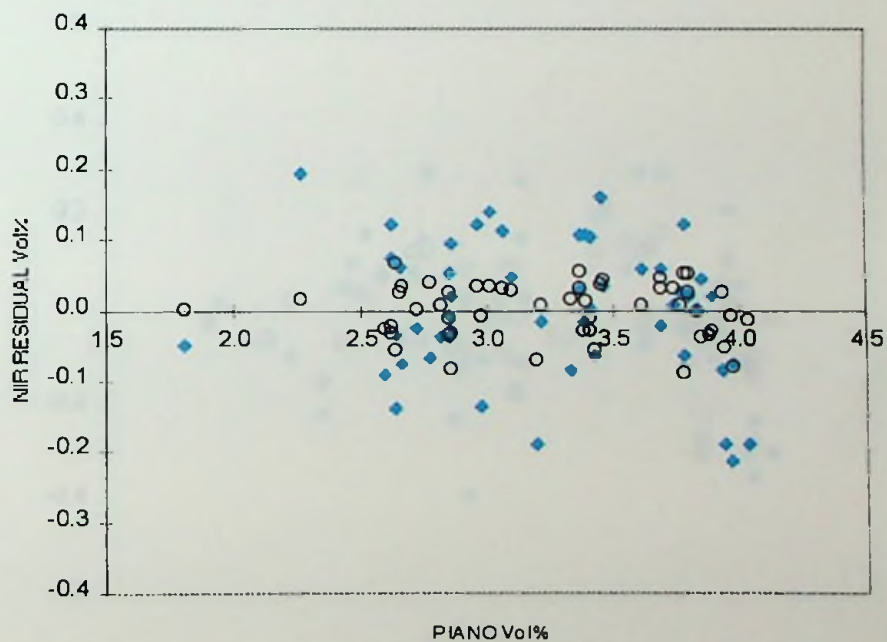
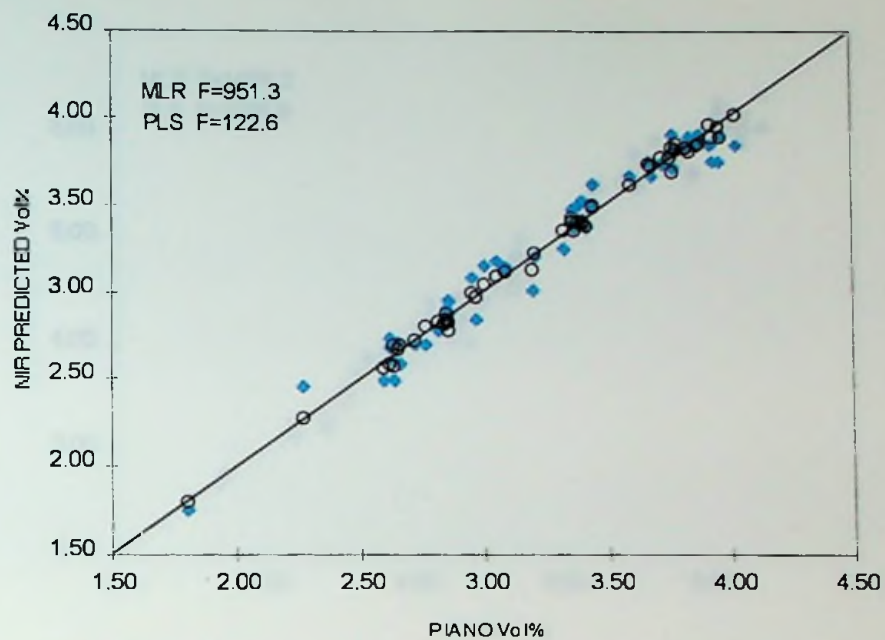


Figure 16. (top) PIANO vs. NIR Predictions for *p*-Xylene in the Original Calibration Set by MLR and PLS. (bottom) NIR Residuals for *p*-Xylene in the Original Calibration Set by MLR and PLS. The blue diamonds represent the MLR data, and the black circles represent the PLS data.

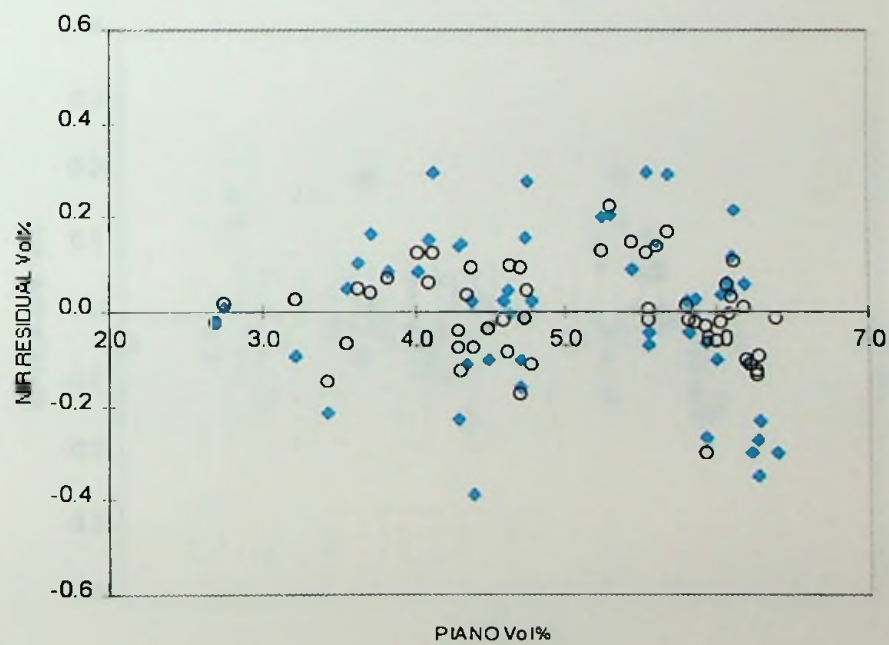
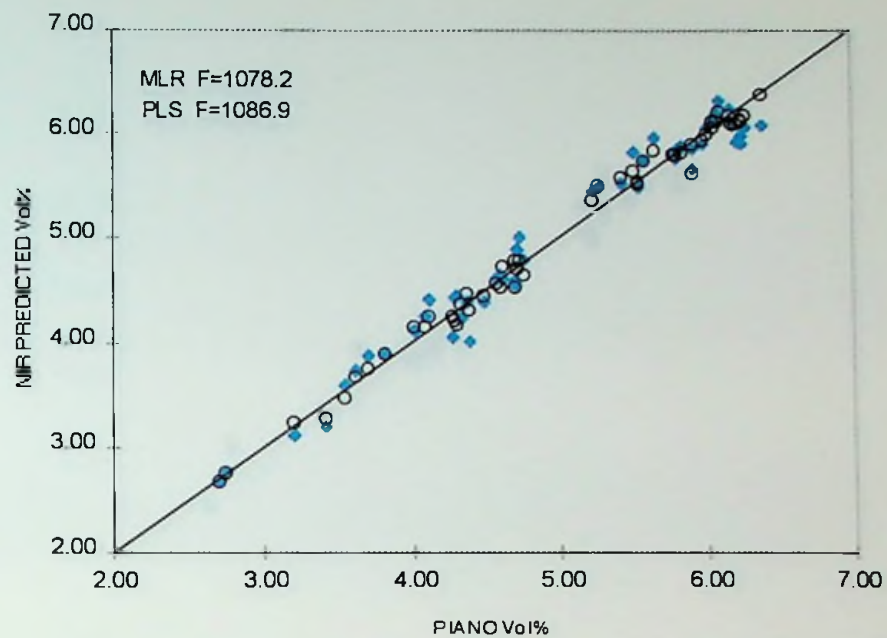


Figure 17. (top) PIANO vs. NIR Predictions for *o*-Xylene in the Original Calibration Set by MLR and PLS. (bottom) NIR Residuals for *o*-Xylene in the Original Calibration Set by MLR and PLS. The blue diamonds represent the MLR data, and the black circles represent the PLS data.

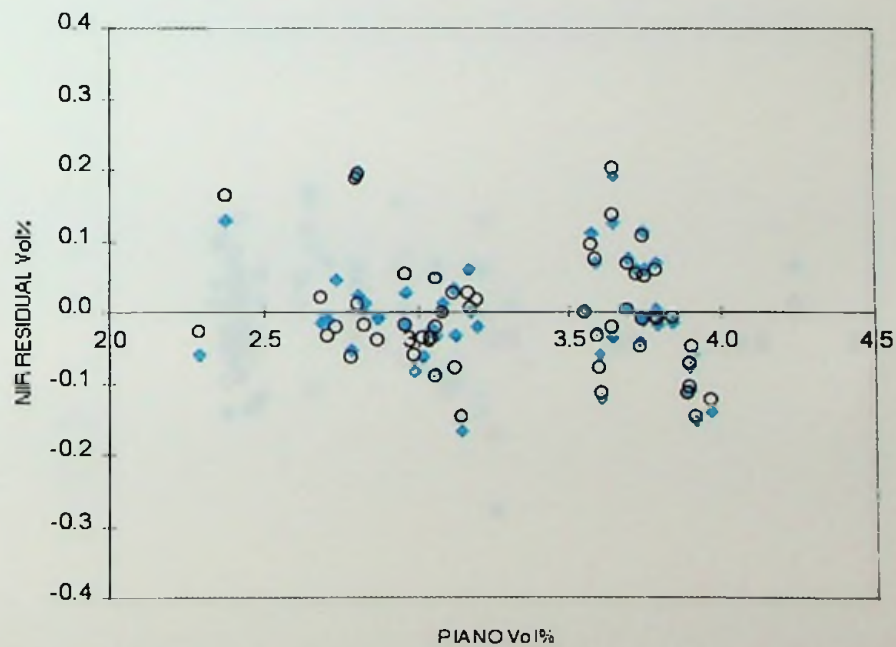
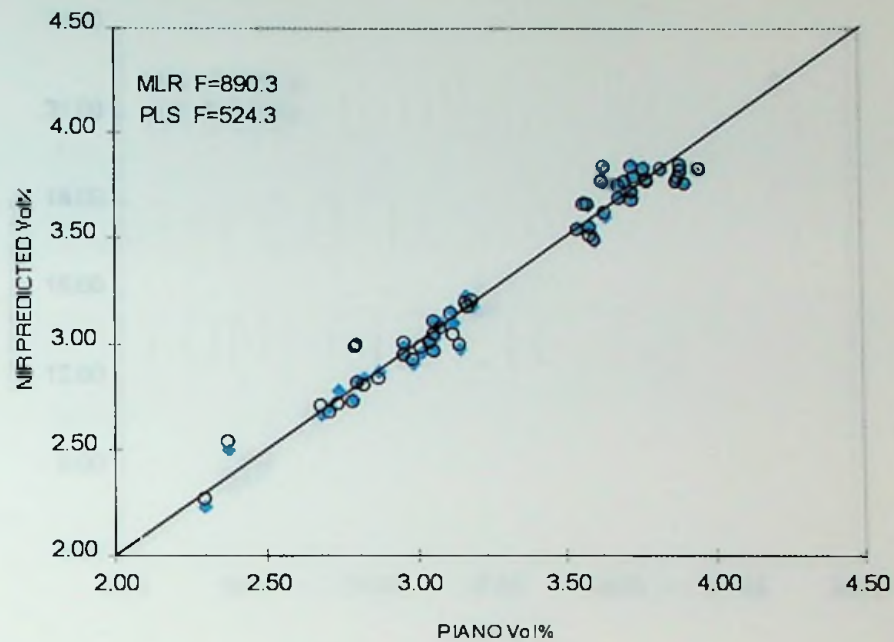


Figure 18. (top) PIANO vs. NIR Predictions for Ethylbenzene in the Original Calibration Set by MLR and PLS. (bottom) NIR Residuals for Ethylbenzene in the Original Calibration Set by MLR and PLS. The blue diamonds represent the MLR data, and the black circles represent the PLS data.

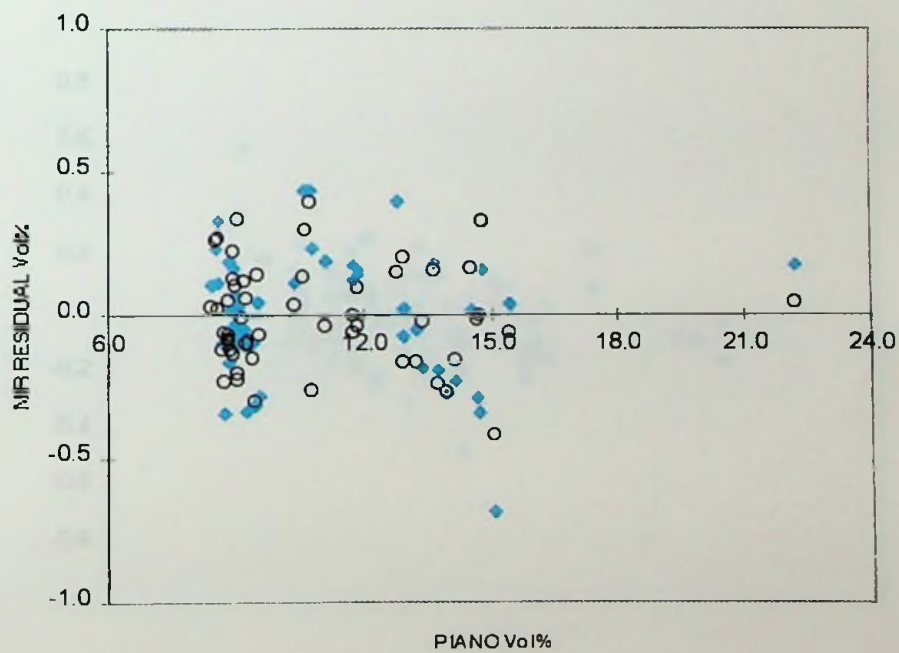
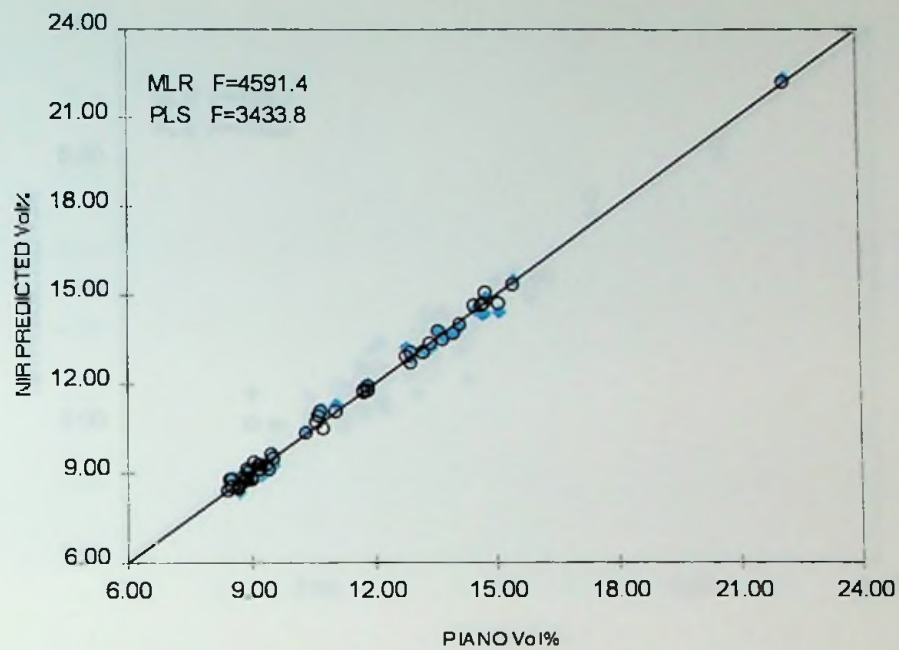


Figure 19. (top) PIANO vs. NIR Predictions for Total Paraffins in the Original Calibration Set by MLR and PLS. (bottom) NIR Residuals for Total Paraffins in the Original Calibration Set by MLR and PLS. The blue diamonds represent the MLR data, and the black circles represent the PLS data.

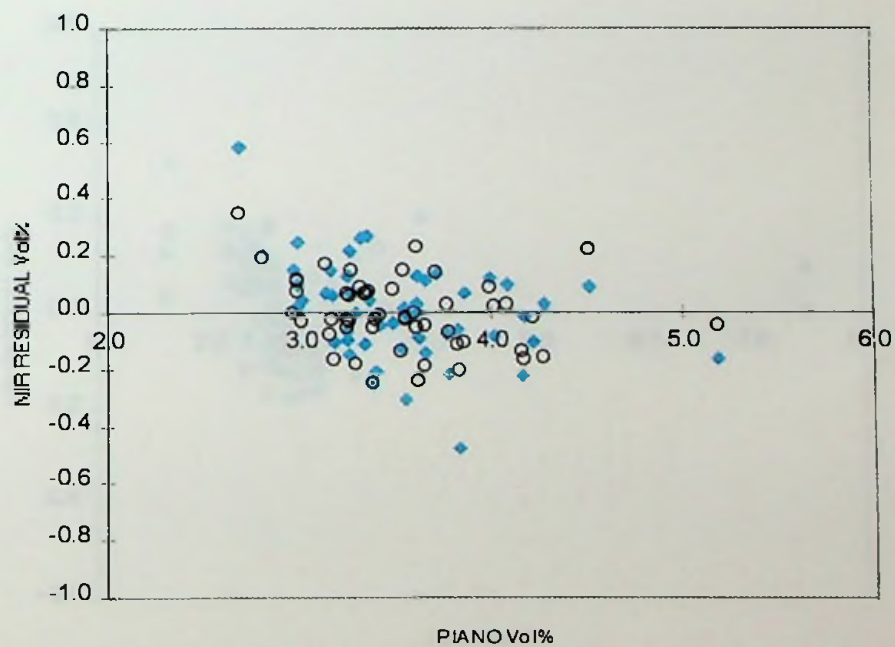
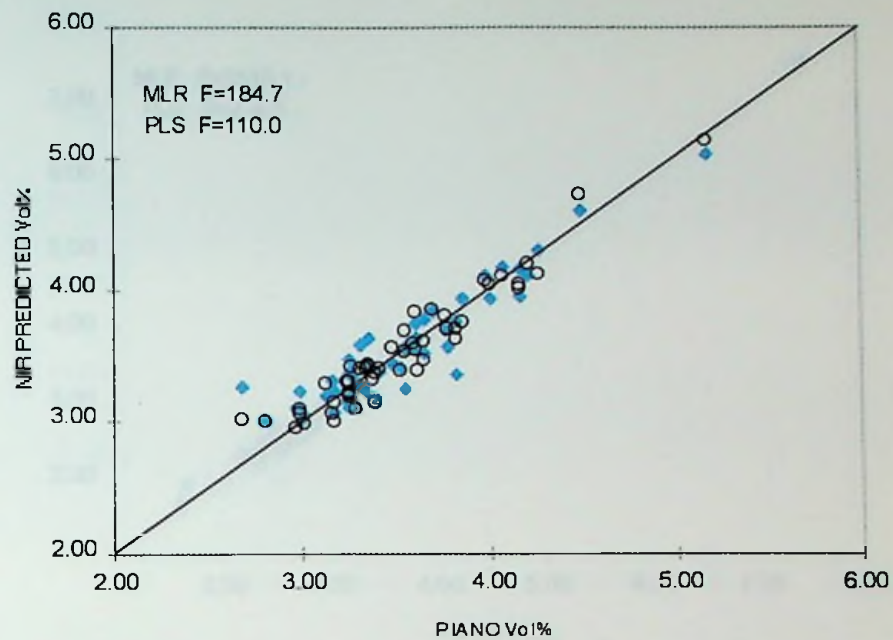


Figure 20. (top) PIANO vs. NIR Predictions for *n*-Hexane in the Original Calibration Set by MLR and PLS. (bottom) NIR Residuals for *n*-Hexane in the Original Calibration Set by MLR and PLS. The blue diamonds represent the MLR data, and the black circles represent the PLS data.

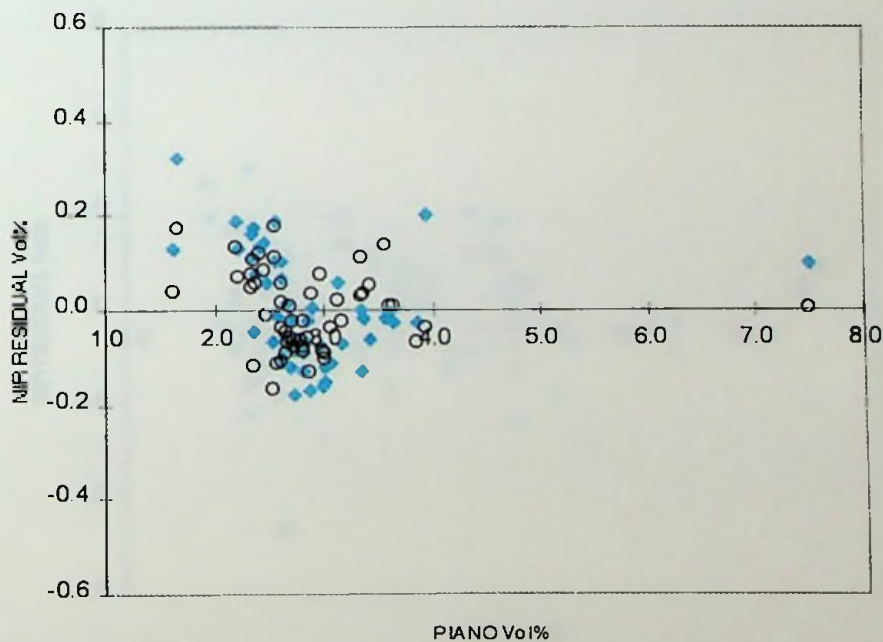
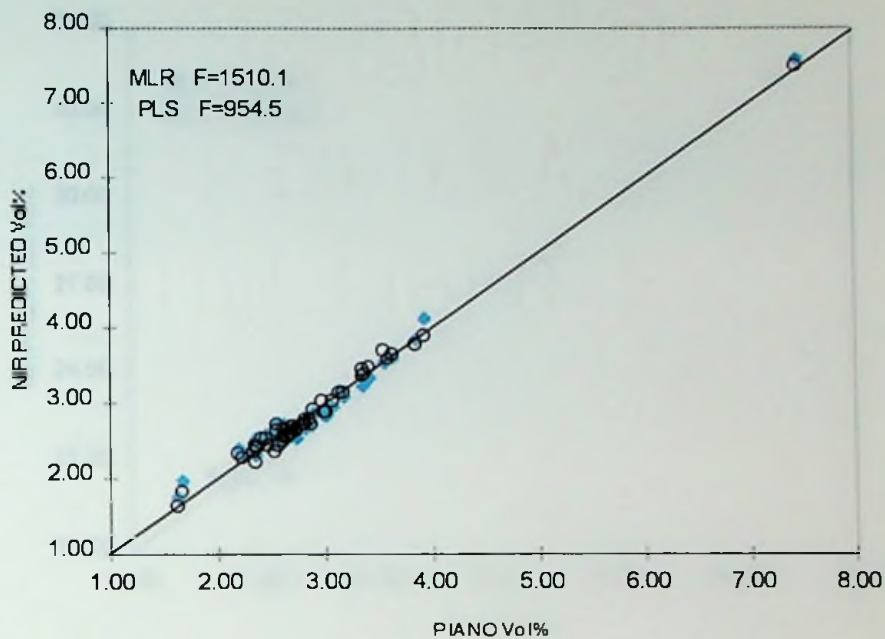


Figure 21. (top) PIANO vs. NIR Predictions for *n*-Heptane in the Original Calibration Set by MLR and PLS. (bottom) NIR Residuals for *n*-Heptane in the Original Calibration Set by MLR and PLS. The blue diamonds represent the MLR data, and the black circles represent the PLS data.

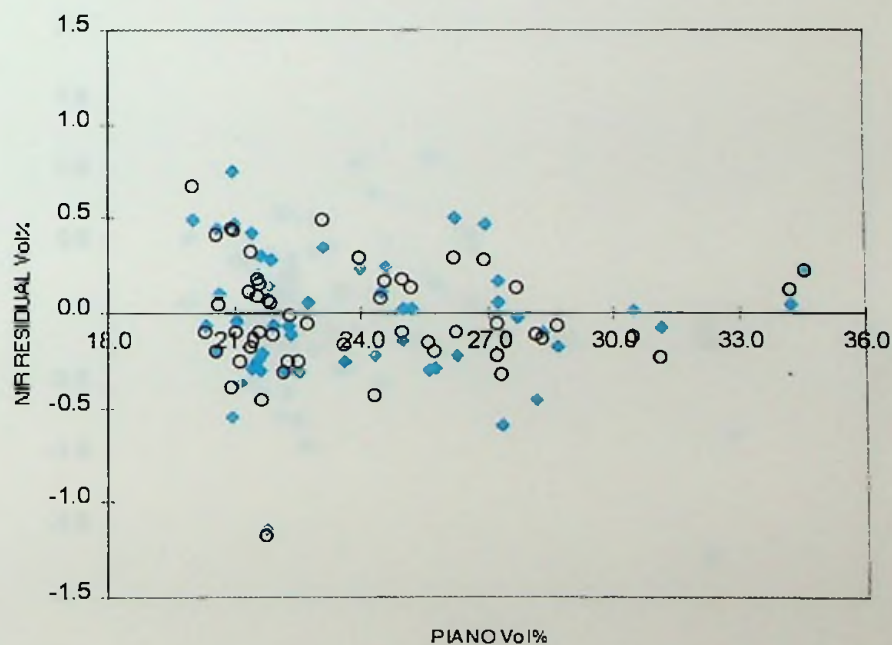
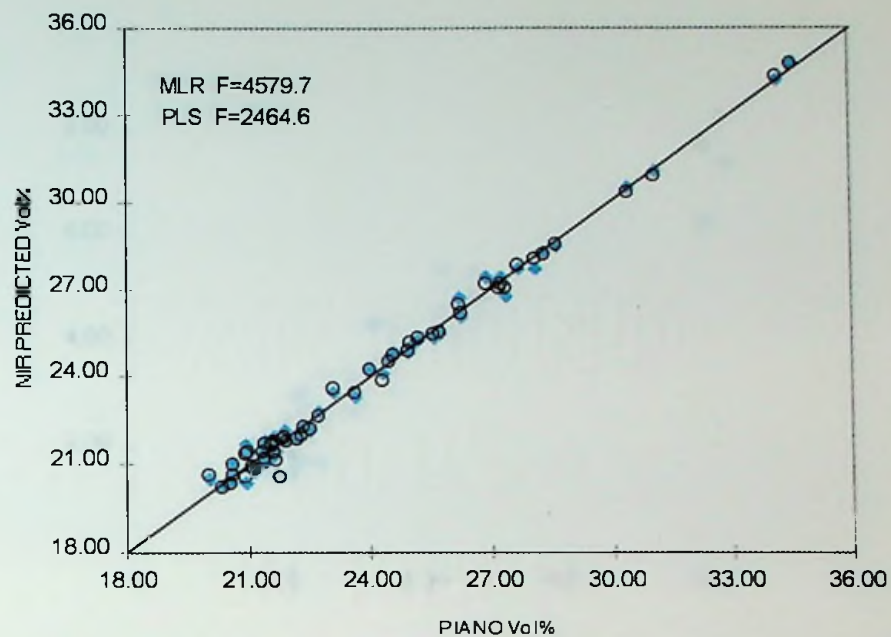


Figure 22. (top) PIANO vs. NIR Predictions for Isoparaffins in the Original Calibration Set by MLR and PLS. (bottom) NIR Residuals for Isoparaffins in the Original Calibration Set by MLR and PLS. The blue diamonds represent the MLR data, and the black circles represent the PLS data.

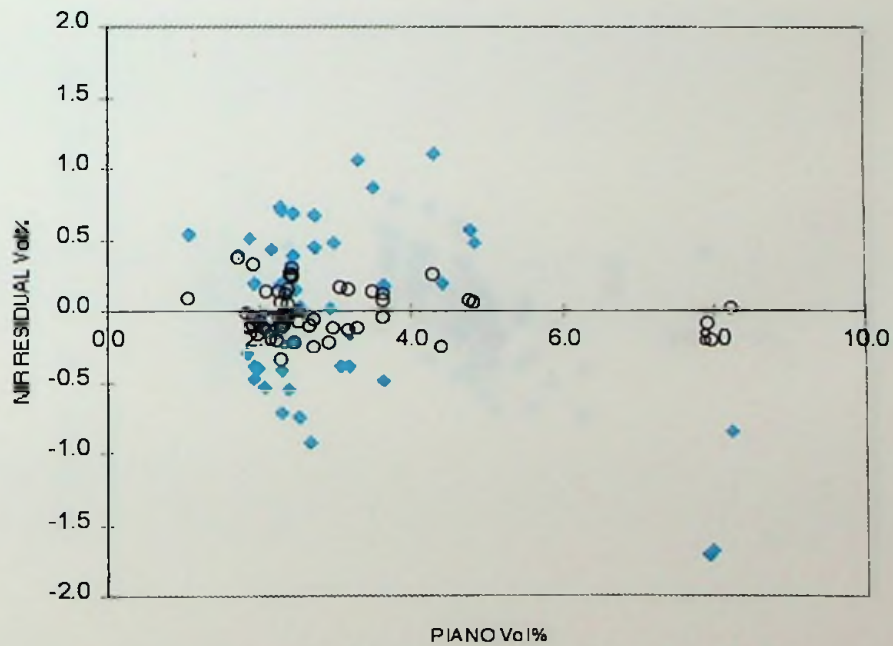
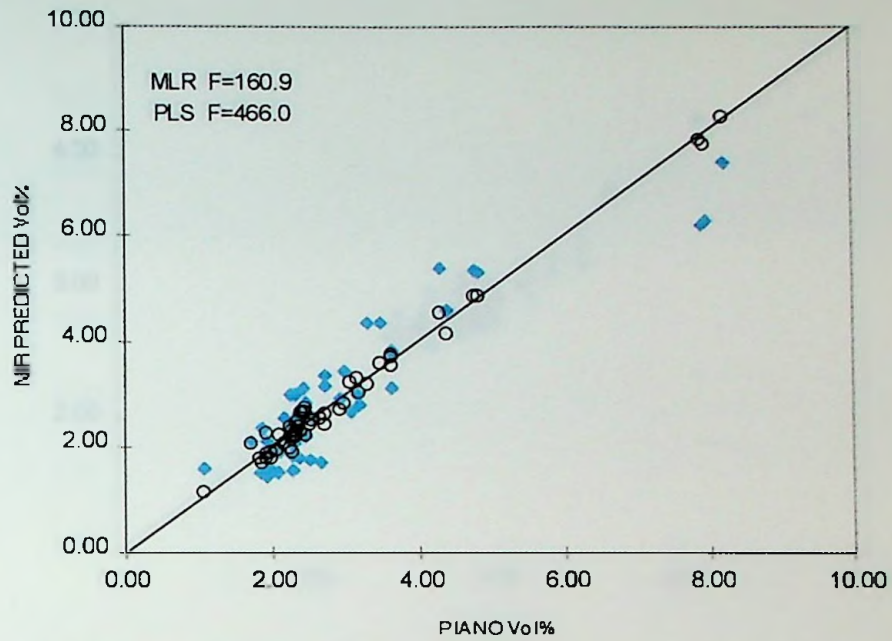


Figure 23. (top) PIANO vs. NIR Predictions for Isopentane in the Original Calibration Set by MLR and PLS. (bottom) NIR Residuals for Isopentane in the Original Calibration Set by MLR and PLS. The blue diamonds represent the MLR data, and the black circles represent the PLS data.

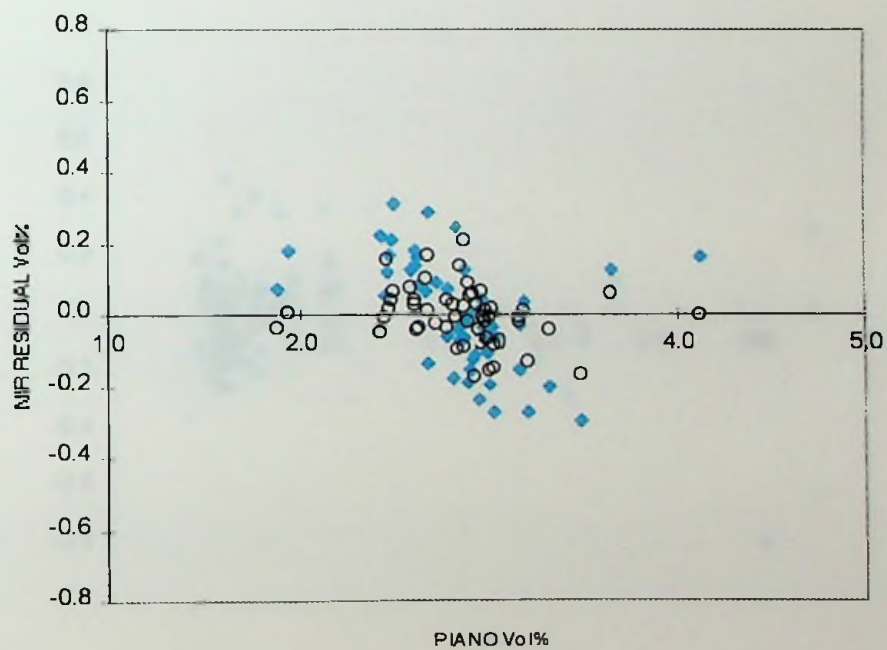
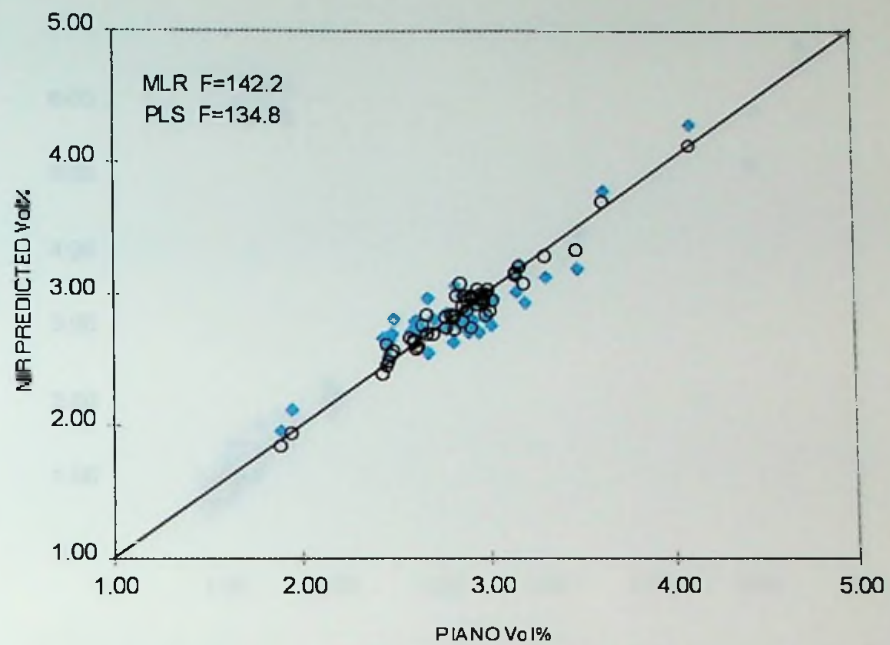


Figure 24. (top) PIANO vs. NIR Predictions for 2-Methylhexane in the Original Calibration Set by MLR and PLS. (bottom) NIR Residuals for 2-Methylhexane in the Original Calibration Set by MLR and PLS. The blue diamonds represent the MLR data, and the black circles represent the PLS data.

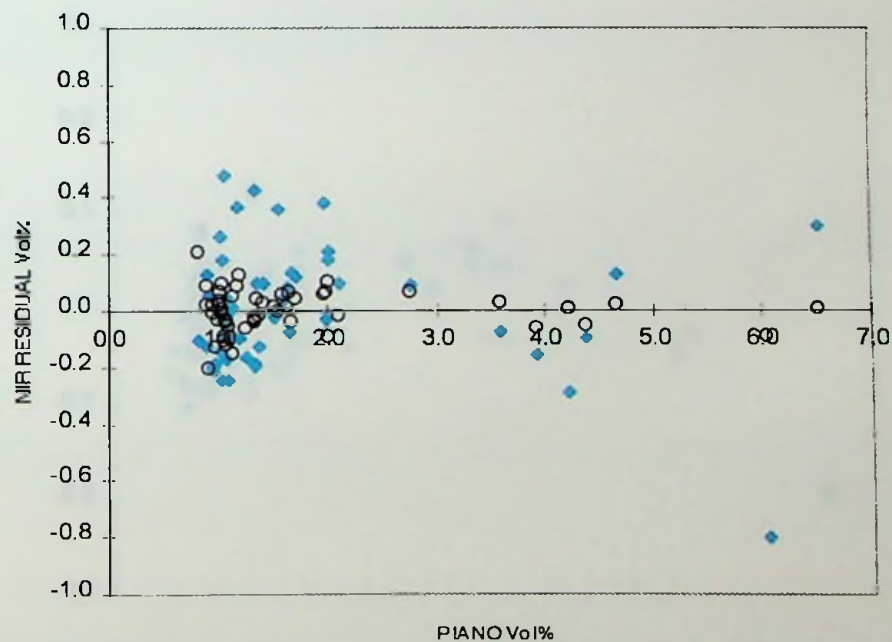
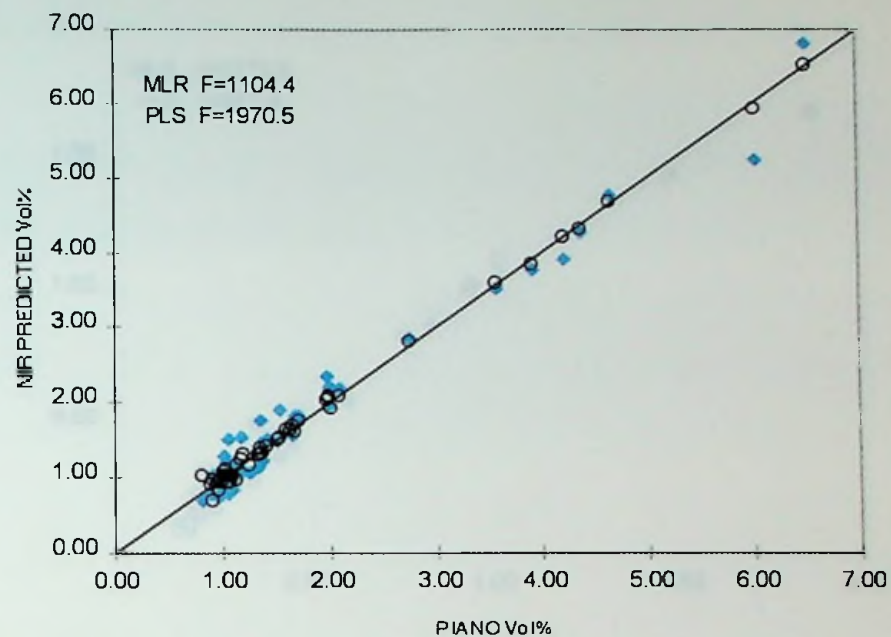


Figure 25. (top) PIANO vs. NIR Predictions for Naphthenes in the Original Calibration Set by MLR and PLS. (bottom) NIR Residuals for Naphthenes in the Original Calibration Set by MLR and PLS. The blue diamonds represent the MLR data, and the black circles represent the PLS data.

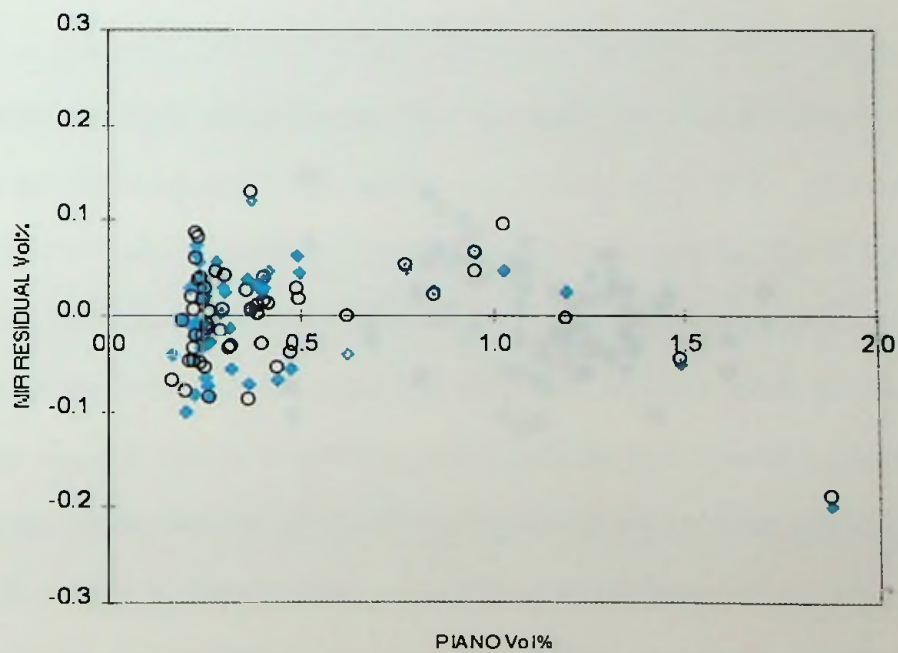
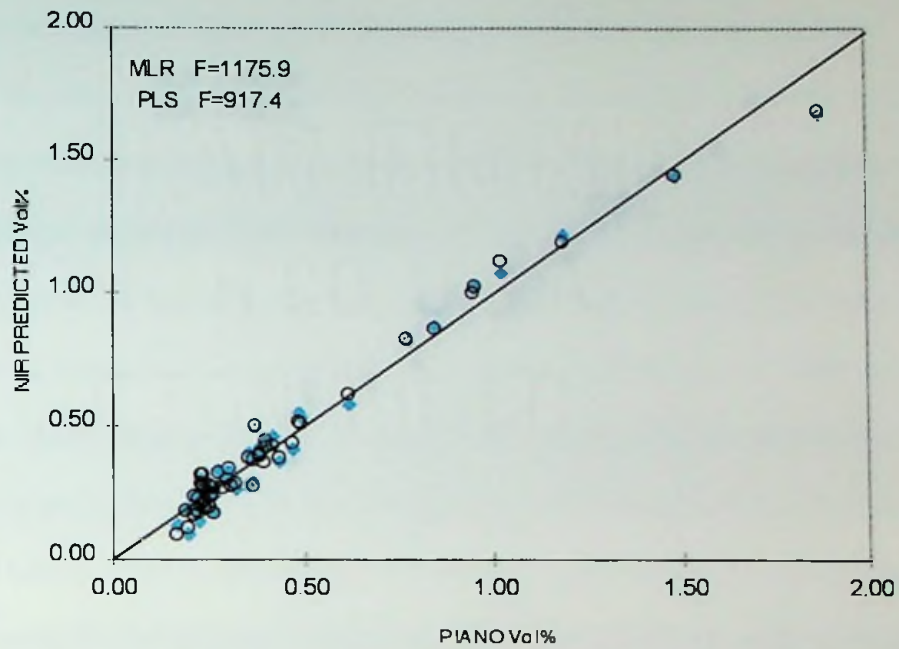


Figure 26. (top) PIANO vs. NIR Predictions for Methylcyclopentane in the Original Calibration Set by MLR and PLS. (bottom) NIR Residuals for Methylcyclopentane in the Original Calibration Set by MLR and PLS. The blue diamonds represent the MLR data, and the black circles represent the PLS data.

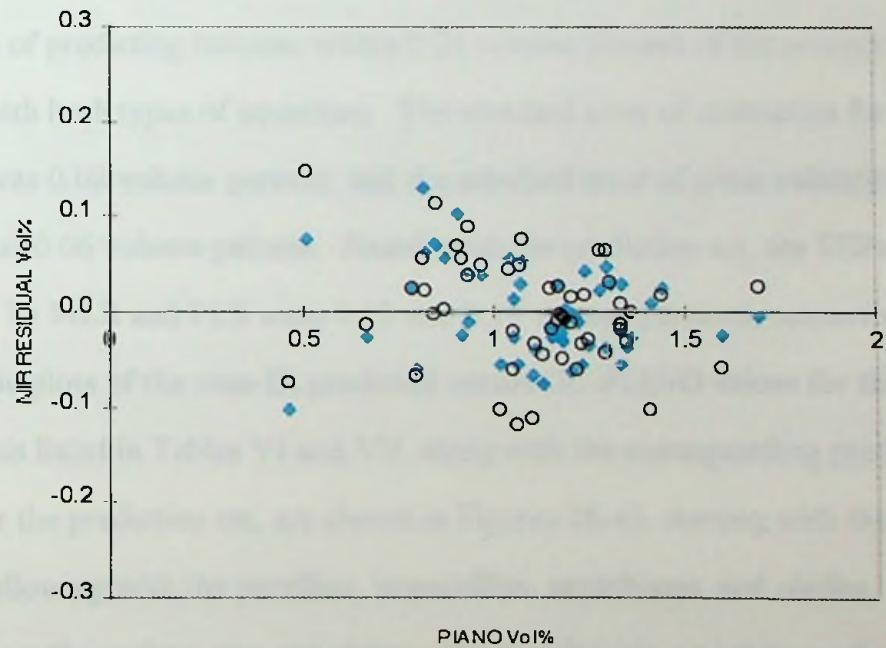
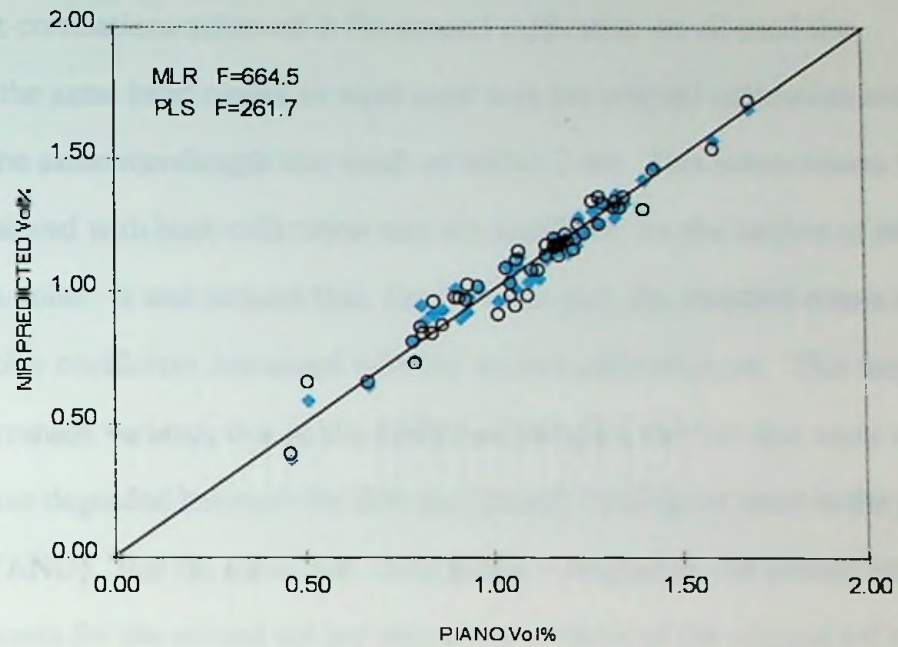


Figure 27. (top) PIANO vs. NIR Predictions for Total Olefins in the Original Calibration Set by MLR and PLS. (bottom) NIR Residuals for Total Olefins in the Original Calibration Set by MLR and PLS. The blue diamonds represent the MLR data, and the black circles represent the PLS data.

The best correlations achieved in the second calibration set all used the wavelengths in the same band ranges as were used with the original calibration set. For the most part, the same wavelength was used or within 2 nm. This substantiates that the correlations achieved with both calibration sets are significant for the analyte of interest and not random noise. It was noticed that, for the most part, the standard errors increased and the correlation coefficient decreased with the second calibration set. This may be attributed to increased variance due to the additional samples, the fact that some of the samples may have degraded between the first and second running, or error in the primary method (GC-PIANO). For the most part, this change is negligible. Of greater importance is that the constants for the second set are very close to those of the original set in the MLR equations. The MLR and PLS results for the second calibration set are listed in Tables VI and VII, respectively.

The goal of predicting benzene within 0.21 volume percent of the primary method was again met with both types of equations. The standard error of calibration for the MLR equation was 0.08 volume percent, and the standard error of cross validation for the PLS equation was 0.06 volume percent. Based upon the prediction set, the SEPs for benzene content by MLR and PLS were 0.12 and 0.10 volume percents, respectively.

Schematic plots of the near-IR predicted versus GC-PIANO values for the calibration models listed in Tables VI and VII, along with the corresponding predicted and residuals plot for the prediction set, are shown in Figures 28-45, starting with the aromatics and following with the paraffins, isoparaffins, naphthenes, and olefins, respectively. From these plots, one can observe the correlations, and their performance with samples not in the calibration set.

The standard errors of calibration for total aromatics are slightly higher for both the MLR and PLS models in the second calibration set compared to the original calibration set. In Figure 28 (top), the evidence of the linearity is clear, as observed in the original calibration set. When using the equations to determine the total aromatics in the

Table VI. MLR results for the second calibration set.

Compound	Volume % Range	Constants				Wavelengths (nm)			NIR STD	
		k(0)	k(1)	k(2)	k(3)	1	2	3	R	ERROR (Vol%)
Total Aromatics	35.9 - 68.3	75.966	88.065	68.748	-96.629	1834 v(CH ₂)	1622 v(Ar-H)	1234 v(CH ₂), v(CH)	0.998	0.48
Benzene	1.79 - 5.73	22.075	-19.167	-74.299	17.596	2128 v(Ar-H)	1622 v(Ar-H)	1832 v(CH ₂)	0.994	0.08
Toluene	8.77 - 16.2	11.906	-39.118	86.410	-144.518	1650 v(Ar-H)	1796 v(CH ₂)	1224 v(CH)	0.989	0.24
Total Xylenes	8.51 - 20.0	-125.538	1162.151	63.009	488.014	1458 v(CH ₂)	2028 v(CH ₃)	1622 v(Ar-H)	0.975	0.59
<i>m</i> -Xylene	4.01 - 9.57	19.287	-42.438	-473.032	-173.995	1652 v(Ar-H)	1502 v(CH ₂)	1404 v(CH ₃)	0.970	0.30
<i>p</i> -Xylene	1.80 - 4.03	10.592	30.348	101.189	-17.774	1204 v(CH ₂)	1356 v(CH ₃)	1646 v(Ar-H)	0.980	0.10
<i>o</i> -Xylene	2.70 - 6.39	12.332	-56.563	15.329	-59.610	2148 v(Ar-H)	1830 v(CH ₂)	1642 v(Ar-H)	0.976	0.21
Ethyl-Benzene	2.29 - 3.96	19.816	-16.797	-17.312	-24.271	1174 v(CH ₃)	1642 v(Ar-H)	1230 v(CH ₂), v(CH)	0.973	0.10
Olefins	0.464 - 1.70	2.861	122.816	29.866	101.53	1612 v(=CH)	1200 v(CH ₃)	1140 v(Ar-H)	0.947	0.08
Paraffins	6.65 - 22.4	-49.215	195.465	-133.584	264.535	1976 v(CH ₃)	2064 v(=CH)	1232 v(CH ₂), v(CH)	0.994	0.30
<i>n</i> -Hexane	1.28 - 5.19	7.969	-17.401	-29.303	-71.100	1844 v(CH ₂)	2022 v(CH ₃)	1624 v(Ar-H)	0.909	0.23
<i>n</i> -Heptane	1.61 - 7.48	29.617	21.102	67.157	114.337	1664 v(Ar-H)	1186 v(CH ₃)	1418 v(CH ₃)	0.975	0.17
Isoparaffins	19.2 - 34.6	102.703	-290.240	116.868	-192.888	2084 v(=CH)	1936 v(CH ₃)	1230 v(CH ₂), v(CH)	0.990	0.48
Isopentane	1.06 - 8.25	-55.845	284.816	127.845	-306.955	1970 v(CH ₃)	2114 v(Ar-H)	1460 v(CH ₂)	0.876	0.71
2-Methylhexane	1.88 - 4.12	49.710	-31.151	-56.069	-84.683	1804 v(CH ₂)	1600 v(=CH)	1240 v(CH ₂)	0.803	0.21
Naphthenes	0.811 - 6.51	-21.232	261.987	759.142	64.960	1368 v(CH ₃)	1292 v(CH ₃)	1802 v(CH ₂)	0.985	0.21
Methylcyclopentane	0.165 - 1.88	-0.081	-40.481	97.619	-47.259	1192 v(CH ₃)	1374 v(CH ₃)	1234 v(CH ₂)	0.968	0.08

prediction set, the standard errors of prediction are slightly higher than 1.0 percent by volume (Figure 28, bottom). As predictors, both models appear to be similar. The standard errors of predictions observed imply that the near-IR models are better than the traditional methods.

In Figure 29 (top), the correlations between the GC-PIANO values for benzene and the near-IR predicted benzene by MLR and PLS are given. It is evident that both models are again linear. The PLS results for the prediction set have for the most part smaller residuals than the MLR results, but one of the PLS residuals is larger than any of the

Table VII. PLS results for the second calibration set.

Compound	Volume %		Wavelength Range (nm)	Factors	R	NIR STD
	Range					ERROR (Vol%)
Total Aromatics	35.9 - 68.0		1214 - 1260 ; 1600 - 1670 ; 1780 - 1858 v(CH), v(CH ₂); v(=CH), v(Ar-H); v(CH ₂)	3	0.997	0.58
Benzene	1.79 - 5.73		1132 - 1260 ; 1600 - 1670 ; 1780 - 1858 ; 2100 - 2160 v(Ar-H), v(CH ₃), v(CH), v(CH ₂); v(Ar-H); v(CH ₂); v(Ar-H)	8	0.994	0.08
Toluene	8.77 - 16.2		1214 - 1230 ; 1600 - 1670 ; 1780 - 1858 ; 2000 - 2160 v(CH), v(Ar-H), v(CH ₂); v(CH ₃), v(=CH), v(Ar-H)	8	0.998	0.12
Total Xylenes	8.51 - 20.0		1132 - 1214 ; 1320 - 1530 ; 1600 - 1670 ; 2000 - 2040 v(Ar-H), v(CH ₃), v(CH ₂), v(=CH), v(Ar-H), v(CH ₃)	13	0.998	0.18
<i>m</i> -Xylene	4.01 - 9.57		1320 - 1430 ; 1480 - 1530 ; 1600 - 1670 ; 2000 - 2040 v(CH ₂), v(CH ₂), v(=CH), v(Ar-H), v(CH ₂)	9	0.995	0.13
<i>p</i> -Xylene	1.80 - 4.03		1156 - 1214 ; 1320 - 1430 ; 1600 - 1670 ; 2000 - 2040 v(CH ₂), v(CH ₃), v(=CH), v(Ar-H), v(CH ₃)	14	0.997	0.04
<i>o</i> -Xylene	2.70 - 6.39		1600 - 1670 ; 1780 - 1858 ; 2000 - 2040 ; 2100 - 2160 v(=CH), v(Ar-H), v(CH ₂), v(CH ₃), v(Ar-H)	9	0.995	0.10
Ethyl-Benzene	2.29 - 3.96		1156 - 1264 ; 1600 - 1670 v(CH ₂), v(CH), v(CH ₂), v(=CH), v(Ar-H)	12	0.992	0.06
Olefins	0.464 - 1.70		1132 - 1214 ; 1600 - 1670 v(Ar-H), v(CH ₃), v(=CH), v(Ar-H)	8	0.965	0.07
Paraffins	6.65 - 22.4		1214 - 1264 ; 1940 - 2100 v(CH), v(CH ₂), v(CH ₃), v(=CH)	9	0.999	0.14
<i>n</i> -Hexane	1.28 - 5.19		1436 - 1480 ; 1780 - 1858 v(CH ₂), v(CH ₂)	9	0.944	0.19
<i>n</i> -Heptane	1.61 - 7.48		1156 - 1214 ; 1320 - 1480 ; 1600 - 1670 v(CH ₂), v(CH ₃), v(CH ₂), v(=CH), v(Ar-H)	6	0.988	0.12
Isoparaffins	19.2 - 34.57		1214 - 1264 ; 1920 - 2100 v(CH), v(CH ₂), v(CH ₃)	5	0.990	0.50
Isopentane	1.06 - 8.25		1430 - 1500 ; 1940 - 2040 ; 2100 - 2160 v(CH ₂), v(CH ₃), v(Ar-H)	10	0.981	0.30
2-Methylhexane	1.88 - 4.12		1214 - 1256 ; 1560 - 1626 ; 1780 - 1850 v(CH), v(CH ₂), v(=CH), v(CH ₂)	11	0.950	0.12
Naphthenes	0.81 - 6.51		1264 - 1430 ; 1780 - 1858 v(CH ₂), v(CH ₂), v(CH ₂)	13	0.999	0.05
Methylcyclopentane	0.165 - 1.88		1156 - 1260 ; 1320 - 1430 v(CH ₃), v(CH), v(CH ₂), v(CH ₃)	5	0.983	0.06

MLR residuals (Figure 29, bottom). Overall, both models perform similarly as predictors, with results similar to that of traditional methods.

For toluene, linearity is once again observed in both the MLR and PLS models (Figure 30, top). The PLS model is noticeably a better predictor, resulting in a standard error of prediction of 0.16 volume percent, compared to 0.32 volume percent for the MLR model (Figure 30, Bottom). Similar results, with the PLS model proving to be the better predictor, are observed for *m*-xylene, *o*-xylene, *n*-hexane, *n*-heptane, isopentane, total naphthenes, and methylcyclopentane (Figures 32, 34, 37, 38, 40, 42, and 43, respectively).

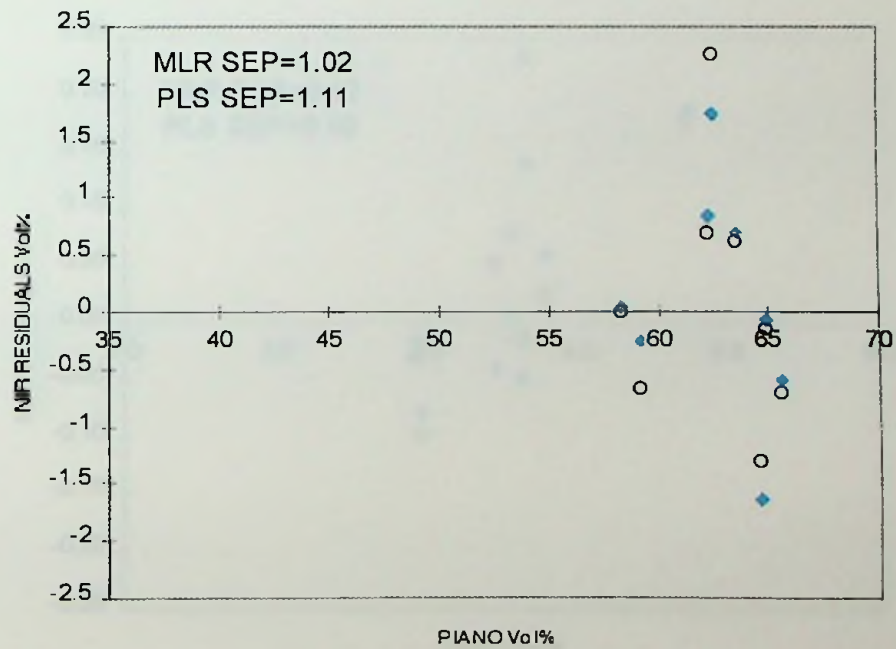
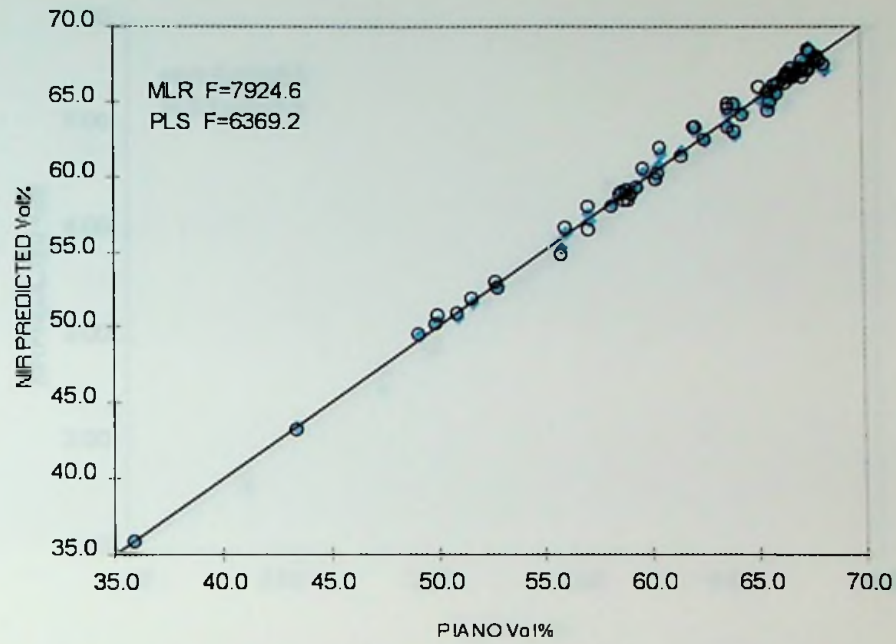


Figure 28. (top) PIANO vs. NIR Predictions for Total Aromatics in the Second Calibration Set by MLR and PLS. (bottom) PIANO vs. NIR Residuals for Total Aromatics in the Prediction Set by MLR and PLS. The blue diamonds represent the MLR data, and the black circles represent the PLS data.

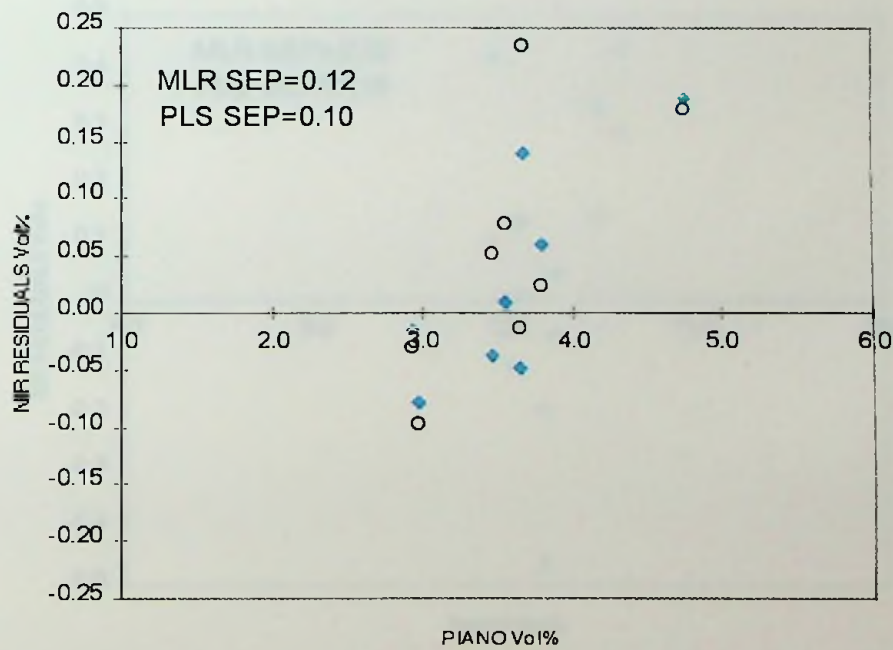
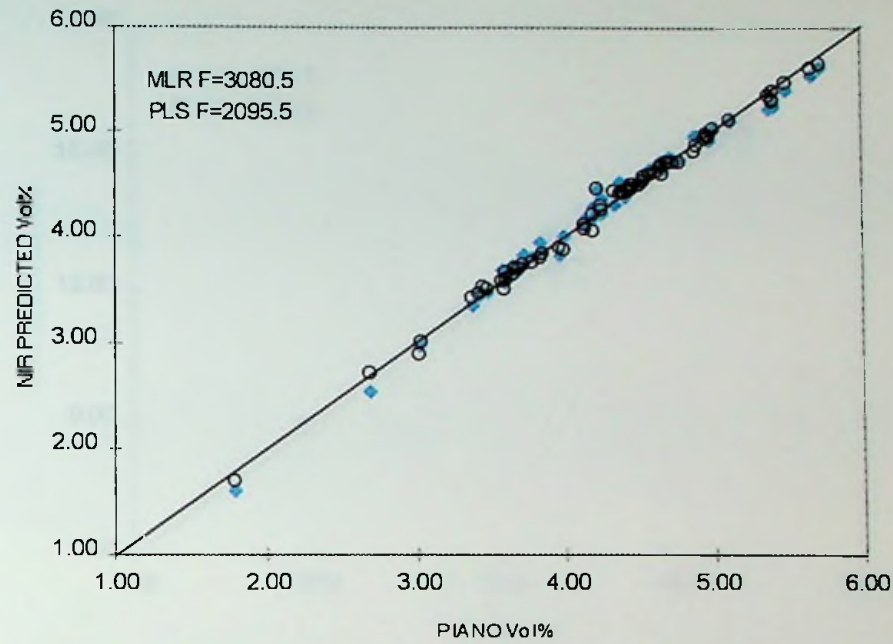


Figure 29. (top) PIANO vs. NIR Predictions for Benzene in the Second Calibration Set by MLR and PLS. (bottom) PIANO vs. NIR Residuals for Benzene in the Prediction Set by MLR and PLS. The blue diamonds represent the MLR data, and the black circles represent the PLS data.

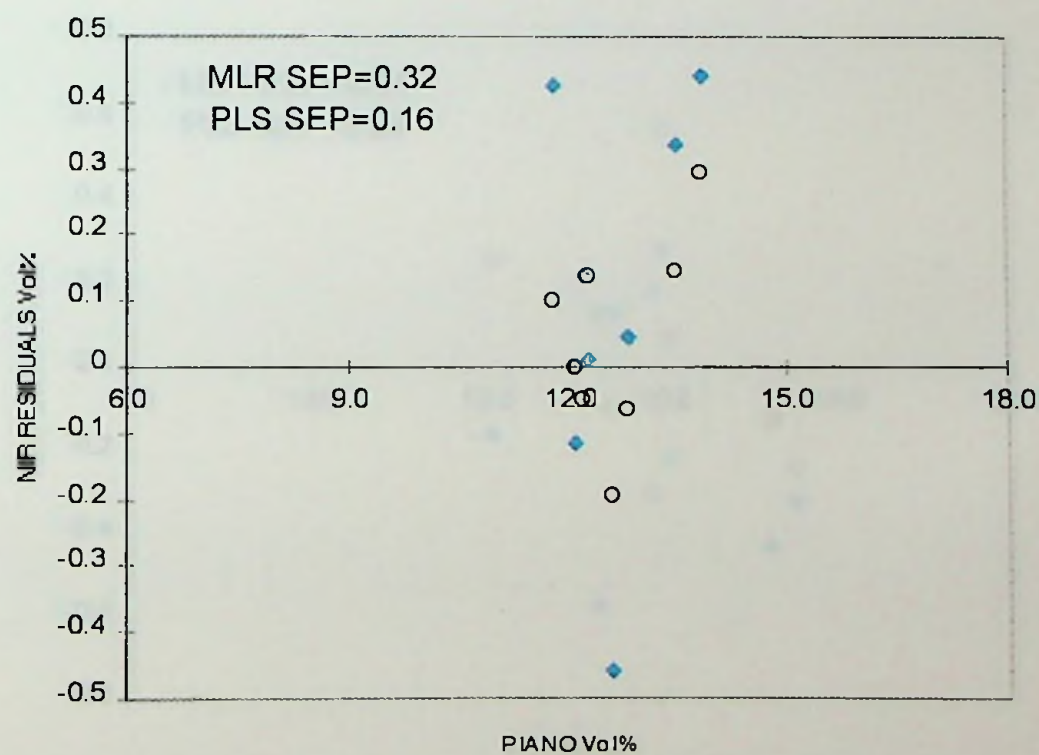
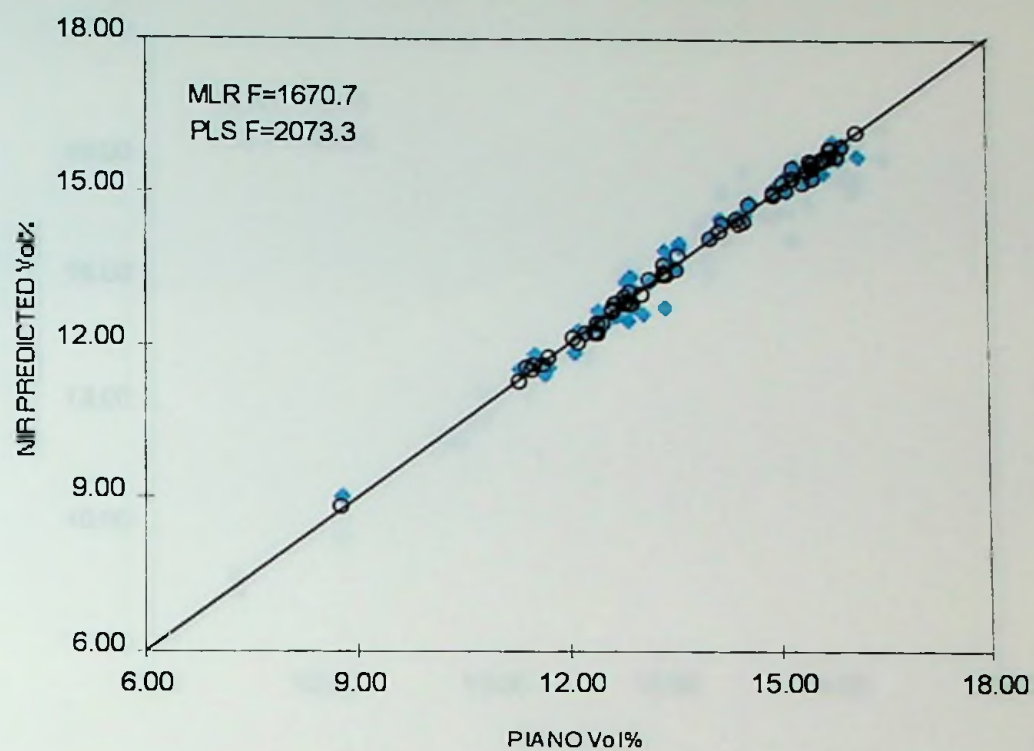


Figure 30. (top) PIANO vs. NIR Predictions for Toluene in the Second Calibration Set by MLR and PLS. (bottom) PIANO vs. NIR Residuals for Toluene in the Prediction Set by MLR and PLS. The blue diamonds represent the MLR data, and the black circles represent the PLS data.

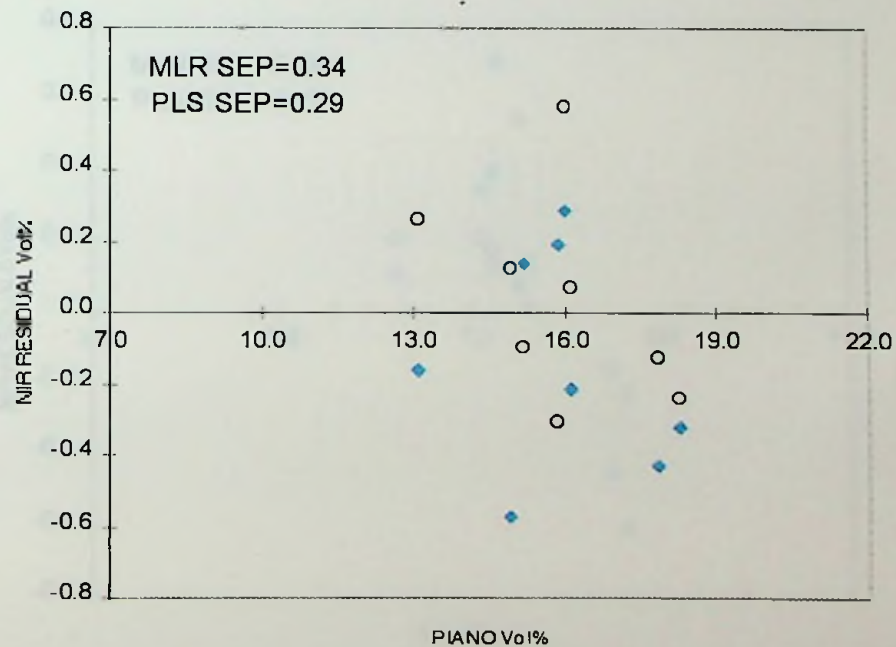
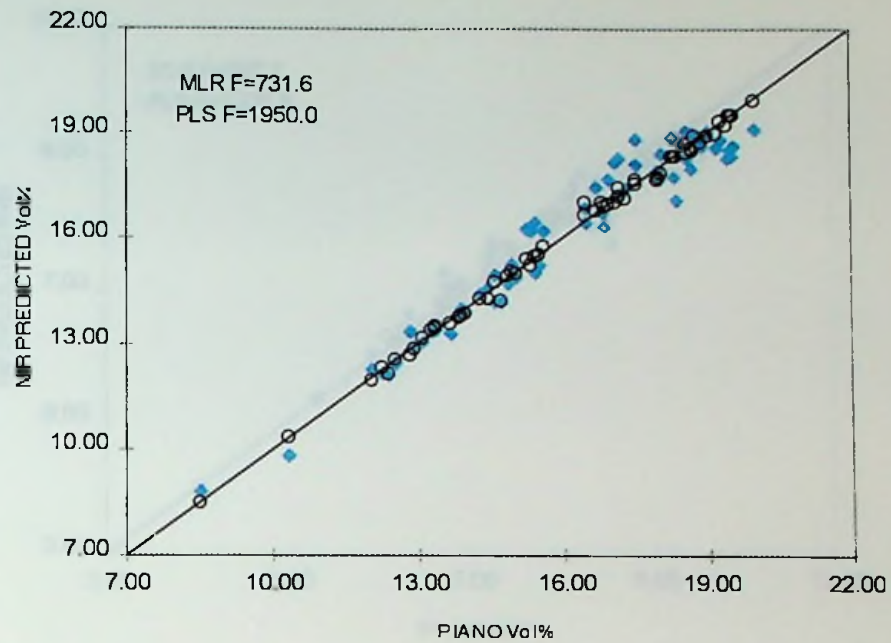


Figure 31. (top) PIANO vs. NIR Predictions for Total Xylenes in the Second Calibration Set by MLR and PLS. (bottom) PIANO vs. NIR Residuals for Total Xylenes in the Prediction Set by MLR and PLS. The blue diamonds represent the MLR data, and the black circles represent the PLS data.

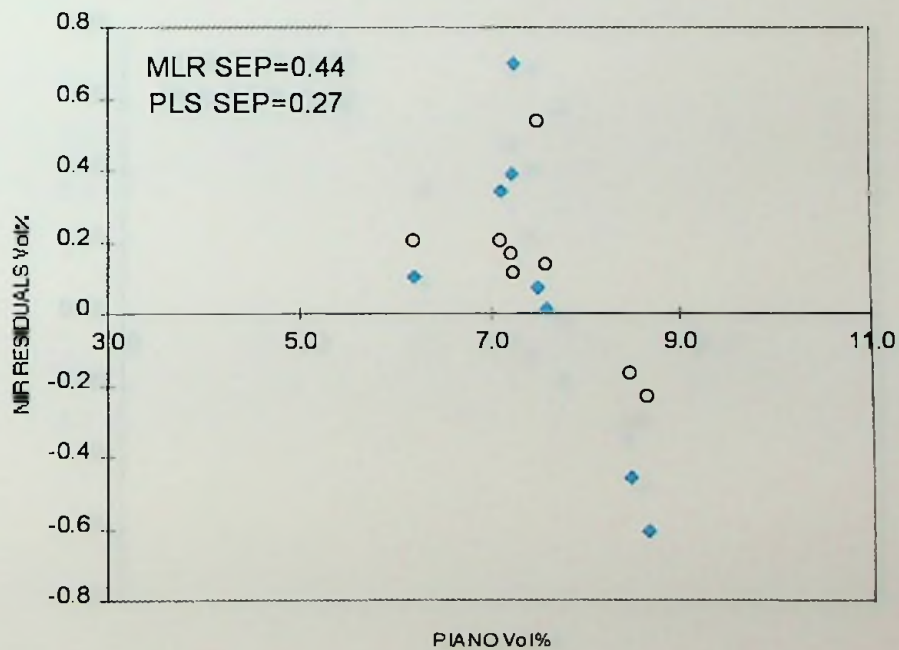
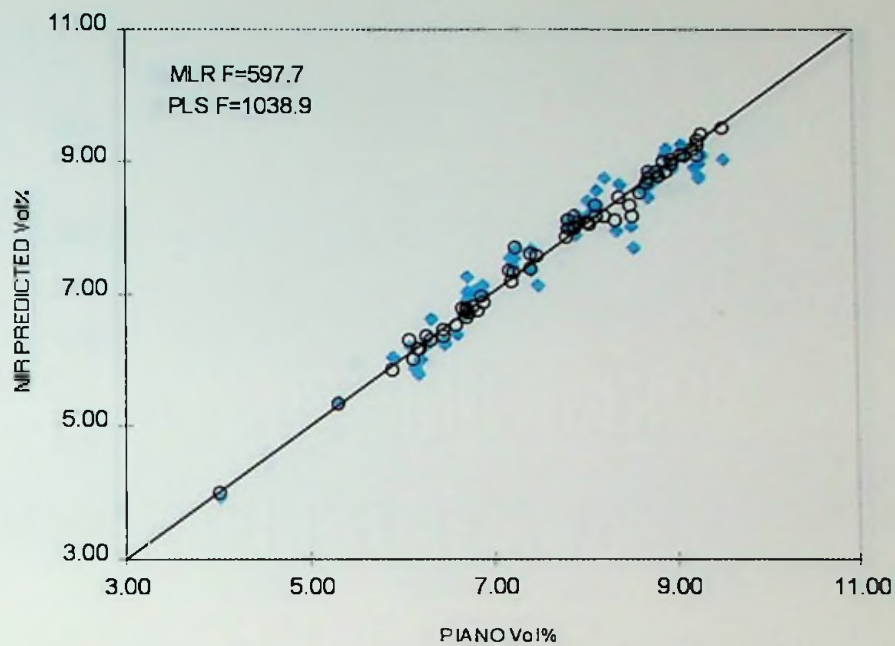


Figure 32. (top) PIANO vs. NIR Predictions for *m*-Xylene in the Second Calibration Set by MLR and PLS. (bottom) PIANO vs. NIR Residuals for *m*-Xylene in the Prediction Set by MLR and PLS. The blue diamonds represent the MLR data, and the black circles represent the PLS data.

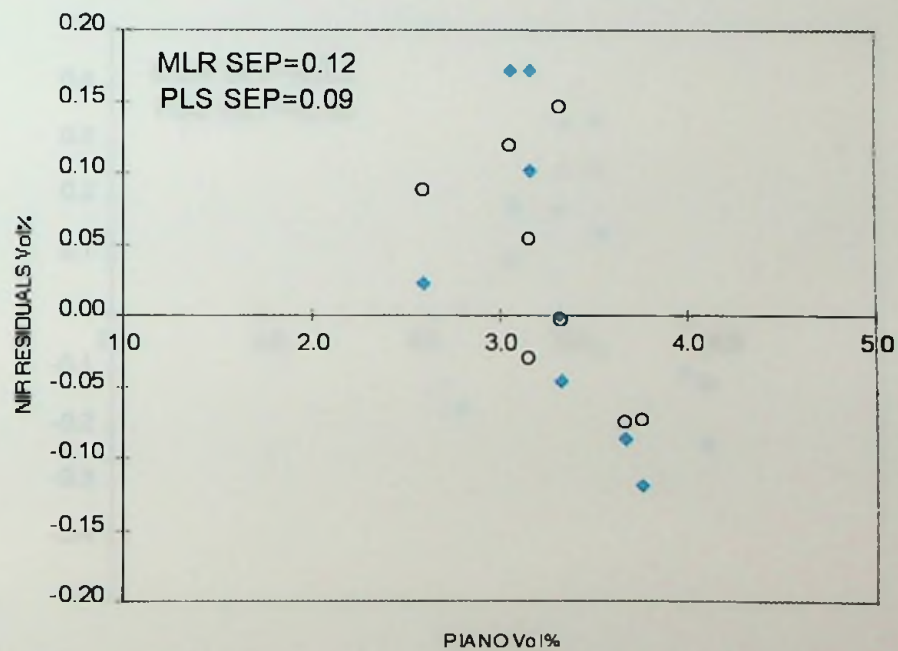
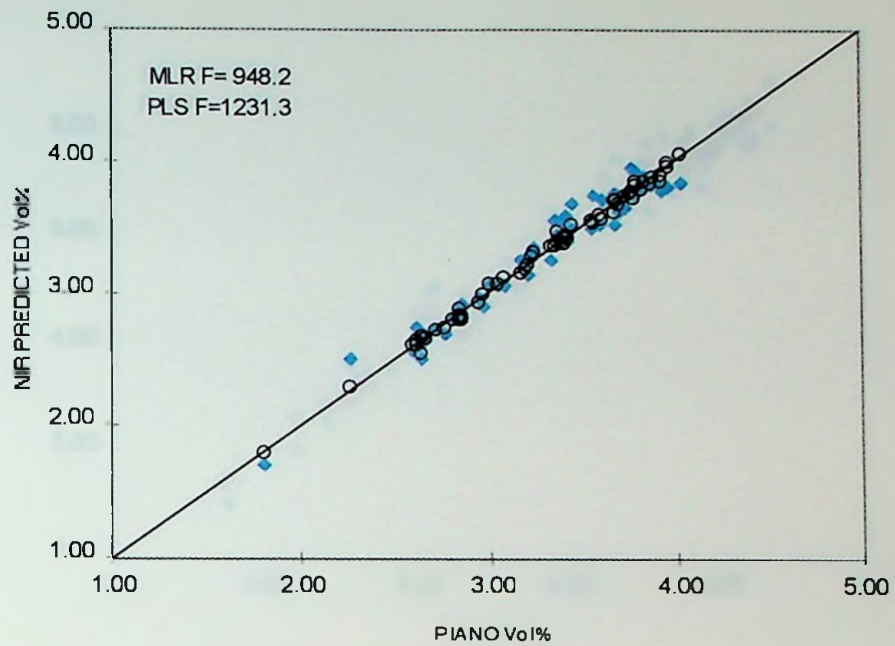


Figure 33. (top) PIANO vs. NIR Predictions for *p*-Xylene in the Second Calibration Set by MLR and PLS. (bottom) PIANO vs. NIR Residuals for *p*-Xylene in the Prediction Set by MLR and PLS. The blue diamonds represent the MLR data, and the black circles represent the PLS data.

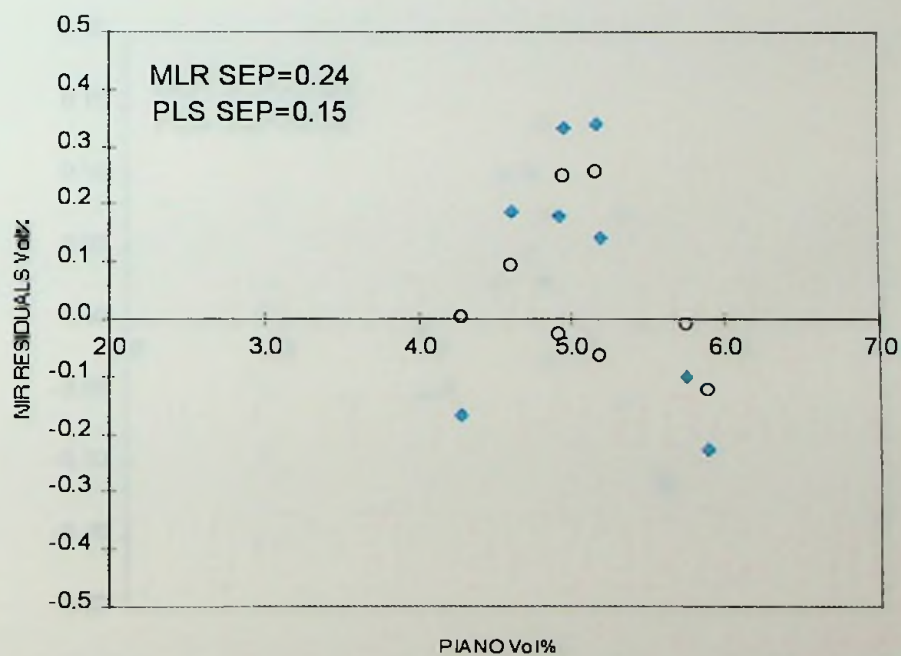
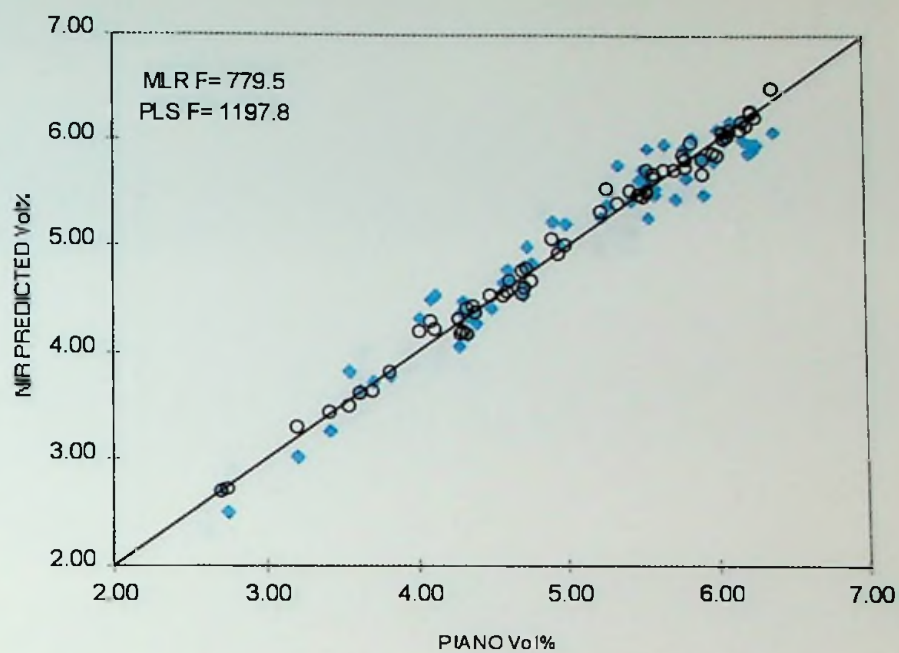


Figure 34. (top) PIANO vs. NIR Predictions for *o*-Xylene in the Second Calibration Set by MLR and PLS. (bottom) PIANO vs. NIR Residuals for *o*-Xylene in the Prediction Set by MLR and PLS. The blue diamonds represent the MLR data, and the black circles represent the PLS data.

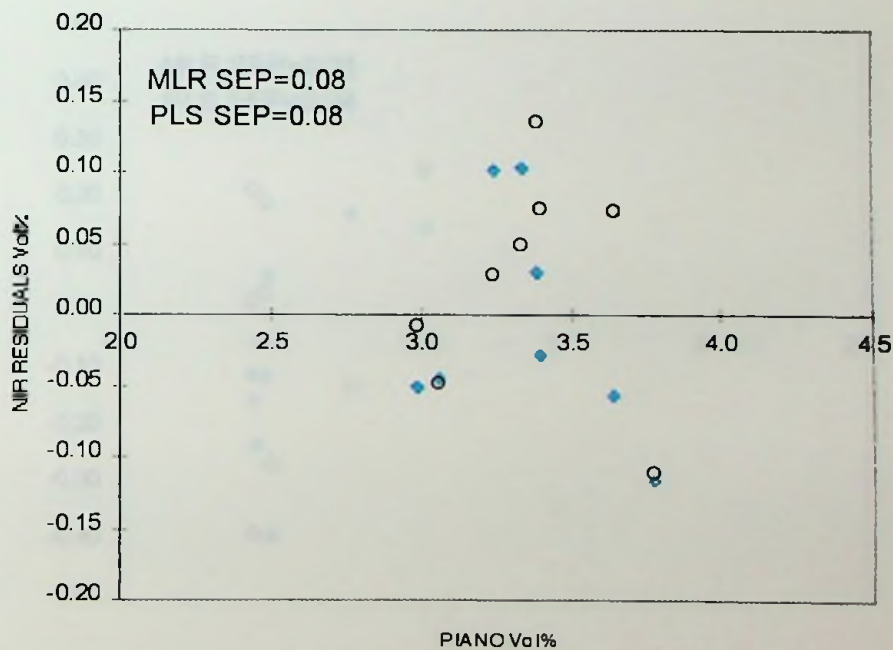
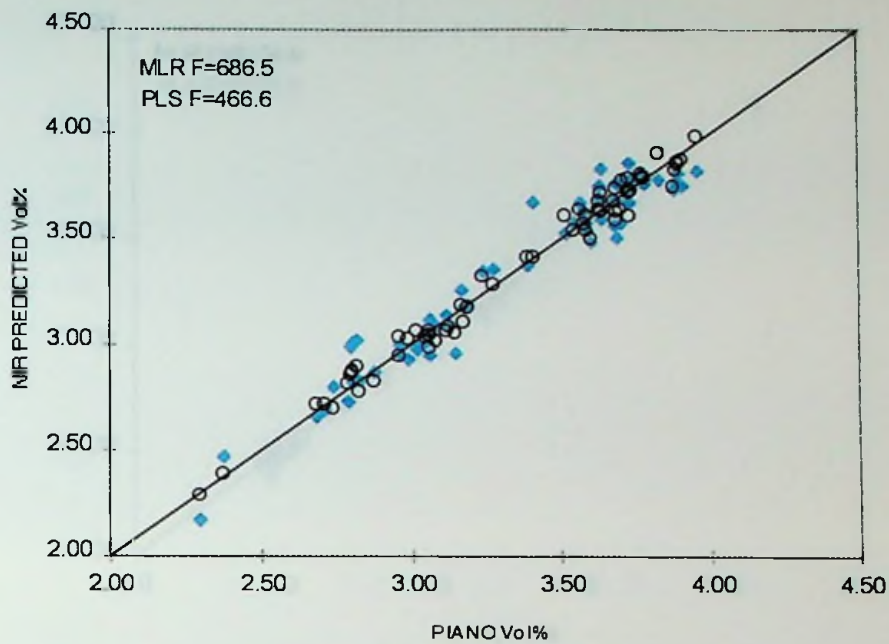


Figure 35. (top) PIANO vs. NIR Predictions for Ethylbenzene in the Second Calibration Set by MLR and PLS. (bottom) PIANO vs. NIR Residuals for Ethylbenzene in the Prediction Set by MLR and PLS. The blue diamonds represent the MLR data, and the black circles represent the PLS data.

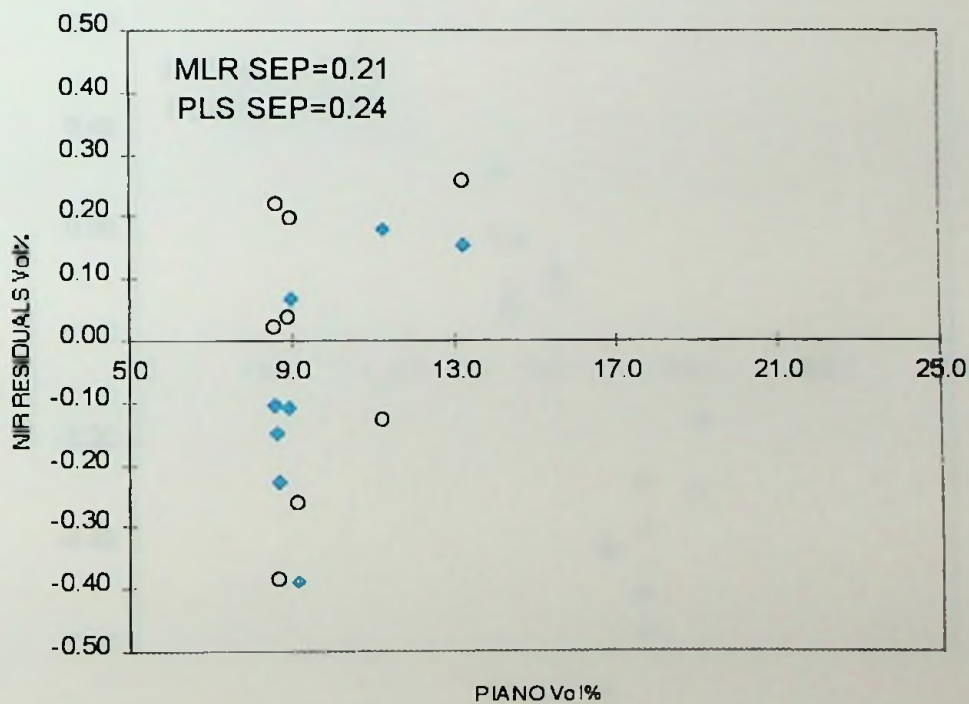
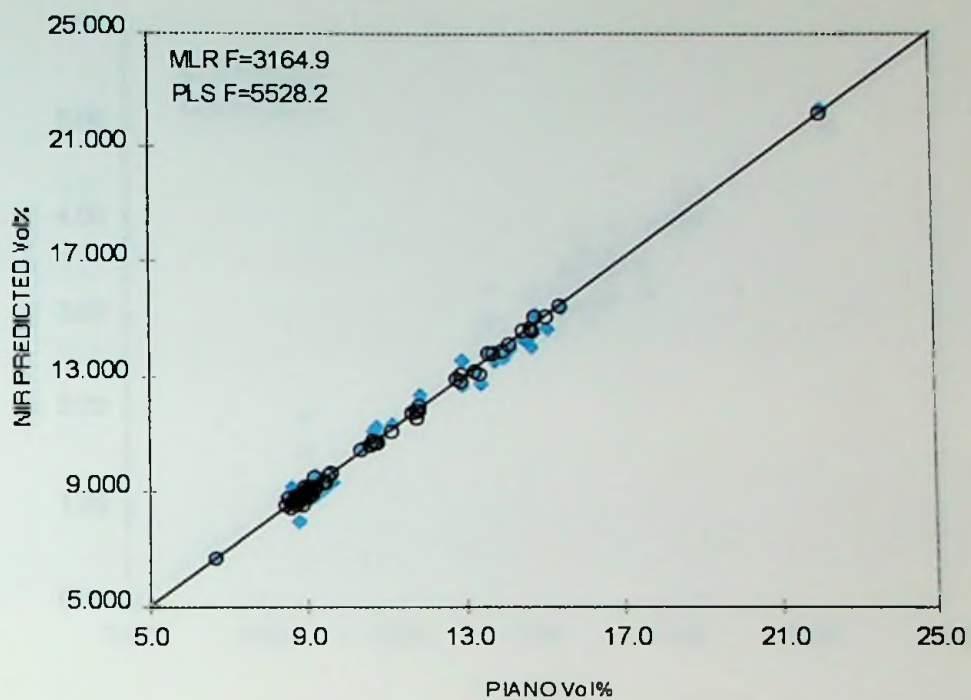


Figure 36. (top) PIANO vs. NIR Predictions for Paraffins in the Second Calibration Set by MLR and PLS. (bottom) PIANO vs. NIR Residuals for Paraffins in the Prediction Set by MLR and PLS. The blue diamonds represent the MLR data, and the black circles represent the PLS data.

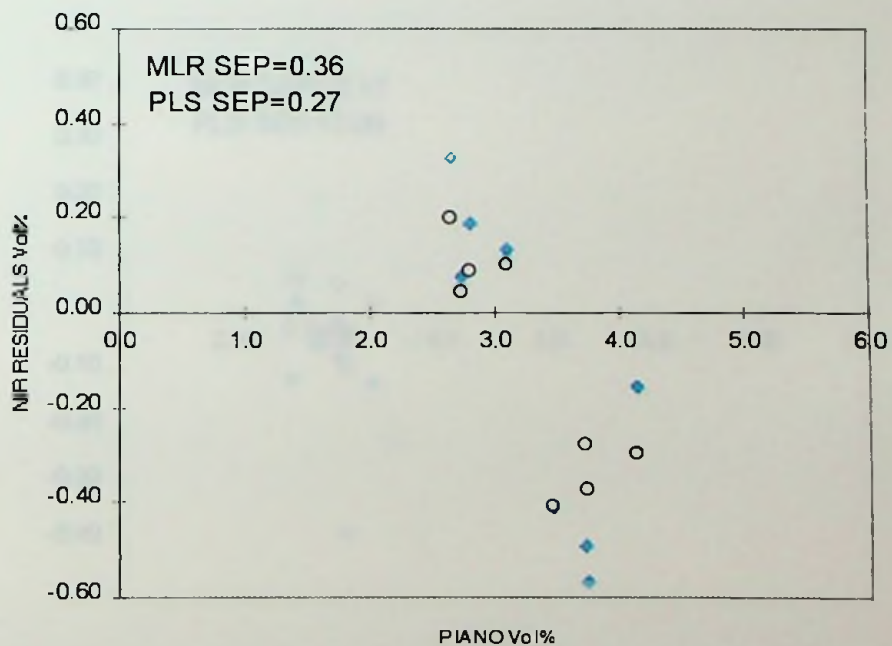
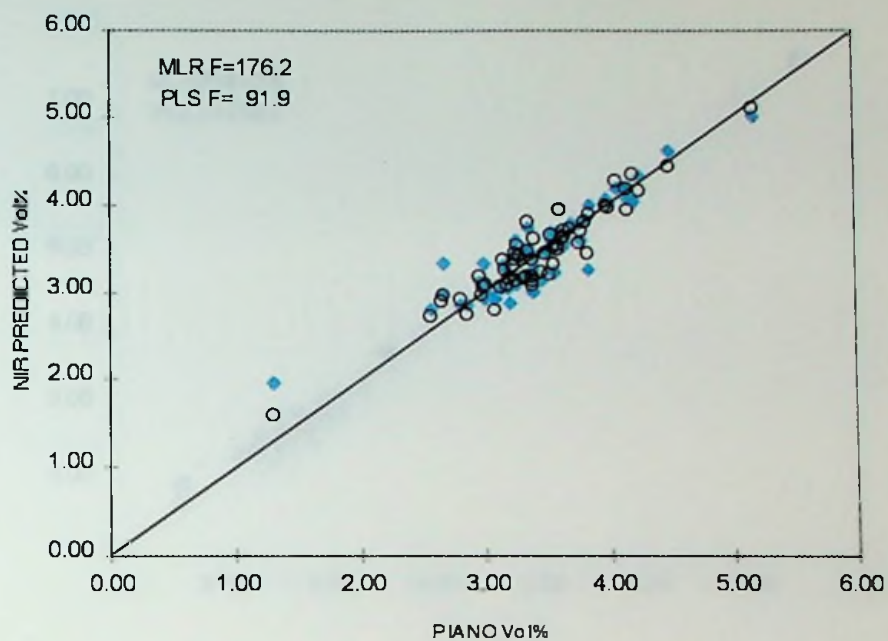


Figure 37. (top) PIANO vs. NIR Predictions for *n*-Hexane in the Second Calibration Set by MLR and PLS. (bottom) PIANO vs. NIR Residuals for *n*-Hexane in the Prediction Set by MLR and PLS. The blue diamonds represent the MLR data, and the black circles represent the PLS data.

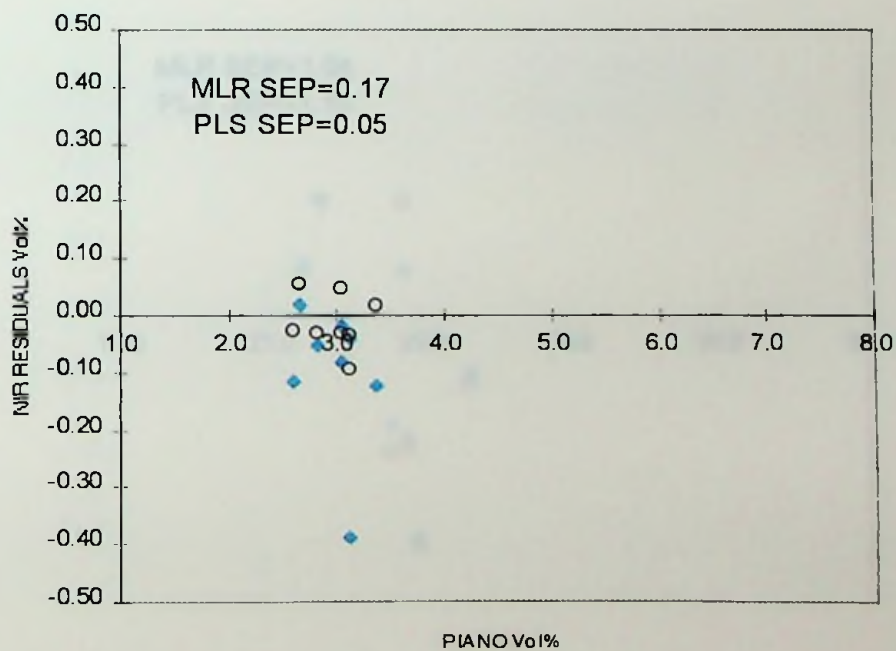
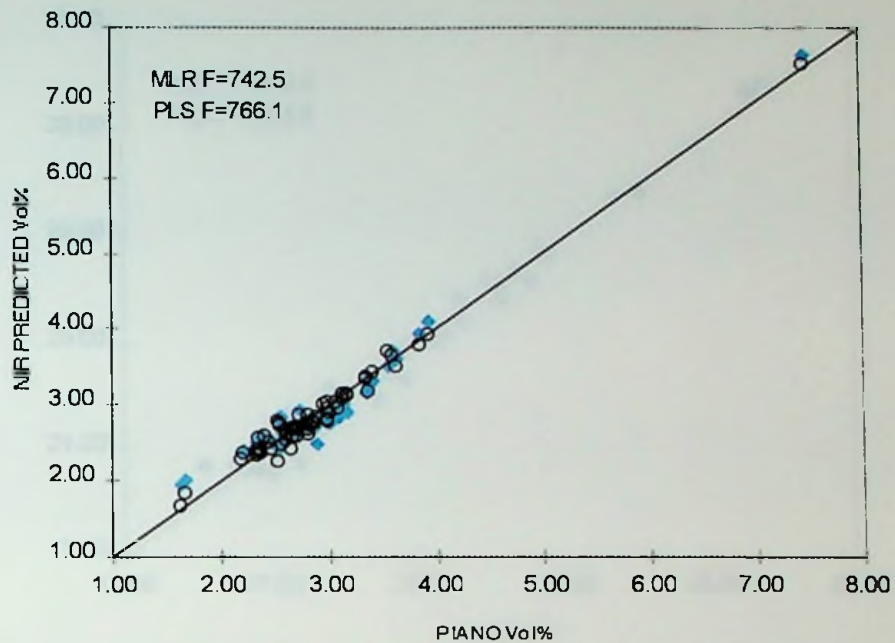


Figure 38. (top) PIANO vs. NIR Predictions for *n*-Heptane in the Second Calibration Set by MLR and PLS. (bottom) PIANO vs. NIR Residuals for *n*-Heptane in the Prediction Set by MLR and PLS. The blue diamonds represent the MLR data, and the black circles represent the PLS data.

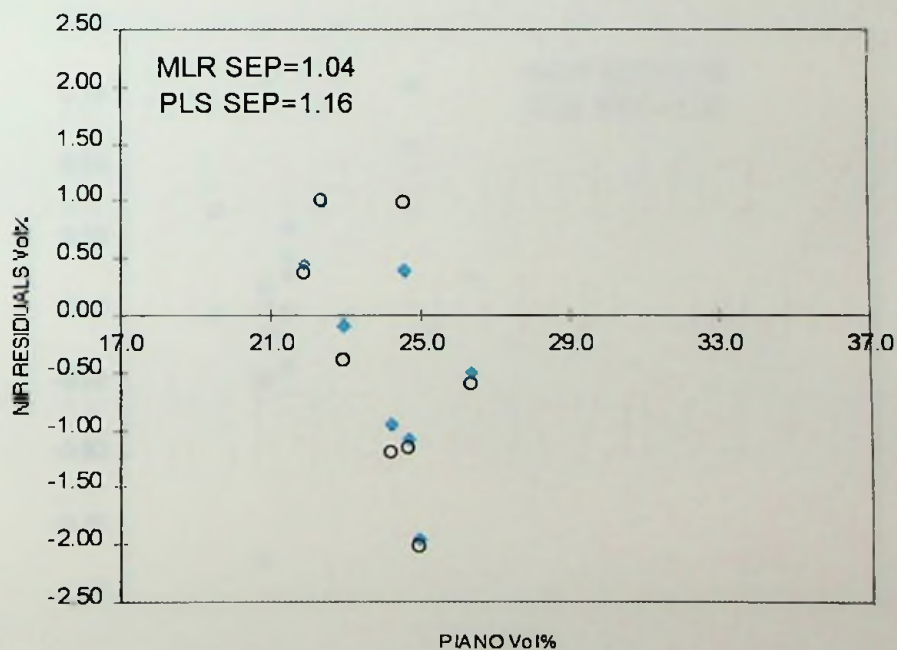
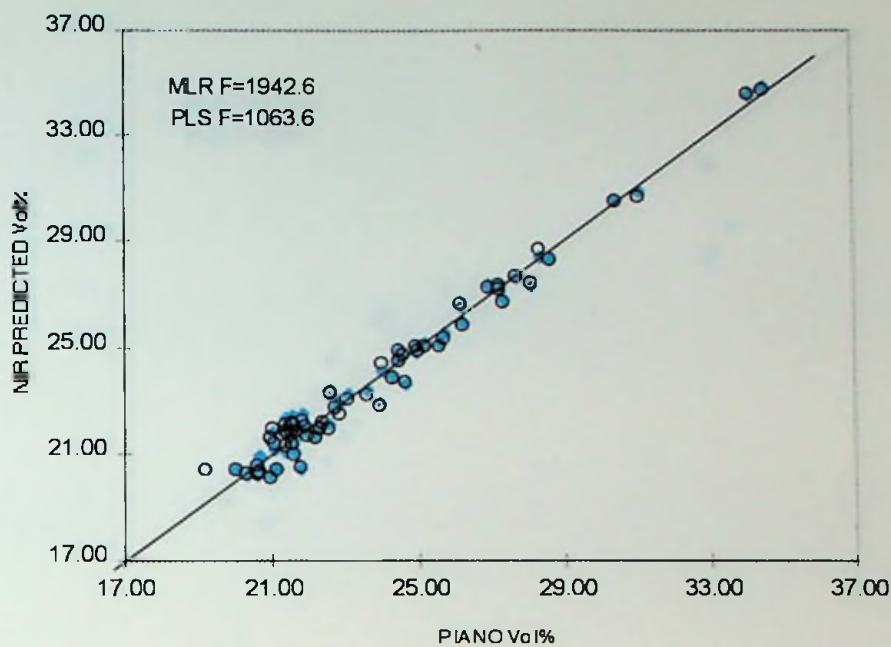


Figure 39. (top) PIANO vs. NIR Predictions for Isoparaffins in the Second Calibration Set by MLR and PLS. (bottom) PIANO vs. NIR Residuals for Isoparaffins in the Prediction Set by MLR and PLS. The blue diamonds represent the MLR data, and the black circles represent the PLS data.

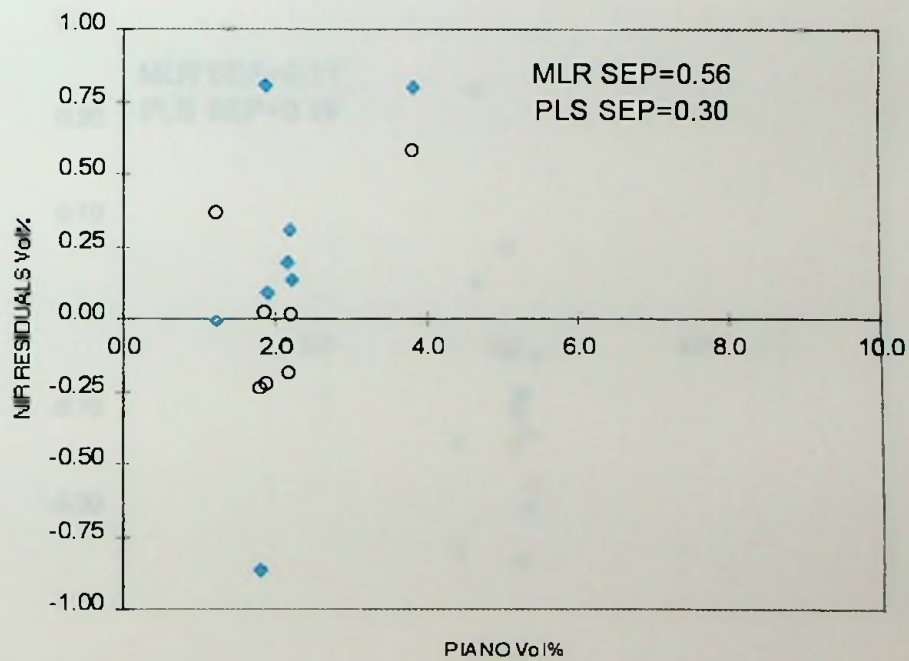
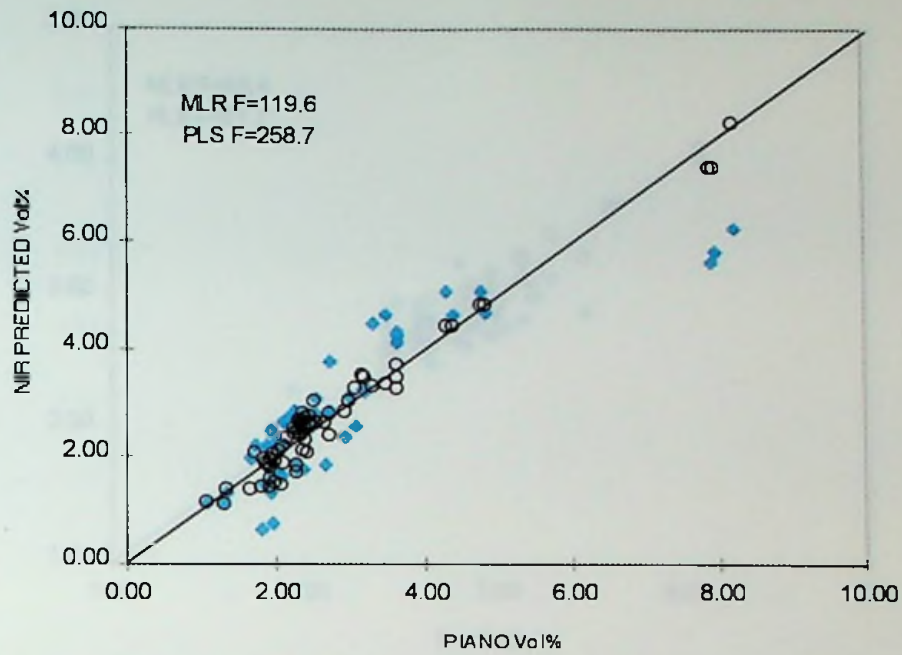


Figure 40. (top) PIANO vs. NIR Predictions for Isopentane in the Second Calibration Set by MLR and PLS. (bottom) PIANO vs. NIR Residuals for Isopentane in the Prediction Set by MLR and PLS. The blue diamonds represent the MLR data, and the black circles represent the PLS data.

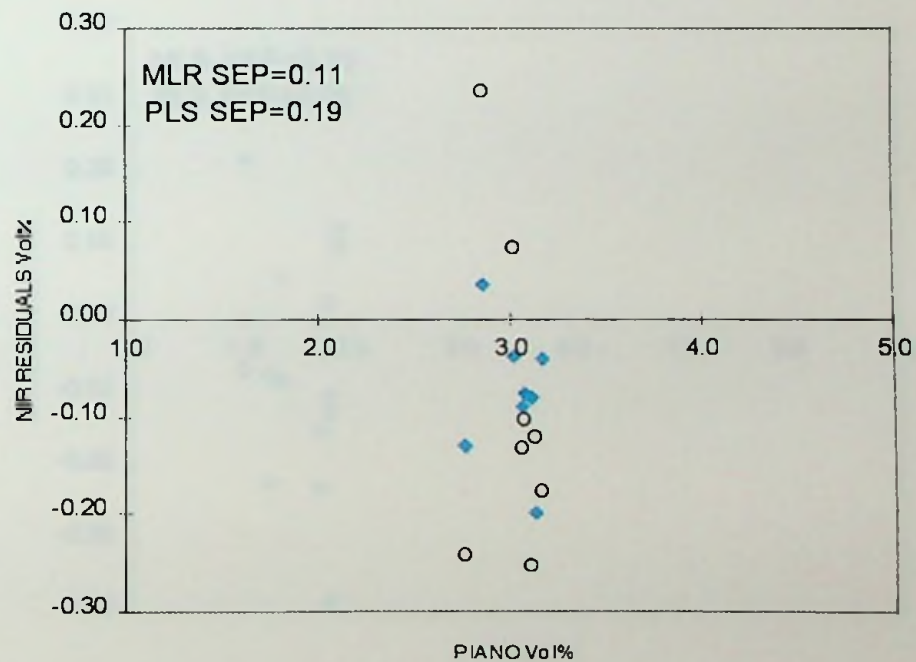
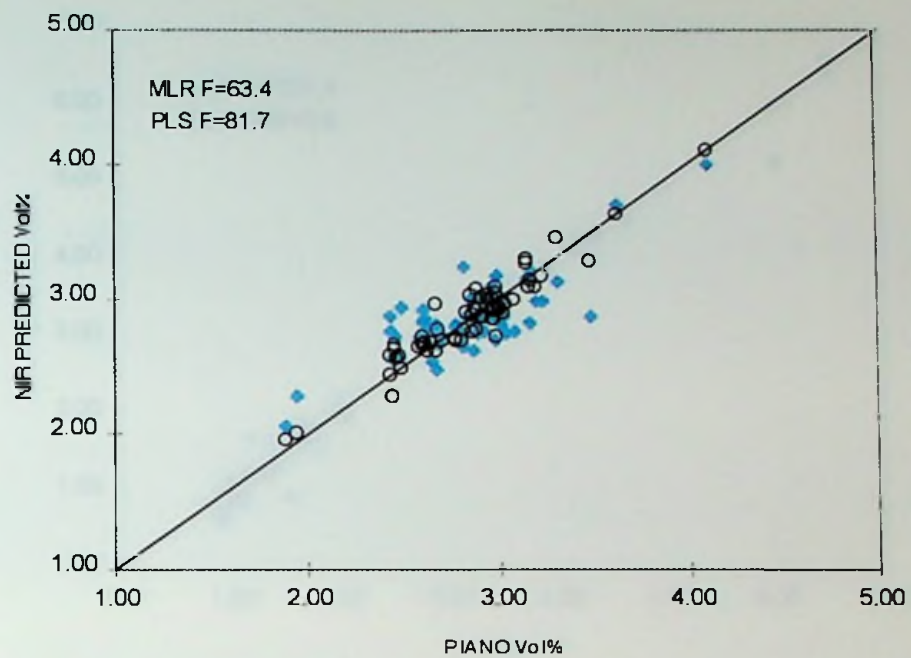


Figure 41. (top) PIANO vs. NIR Predictions for 2-Methylhexane in the Second Calibration Set by MLR and PLS. (bottom) PIANO vs. NIR Residuals for 2-Methylhexane in the Prediction Set by MLR and PLS. The blue diamonds represent the MLR data, and the black circles represent the PLS data.

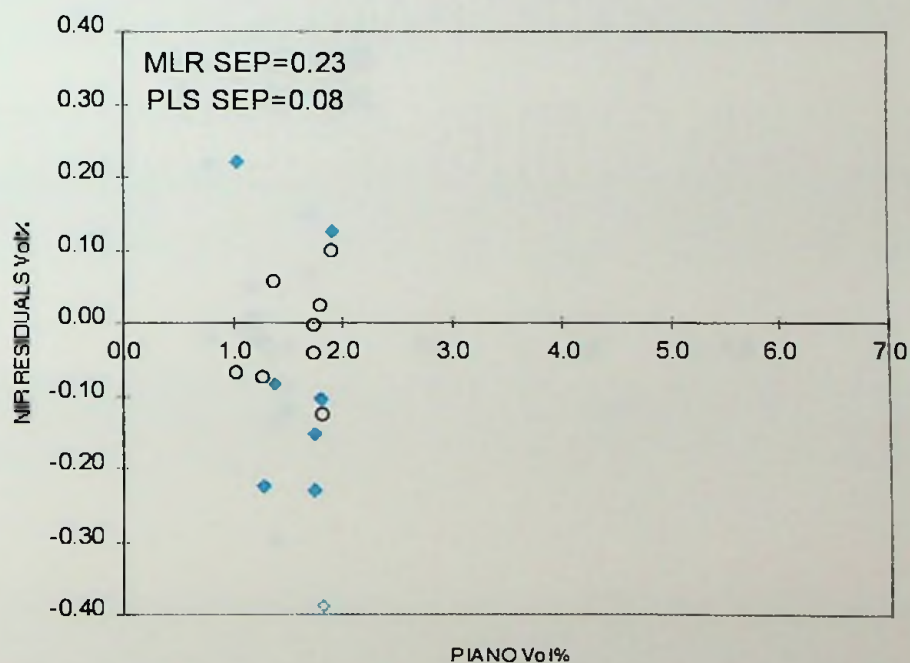
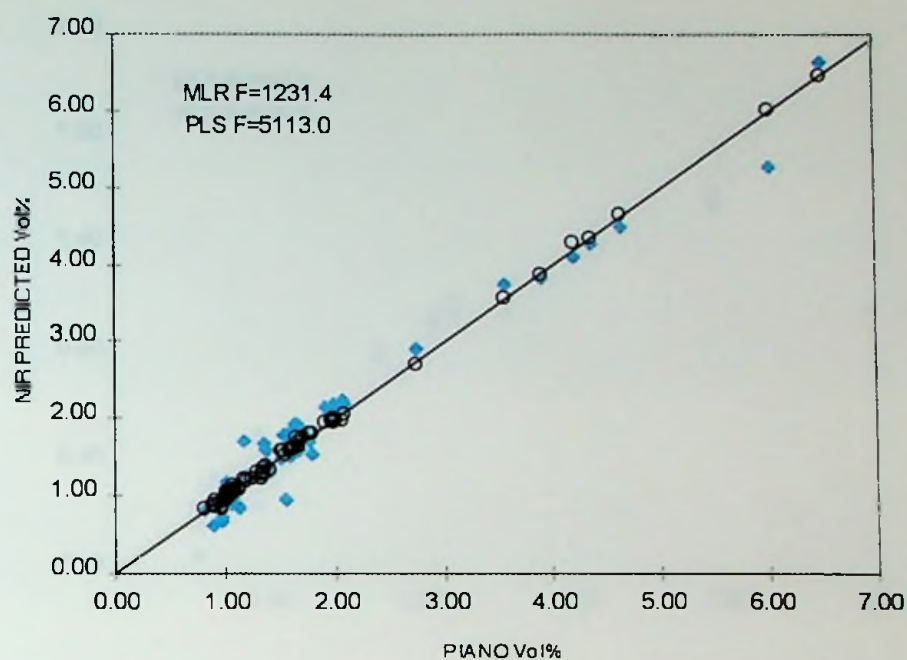


Figure 42. (top) Piano vs. NIR Predictions for Naphthenes in the Second Calibration Set by MLR and PLS. (bottom) Piano vs. NIR Residuals for Naphthenes in the Prediction Set by MLR and PLS. The blue diamonds represent the MLR data, and the black circles represent the PLS data.

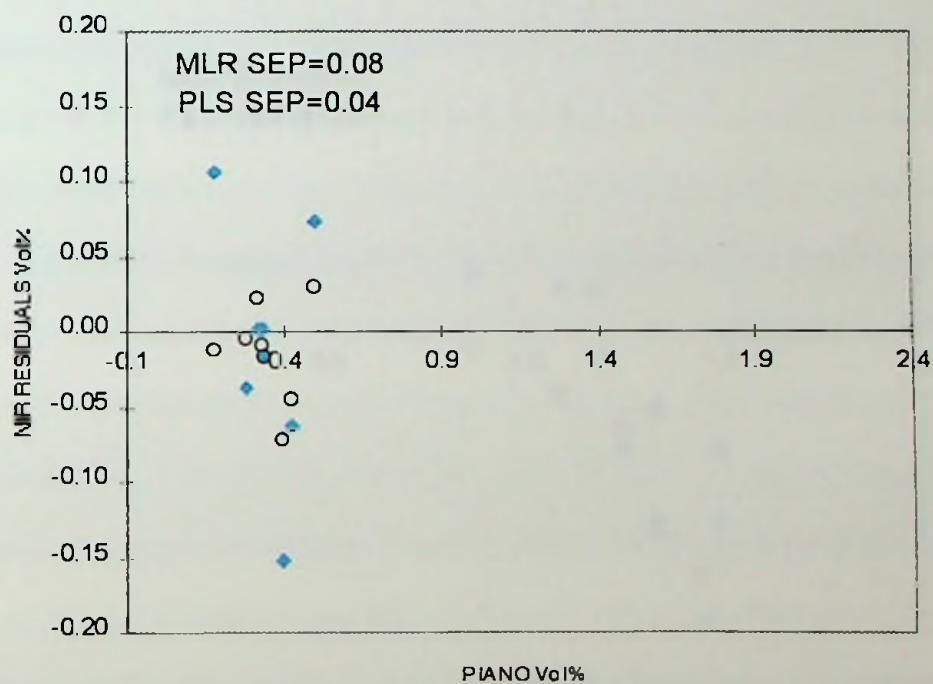
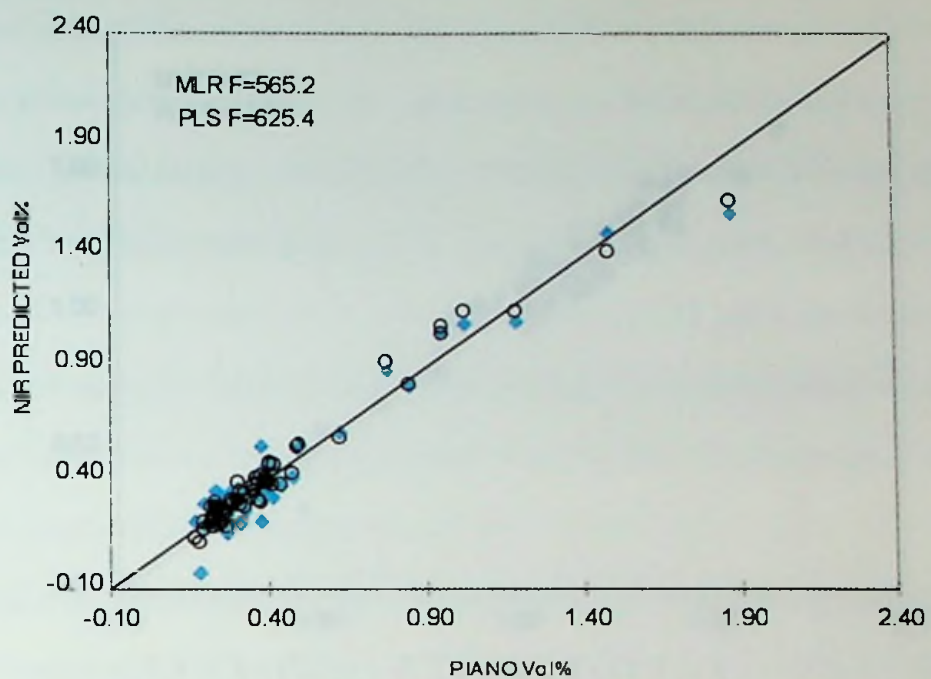


Figure 43. (top) Piano vs. NIR Predictions for Methycyclopentane in the Second Calibration Set by MLR and PLS. (bottom) Piano vs. NIR Residuals for Methycyclopentane in the Prediction Set by MLR and PLS. The blue diamonds represent the MLR data, and the black circles represent the PLS data.

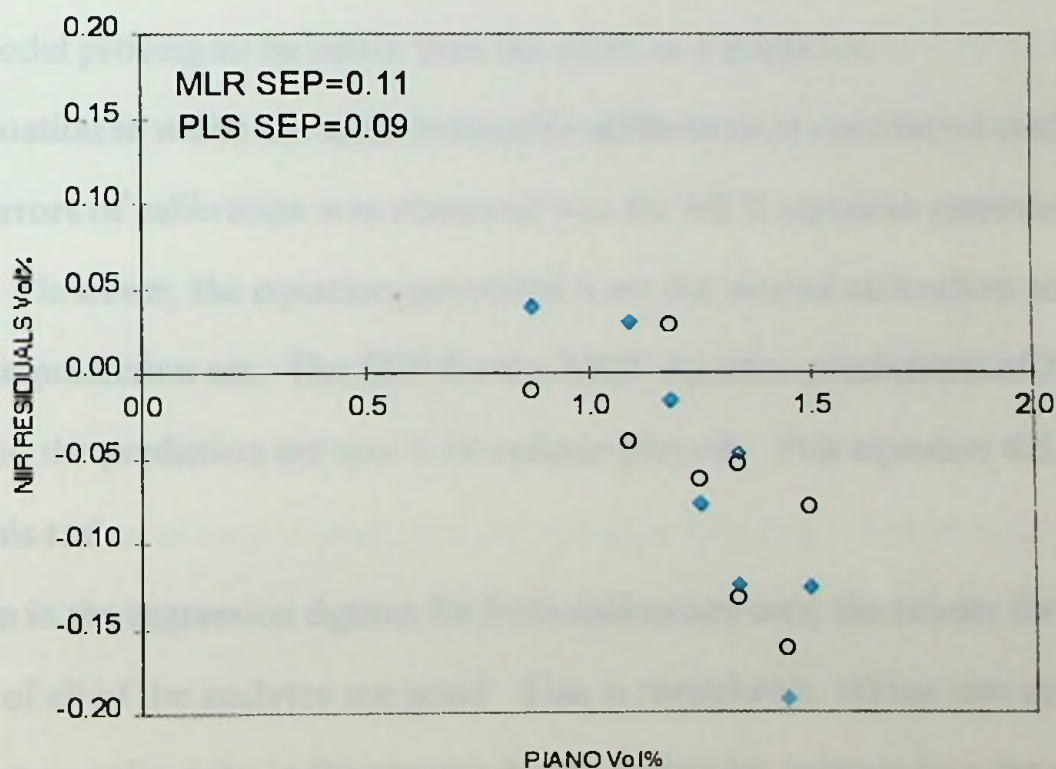
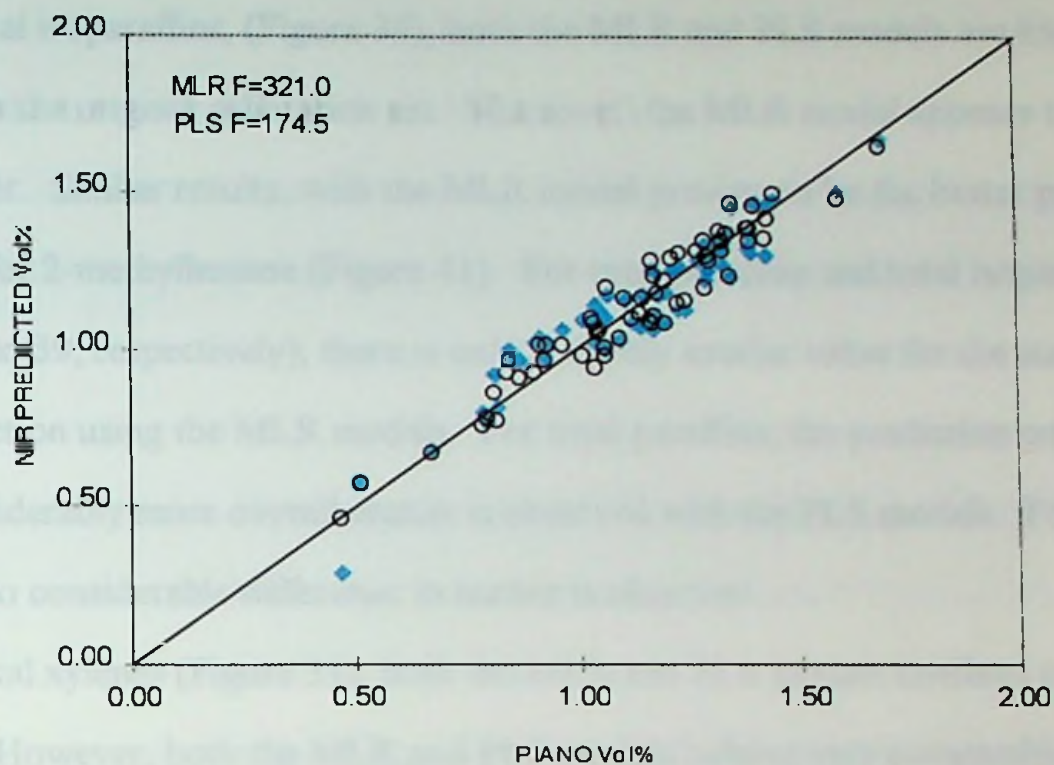


Figure 44. (top) Piano vs. NIR Predictions for Olefins in the Second Calibration Set by MLR and PLS. (bottom) Piano vs. NIR Residuals for Olefins in the Prediction Set by MLR and PLS. The blue diamonds represent the MLR data, and the black circles represent the PLS data.

For total isoparaffins, (Figure 39), both the MLR and PLS models are linear, as they were with the original calibration set. Moreover, the MLR model appears to be the better predictor. Similar results, with the MLR model proving to be the better predictor, are observed for 2-methylhexane (Figure 41). For total paraffins and total isoparaffins (Figures 36 and 39, respectively), there is only a slightly smaller value for the standard error of prediction using the MLR models. For total paraffins, the prediction set chart indicates considerably more overall scatter is observed with the PLS models. For total isoparaffins, no considerable difference in scatter is observed.

For total xylenes (Figure 31), both the MLR and PLS models conform to linear correlations. However, both the MLR and PLS models behave very comparable as predictors, neither model proving to be better than the other. Likewise, similar results are observed with *p*-xylene, ethylbenzene, and olefins (Figures 33, 35, and 44, respectively), with neither model proving to be better than the other as a predictor.

The equation in which the most noticeable differences in correlation coefficients and standard errors of calibration was observed was the MLR equation generated for 2-methylhexane. However, the equation generated from the second calibration set was tested using the prediction set. The SEP for the MLR equation predictions of 2-methylhexane in the prediction set was 0.19 volume percent. This equation did perform quite well at this task.

As seen in the regression figures for both calibration sets, the results for the determination of all of the analytes are good. This is remarkable, taking into consideration that there is some nonlinearity in the spectra due to molecules surrounding the analytes of interest.¹³ This overcoming of the nonlinearity was achieved by converting the spectra to second derivatives and applying multivariate analysis. The extremely good repeatability results of the P.I.A.N.O. analysis also contributed to this. The good repeatability results provide a sense of reliability from run-to-run, and day-to-day in the P.I.A.N.O. data that were used to perform the near-IR correlations.

VI. APPLICATION FOR ON-LINE ANALYSIS

Four of the equations from this work are used on-line in conjunction with the on-line near-IR InfraTane® system located at Ashland's Catlettsburg, Kentucky refinery's LPCCR. The four equations were the MLR equations for total aromatics, olefins, benzene, and toluene. As an added package for quality assurance, the unit has a profuel system installed. A profuel is a sample of a particular fuel or stream with known concentrations of analytes. There are three profuels included in this system. The system is designed to run these profuels to monitor the equations, based upon set tolerance limits. If the equations need to be adjusted, the system does that automatically. It also has the capability to run one profuel only. This is used where there may be a question about the prediction of the stream and a quick check on the calibration is requested. The three profuels that were initially collected had concentrations of total aromatics, benzene, toluene, and olefins too close together. These were too similar because the initial collection times were based only upon the octane numbers of the stream. It was desired to have concentrations over a large range. One of the three profuels was kept. The other two were discarded, and two more profuels were collected. With the addition of the two new profuels, the ranges for all analytes, except benzene, were sufficient enough for use. In the case of benzene, spectra of several grab samples were collected off-line.

The stream has primarily been used for gasoline blending. The stream is primarily being monitored for its research octane number and benzene content (Table VIII). A weekly check sample is obtained for benzene analysis by ASTM D 3606. This method agrees extremely well with GC-PIANO. However, the results of this sample and a standard are completed in approximately one hour. This is faster than the GC-PIANO method, and since only one analyte is being monitored, it is more efficient for this purpose. The only analyte from this work that is being closely monitored at this time is benzene. These results show that the goal of being able to determine benzene within 0.21% by volume has been achieved. In this six month period, the difference between the on-line

Table VIII. Six Month Study Results from Weekly Benzene Check Sample

DATE	TIME	Volume % Benzene		DIFFERENCE
		D3606	ON-LINE NIR	d3606 - NIR
08/30/95	15:45	2.700	2.780	-0.080
09/08/95	15:00	2.830	2.740	0.090
09/12/95	09:00	2.630	2.520	0.110
09/19/95	10:15	2.920	2.990	-0.070
09/26/95	09:00	2.260	2.200	0.060
10/02/95	13:35	4.190	4.050	0.140
10/10/95	13:50	2.600	2.643	-0.043
10/17/95	10:00	4.194	4.231	-0.037
10/26/95	07:30	1.890	1.870	0.020
11/06/95	09:05	1.920	1.840	0.080
11/09/95	22:32	2.520	2.540	-0.020
11/14/95	10:30	2.569	2.608	-0.039
11/21/95	07:50	2.150	2.196	-0.046
11/28/95	14:00	2.510	2.355	0.155
12/05/95	10:00	2.260	2.000	0.260
12/12/95	09:30	1.900	1.840	0.060
01/05/96	07:00	1.617	1.492	0.125
01/12/96	15:05	2.340	2.530	-0.190
01/26/96	14:45	2.200	2.280	-0.080
02/01/96	15:00	2.415	2.230	0.185
02/06/96	13:30	2.540	2.370	0.170
02/13/96	14:00	1.210	1.290	-0.080
02/23/96	13:20	1.700	1.870	-0.170
02/27/96	14:30	1.990	2.030	-0.040
SEP				0.118

near-IR exceeded 0.21% by volume one time, with a standard error of prediction of 0.12% by volume over this six month period.

Every five months, the lamp is replaced with a new lamp because the life of the lamps are estimated at six months. Instead of running all of the calibration samples again, the MLR calibrations can be transferred for use with the new lamp, because, technically, changing a lamp is similar to changing an instrument. The calibrations are transferred via Maggard's method.¹⁰⁴ The equations are then slope and bias adjusted for all parameters, except benzene, using the three protofuels. The benzene equation is adjusted using a set of samples run off-line.

VI. CONCLUSION

This research does verify that near infrared spectroscopy can be used as a quantitative technique employing multiple linear regression and partial least squares regression for determining the concentration of hydrocarbon groups and individual hydrocarbons amongst a complex mixture of hydrocarbons. Models have been generated and presented here for total aromatics, benzene, toluene, total xylenes and individual xylene isomers, ethylbenzene, total paraffins, *n*-hexane, *n*-heptane, total isoparaffins, isopentane, 2-methylhexane, total naphthenes, methylcyclopentane, and total olefins. Techniques described in this thesis have been successfully applied on-line, and in the laboratory, and are performing well. The standard error of performance over a six month period for the on-line prediction of the benzene concentration of a reformat stream was determined to be 0.12% by volume.

The technique described here serves as a faster method of analysis. The near-IR technique takes less than a minute to perform the operation, and results of several analytes are determined simultaneously. The primary methods of gas chromatography can take in excess of three hours to perform. Therefore, near-IR is a fast method of providing reliable data. This faster analysis can enhance the economics concerning analysis time and can be used on-line for advanced control of a refinery process.

Patent applications have been filed for this technology in the United States and other countries.

REFERENCES

1. Wetzel, D. L. *Anal. Chem.* **1983**, *55*, 1165A-1176A.
2. Ciurczak, E. W. *CHEMTECH* **1992**, *22*, 374-380.
3. *Near Infra-red Spectroscopy Bridging the Gap between Data Analysis and NIR Applications*; Hildrum, K. I.; Isaksson, T.; Naes, T.; Tandberg, A., Eds.; Ellis Horwood Limited, Chichester, West Sussex, England, 1992.
4. Martin, K. A. *Appl. Spectrosc. Rev.* **1992**, *27*, 325-383.
5. Massie, D. R.; Norris, K. H. *Trans. Am. Soc. Agric. Eng.* **1965**, *8*, 598-600.
6. Norris, K. H.; Barnes, R. F.; Moore, J. E.; Shenk, J. S. *J. Anim. Sci.* **1976**, *43*, 889-897.
7. Osborne, B. G.; Fearn, T. *Near Infrared Spectroscopy in Food Analysis*; Longman Scientific & Technical: Essex, England; John Wiley & Sons: New York, 1986, 36-41.
8. Orman, B. A.; Schumann, Jr. R. A. *J. Agric. Food Chem.* **1991**, *39*, 883-886.
9. Davies, A. M. C. *Anal. Proceed.* **1992**, *29*, 198-200.
10. Jouan-Rimbaud, D.; Walczak, B.; Massart, D. L.; Last, I. R.; Prebble, K. A. *Anal. Chim. Acta* **1995**, *304*, 285-295.
11. Blanco, M.; Coello, J.; Iturriaga, H.; Maspoch, S.; de la Pezuela, C. *Anal. Chim. Acta* **1996**, *333*, 147-156.
12. Nickel, D.; Schneider, G. M. *J. Chem. Thermodynamics* **1989**, *21*, 293-305.
13. DiFoggio, R. *Appl. Spectrosc.* **1995**, *49*, 67-75.
14. Baptista, M. S.; Tran, C. D.; Gao, G. *Anal. Chem.* **1996**, *68*, 971-976.
15. Bjørsvik, H. *Appl. Spectrosc.* **1996**, *50*, 1541-1544.
16. Wong, J. L.; Jaselskis, B. *Analyst* **1982**, *107*, 1282-1285.
17. Honigs, D. E.; Freelin, J. M.; Hieftje, G. M.; Hirschfeld, T. B. *Appl. Spectrosc.* **1983**, *37*, 491-497.

18. Buchanan, B. R.; Honigs, D. E. *Appl. Spectrosc.* **1987**, *41*, 1388-1392.
19. Donahue, S. M.; Brown, C. W.; Caputo, B.; Modell, M. D. *Anal. Chem.* **1988**, *60*, 1873-1878.
20. Espinosa, A.; Lambert, D.; Martens, A.; Ventron, G. European Patent 304 232, 1988.
21. Hieftje, G. M.; Honigs, D. E.; Hirschfeld, T. B. U.S. Patent 4 800 279, 1989.
22. Kelly, J. J.; Barlow, C. H.; Jinguji, T. M.; Callis, J. B. *Anal. Chem.* **1989**, *61*, 313-320.
23. Maggard, S. M. U.S. Patent 4 963 745, 1990.
24. Kelly, J. J.; Callis, J. B. *Anal. Chem.* **1990**, *62*, 1444-1451.
25. Maggard, S. M., Presented at the National Meeting of the American Chemical Society, Boston, MA, April 1990.
26. Asker, N.; Kokot, S. *Appl. Spectrosc.* **1991**, *45*, 1153-1157.
27. Lambert, D.; Martens, A. European Patent 285 251, 1991.
28. Davidson, T. M.; DeConde K.; Hake, R.; Tracy, D.; Gantz, A.; McDermott, L., *SPIE* **1992**, 1681, 231-235.
29. Swarin, S. J.; Drumm, C. A. *Spectrosc.* **1992**, *7*, 42-49.
30. Welch, W. T., Presented at the National Fuels and Lubricants Meeting of the National Petroleum Refiners Association, Houston, TX, November 1993, paper FL-93-114.
31. InfoMetrix, Inc. *Chemometrics Application Note*, Publication No. 11-6/93.
32. Brown, C. W.; Lo, S. *Appl. Spectrosc.* **1993**, *47*, 812-815.
33. Espinosa, A.; Martens, A.; Ventron, G.; Lambert, D.; Pasquier, A. European Patent 305 090, 1993.
34. DiFoggio, R.; Sadhukhan, M.; Ranc, M. L. *Oil & Gas J.* **1993**, *91*(18), 87-90.
35. Welch, W. T.; Bain, M. L.; Maggard, S. M.; May, J. M. *Oil & Gas J.* **1994**, *92*(26), 48-56.

36. Maggard, S. M.; Welch, W. T. U.S. Patent 5 348 645, 1994.
37. Maggard, S. M. U.S. Patent 5 349 188, 1994.
38. Maggard, S. M. U.S. Patent 5 349 189, 1994.
39. Coates, J. P. *Spectrosc.* **1994**, *9*, 36-40.
40. Espinosa, A.; Sanchez, M.; Osta, S.; Boniface, C.; Gil, J.; Martens, A.; Descales, B.; Lambert, D.; Valleur, M. *Oil & Gas J.* **1994**, *92(42)*, 49-56.
41. Lambert, D.; Descales, B.; Bages, S.; Bellet, S.; Llinas, J. R.; Loublier, M.; Maury, J. P.; Martens, A. *Hydrocarb. Process.* **1995**, *74(12)*, 103-108.
42. Espinosa, A.; Lambert, D.; Martens, A.; Ventron, G. U.S. Patent 5 452 232, 1995.
43. Choquette, S. J.; Chesler, S. N.; Duewer, D. L. *Anal. Chem.* **1996**, *68*, 3525-3533.
44. Cooper, J. B.; Wise, K. L.; Welch, W. T.; Bledsoe, R. R.; Sumner, M. B. *Appl. Spectrosc.* **1996**, *50*, 917-921.
45. Korsman, T.; Nilsson, M.; Öhman, J.; Renberg, I. *Environ. Sci. Technol.* **1992**, *26*, 2122-2126.
46. Small, G. W.; Arnold, M. A.; Marquardt, L. A. *Anal. Chem.* **1993**, *65*, 3279-3289.
47. Sun, J. *J. Chemometrics* **1996**, *10*, 1-9.
48. Carlson, R.; Smythe, W.; Baines, K.; Barbanis, E.; Becker, K.; Burns, R.; Calcutt, S.; Calvin, W.; Clark, R.; Danielson, G.; Davies, A.; Drossart, P.; Encrenaz, T.; Fanale, F.; Granahan, J.; Hansen, G.; Herrera, P.; Hibbitts, C.; Hui, J.; Irwin, P.; Johnson, T.; Kamp, L.; Kieffer, H.; Leader, F.; Lellouch, E.; Lopes-Gautier, R.; Matson, D.; McCord, T.; Mehlman, R.; Ocampo, A.; Orton, G.; Roos-Serote, M.; Segura, M.; Shirley, J.; Soderblom, L.; Stevenson, A.; Taylor, F.; Torson, J.; Weir, A.; Weissman, P. *Science* **1996**, *274*, 385-388.
49. Bangalore, A. S.; Shaffer, R. E.; Small, G. W.; Arnold, M. A. *Anal. Chem.* **1996**, *68*, 4200-4212.

50. Phelan, M. K.; Barlow, C. H.; Kelly, J. J.; Jinguji, T. M.; Callis, J. B. *Anal. Chem.* **1989**, *61*, 1419-1424.
51. Lin, J.; Zhou, J.; Brown, C. W. *Appl. Spectrosc.* **1996**, *50*, 444-448.
52. Skoog, D. A.; Leary, J. J. *Principles of Instrumental Analysis, Fourth Edition*, Harcourt Brace Publishers, New York, 1992, 46-56, 126-138, 252-295.
53. Brown, C. W.; Donohue, S. M.; Lo, S. In *Advances In Near Infrared Measurements*, Potany, G., Ed.; JAI Press Inc., Greenwich, Cn., 1993, 1-22.
54. Rankin, J. G., Marshall University, personal communication, 1994.
55. Harris, D. C.; Bertolucci, M. D. *Symmetry and Spectroscopy*, Dover Publications, New York, 1978, 93-224.
56. Wetzel, D. L.; Kemeny, G. J. *Applied Near-Infrared Spectroscopy, Analytical Near-IR Spectroscopy*, 1989, (whole).
57. Wetzel, D. L.; Kemeny, G. J. Applied Near-Infrared Spectroscopy, Short course presented by Society for Applied Spectroscopy in conjunction with the Twenty-First Annual Conference of the Federation of Analytical Chemistry and Spectroscopy Societies, St. Louis, MO, Oct. 1994.
58. *Manual for Near Infrared Spectral Analysis Software (NSAS)*, 1990, SM-1 - SM-20, A-1-1 - A-1-31.
59. Bonanno, A. S.; Olinger J. M.; Griffiths, P. R. In *Near Infra-red Spectroscopy Bridging the Gap between Data Analysis and NIR Applications*; Hildrum, K. I.; Isaksson, T.; Naes, T.; Tandberg, A., Eds.; Ellis Horwood Limited, Chichester, West Sussex, England, 1992, 19-28.
60. Cooper, J. B., Fletcher, P. E., Vess, T. M., Welch, W. T., *Appl. Spectrosc.*, 1995, *49*, 586-592.
61. Gary, J. H.; Handwerk, G. E. *Petroleum Refining Technology and Economics*, Marcel Dekker, New York, 1987, Vol. 5, 65-85.

62. Kulakowski, M. *Preprints*, Division of Petroleum Chemistry, Inc., American Chemical Society, Washington, DC, 1994, 39, 494-500.
63. Zilberman, I.; Bigman, J.; Sela, I.; Hiram, A.; Haviv, D. *Hydrocarb. Process.* **1996**, 75(5), 91-97.
64. *Kirk-Othmer Encyclopedia of Chemical Technology*, Third Edition; Grayson, M., Ed.; John Wiley & Sons, New York, Vol. 17, 1982, 218-220.
65. *Handbook of Petroleum Refining Processes*, Part 3; Meyers, R. A., Ed.; McGraw-Hill, New York, 1986, 1-20.
66. Mark, H. In *Advances In Near Infrared Measurements*; Potany, G., Ed.; JAI Press Inc., Greenwich, Cn., 1993, 55-60.
67. Alberty, R. A.; Silbey, R. J. *Physical Chemistry, First Edition*; John Wiley & Sons: New York, 1992, 491-495.
68. Brown, C. W. Presented at the Twenty-First Annual Conference of the Federation of Analytical Chemistry and Spectroscopy Societies, St. Louis, MO, October 1994; paper 164a.
69. Brown, C. W.; Lynch, P. F.; Obremski, R. J.; Lavery, D. S. *Anal. Chem.* **1982**, 54, 1472-1479.
70. Casal, V.; Martin-Alvarez, P. J.; Herraiz, T. *Anal. Chim. Acta* **1996**, 326, 77-84.
71. Sumner, M. B., Ashland Petroleum Company, personal communication, 1994.
72. Wold, H. In *Research Papers in Statistics. Festschrift for J. Neyman*; David, F. N., Ed.; John Wiley and Sons: New York, 1966; pp 411-444.
73. Wold, H. In *Multivariate Analysis-III*; Krishnaiah, P. R., Ed.; Academic Press: New York, 1973; pp 383-407.
74. Goutis, C. *Annals of Statist.* **1996**, 24, 816-824.
75. Sjöström, M.; Wold, S.; Lindberg, W.; Persson, J.; Martens, H. *Anal. Chim. Acta* **1983**, 150, 61-70.

76. Dunn III, W. J.; Stalling, D. L.; Schwartz, T. R.; Hogan, J. W.; Petty, J. D.; Johansson, E.; Wold, S. *Anal. Chem.* **1984**, *56*, 1308-1313.
77. Otto, M.; Wegscheider, W. *Anal. Chem.* **1985**, *57*, 63-69.
78. Geladi, P.; Kowalski, B. *Anal. Chim. Acta*, **1986**, *185*, 19-32.
79. Beebe, K. R.; Kowalski, B. R. *Anal. Chem.* **1987**, *59*, 1007A-1017A.
80. Haaland, D. M.; Thomas, E. V. *Anal. Chem.* **1988**, *60*, 1202-1208.
81. Haaland, D. M. *Anal. Chem.* **1988**, *60*, 1208-1217.
82. Brekke, T.; Kvalheim, O. M.; Sletten, E. *Anal. Chim. Acta* **1989**, *223*, 123-134.
83. Bak, J.; Larsen, A. *Appl. Spectrosc.* **1995**, *49*, 437-443.
84. Cabanillas, A. G.; Diaz, T. G.; Espinosa-Mansilla, A.; López-de-Alba, P. L.; Lopez, F. L. *Anal. Chim. Acta* **1995**, *302*, 9-19.
85. Hernández, O.; Jiménez, A. I.; Jiménez, F.; Arias, J. J. *Anal. Chim. Acta* **1995**, *310*, 53-61.
86. Urbanski, P.; Kowalska, E. *X-Ray Spectrometry* **1995**, *24*, 70-75.
87. López-de-Alba, P. L.; Wróbel-Kaczmarczyk, K.; Wróbel, K.; López-Martínez, L.; Hernández, J. A. *Anal. Chim. Acta* **1996**, *330*, 19-29.
88. Iob, A.; Ali, M. A.; Tawabini, B. S.; Abbas, N. M. *Fuel* **1996**, *75*, 1060-1064.
89. Moreno, C.; Manuel-Vez, M. P.; Gómez, I.; García-Vargas, M. *Analyst* **1996**, *121*, 1609-1612.
90. Geladi, P.; Kowalski, B. *Anal. Chim. Acta*, **1986**, *185*, 1-17.
91. Haaland, D. M.; Thomas, E. V. *Anal. Chem.* **1988**, *60*, 1193-1202.
92. Protic-Lovasic, G.; Jambrec, N.; Deur-Siftar, D.; Prostenik, M. V. *Fuel* **1990**, *69*, 525-528.
93. Iob, A.; Ali, M. A.; Tawabini, B. S.; Anabtawi, J. A.; Ali, S. A.; Al-Farayedhi, A. *Fuel* **1995**, *74*, 227-231.
94. Ali, S. A.; Anabtawi, J. A.; Alam, K. *Fuel Sci. Tech. Int'l.* **1995**, *13*, 545-558.
95. Von Bargaen, K. NIRSystems, Inc., personal communication, 1997.

96. Brush, P. NIRSystems, Inc., personal communication, 1996.
97. Perstorp Analytical Company, NIRSystems, Inc., *CHEM-ID™ Chemical Identification Analyzers*, Publication No. DS-56.
98. Perstorp Analytical Company, NIRSystems, Inc., *8 Steps to a Better Quantitative Calibration*, Publication No. MS-4.
99. Mark, H., *Principles and Practice of Spectroscopic Calibration*, John Wiley & Sons, Inc., New York, 1991, 26-32, 97-98, 131-137.
100. Weyer, L. G. *Appl. Spectrosc. Rev.* **1985**, *21*, 1-43.
101. Perstorp analytical Company, NIRSystems, Inc., *Near Infrared Absorptions*, Publication No. MS-2.
102. *Annual Book of ASTM Standards*, American Society for Testing and Materials, West Conshohocken, PA, 1993, Section 5.
103. *Annual Book of ASTM Standards*, American Society for Testing and Materials, West Conshohocken, PA, 1996, Section 5.
104. Maggard, S. M. U.S. Patent 5 243 546, 1993.

APPENDIX I.

18/02 '97 10:33

☎ 31 20 4852722

ELSEVIER F&A

001



ELSEVIER
SCIENCE

Elsevier Science - NL

Sara Burgerhartstraat 25
1033 KV Amsterdam
The Netherlands

P.O. Box 521
1000 AM Amsterdam
The Netherlands

Tel (+31) 20 485 2633
Fax (+31) 20 485 2772

gopher:elsevier.nl
URL: <http://www.elsevier.nl>

Mr R.R. Bledsoe, Jr.
Ashland Petroleum Company
Fax: 001 606 924 2560

Direct Line: (20) 4852 751 Amsterdam, 18 February 1997
Direct Fax: (20) 4852 722

Re: *Analytica Chimica Acta* 185 (1986) pgs. 4-17
Your letter 13-02-1997

Dear Mr Bledsoe,

We herewith grant you and University Microfilms Inc. permission to reproduce the material as mentioned on the enclosed copy of your letter in your thesis/dissertation, provided that:

- full acknowledgement is given to the original source of the publication

Yours sincerely,
ELSEVIER SCIENCE - NL
Publishing Support & Services Department



Ms Jantina Veenema
Rights & Permissions

Inspira
Fluvius
Vergamo
North-Holland
Excerpta Medica

Bank van: Hollandsche Bank Unie
Hollandsche Bank Unie
1017 Amsterdam 32150002

18/02 '07 10:33 31 20 4882722
02/13/87 10:14 606 921 2580

ELSEVIER F&A
ASH PETR R&D

002
002

RECEIVED: Rights and Permissions Date 14 FEB. 1997

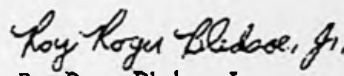
Ms. Tonny Smit
Permissions Dept.
Elsevier Science Ltd.
Amsterdam, The Netherlands

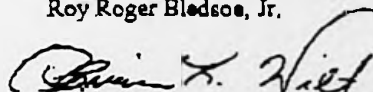
February 13, 1997

Dear Ms. Smit,

I am writing this on behalf of a colleague, Brian Wilt, and myself to ask permission to reprint an algorithm and table that appears in one of Elsevier's published journals, *Analytica Chimica Acta* 1986, Volume 185, pp 1-17 by P. Geladi and B. Kowalski. The algorithm is listed in the appendix on page 16, and the table appears on page 2. We wish to know if Elsevier holds copyright on this material, or if it is in the public domain, or if you could direct us to the holder of the copyright. We are graduate students at Marshall University in Huntington, West Virginia, USA, and this information is desired to be included into our theses. Final copyright of our theses will be held by Ashland Petroleum Company, our employer. Since we are employees of the company that will be copyrighting the papers, would the company also need to send correspondence for permission? We thank you in advance for your prompt attention in this matter. If you have any questions, we can be reached by phone in the United States at 1-606-921-6379. We would like to request your response in writing, so we may have written record. This can be sent by fax at 1-606-921-2580.

Sincerely,


Roy Roger Blodsoe, Jr.


Brian K. Wilt

APPENDIX II.

P.I.A.N.O. ANALYSIS

by

Analytical Automation Specialists, Inc.

Licensed to: Ashland Petroleum Co. - Catlettsburg, KY

Sample: LPCCR	Acquired on: 05-03-1994
File: K524.ATB	Normalized to 100%
RI Data File: product	Processed 254 Peaks

Gas Chromatograph: _____	Sample Size _____
Inj. Temp _____	Split Ratio _____
Det. Temp _____	Carrier Pressure _____
Carrier Gas: Helium	Installed on _____
Column: Supelco DH-100 100M	
Conditions: 35 deg C	
Rate 2: Methane set to 7.00 min.	

Sample: LPCCR

Acquired on: 05-03-1994

Composite ReportHydrocarbon Totals by Group Type

Type	Wt %	Vol%	Mol %
Total Paraffins:	7.321	8.831	8.355
Total Iso-paraffins:	19.136	22.798	20.739
Total Naphthenes:	1.490	1.578	1.531
Total Aromatics:	69.913	64.474	67.429
Total Olefins:	1.246	1.435	1.412
Total C14+	0.431	0.455	0.224
Total Unknowns:	0.463	0.429	0.309
Total:	100.000	100.000	100.000

Totals by Carbon Number

Group	Wt %	Vol %	Mol %	Ave. M.w.	Ave. Sp. Gr.
Methane	0.000	0.000	0.000	0.000	0.000
Ethane	0.000	0.000	0.000	0.000	0.000
Propane	0.000	0.000	0.000	0.000	0.000
Butanes:	0.193	0.270	0.343	58.071	0.575
Pentanes:	2.305	2.961	3.304	72.009	0.626
Hexanes:	13.324	14.974	16.474	83.467	0.716
Heptanes:	27.312	28.401	29.468	95.649	0.773
Octanes:	27.334	26.114	26.307	107.228	0.842
Nonanes:	20.307	18.800	17.410	120.369	0.869
Decanes:	5.401	4.938	4.163	133.870	0.880
C11's:	2.189	1.953	1.533	147.351	0.902
C12's:	0.740	0.706	0.464	164.560	0.844
C13's:	0.000	0.000	0.000	0.000	0.000
C14+	0.431	0.455	0.224		
Unknowns:	0.463	0.429	0.309		
Total:	100.000	100.000	100.000	104.444	0.797

Sample: LPCCR

Acquired on: 05-03-1994

		Types by Carbon Number		
		Wt %	Vol %	Mol %
Paraffins:	C1	0.000	0.000	0.000
	C2	0.000	0.000	0.000
	C3	0.000	0.000	0.000
	C4	0.148	0.206	0.263
	C5	0.874	1.122	1.250
	C6	2.840	3.463	1.400
	C7	2.620	3.082	2.698
	C8	0.701	0.803	0.634
	C9	0.129	0.145	0.104
	C10	0.009	0.010	0.007
	C11	0.000	0.000	0.000
	C12	0.000	0.000	0.000
	C13	0.000	0.000	0.000
Iso-paraffins:	C4	0.040	0.058	0.071
	C5	1.276	1.656	1.825
	C6	5.766	7.054	6.905
	C7	8.913	10.469	9.175
	C8	2.613	2.981	2.363
	C9	0.369	0.409	0.300
	C10	0.012	0.014	0.009
	C11	0.041	0.044	0.027
	C12	0.106	0.113	0.064
	C13	0.000	0.000	0.000
Aromatics:	C6	4.034	3.692	5.329
	C7	14.652	13.592	16.410
	C8	23.381	21.655	22.727
	C9	19.711	18.148	16.927
	C10	5.373	4.907	4.143
	C11	2.149	1.909	1.506
	C12	0.613	0.571	0.387
	C13	0.000	0.000	0.000
Naphthenes:	C5	0.052	0.056	0.076
	C6	0.356	0.381	0.436
	C7	0.339	0.364	0.357
	C8	0.617	0.651	0.563
	C9	0.097	0.098	0.080
	C10	0.006	0.007	0.005
	C11	0.000	0.000	0.000
	C12	0.021	0.021	0.013
	C13	0.000	0.000	0.000
Olefins:	C2	0.000	0.000	0.000
	C3	0.000	0.000	0.000
	C4	0.005	0.007	0.009
	C5	0.104	0.127	0.153
	C6	0.328	0.384	0.403
	C7	0.788	0.893	0.828
	C8	0.022	0.024	0.020
	C9	0.000	0.000	0.000
	C10	0.000	0.000	0.000
	C11	0.000	0.000	0.000
	C12	0.000	0.000	0.000
	C13	0.000	0.000	0.000

Components Listed in Chromatographic Order

pk#	Min.	Index	Component	Area	Wt %	Vol %	Mol %	Grp.	Shift
1	7.67	367.9	i-Butane	4449	0.040	0.058	0.071	I4	2.10
2	7.91	390.3	Butene-1/Isobutylene	272	0.002	0.003	0.004	O4	0.91
3	8.03	400.0	n-Butane	16477	0.148	0.206	0.263	P4	0.00
4	8.15	409.7	t-Butene-2	146	0.001	0.002	0.002	O4	0.58
5	8.35	424.1	c-Butene-2	152	0.001	0.002	0.002	O4	0.21
6	8.92	456.8	3-Methylbutene-1	261	0.002	0.003	0.003	O5	1.19
7	9.32	474.7	i-Pentane	142853	1.276	1.656	1.825	I5	0.22
8	9.69	488.7	pentene-1	476	0.004	0.005	0.006	O5	0.02
9	9.87	495.2	2-Methylbutene-1	2405	0.021	0.026	0.031	O5	0.22
10	10.02	500.0	n-Pentane	97816	0.874	1.122	1.250	P5	0.00
11	10.25	507.3	t-Pentene-2	1591	0.014	0.017	0.020	O5	0.13
12	10.52	515.6	c-Pentene-2	1079	0.009	0.011	0.014	O5	0.45
13	10.69	520.5	2-Methylbutene-2	5848	0.051	0.062	0.075	O5	0.75
14	11.34	537.0	2,2-Dimethylbutane	59789	0.531	0.658	0.636	I6	0.31
15	12.16	554.8	Cyclopentene	310	0.003	0.003	0.004	O5	0.46
16	12.32	558.0	4-Methylpentene-1	938	0.008	0.010	0.010	O6	0.40
17	12.41	559.7	3-Methylpentene-1	1341	0.012	0.014	0.014	O6	0.32
18	12.75	566.0	Cyclopentane/MTBE	5974	0.052	0.056	0.076	N5	0.21
19	12.83	567.4	2,3-Dimethylbutane	61481	0.546	0.664	0.654	I6	0.36
20	12.94	569.2	2,3-Dimethylbutene-1	867	0.008	0.009	0.009	O6	0.46
21	13.06	571.5	2-Methylpentane	297308	2.643	3.254	3.164	I6	0.28
22	13.90	585.1	3-Methylpentane	230156	2.046	2.477	2.450	I6	0.15
23	14.17	589.1	2-Methylpentene-1	5244	0.045	0.053	0.056	O6	0.41
24	14.23	590.0	Hexene-1	1439	0.012	0.015	0.015	O6	0.42
25	14.96	600.0	n-Hexane	319475	2.840	3.463	3.400	P6	0.00
26	15.07	601.7	t-Hexene-3	2749	0.024	0.028	0.029	O6	0.21
27	15.16	603.0	c-Hexene-3	1098	0.010	0.011	0.012	O6	0.33
28	15.26	604.4	t-Hexene-2	5616	0.049	0.057	0.060	O6	0.13
29	15.43	606.8	2-Methylpentene-2	8605	0.075	0.087	0.092	O6	0.03
30	15.67	610.2	2-Methyl-c-pentene-2	6403	0.056	0.064	0.068	O6	0.20
31	15.83	612.5	O13	400	0.003	0.004	0.004	O6	0.21
32	15.95	614.0	c-Hexene-2	3117	0.027	0.031	0.033	O6	0.18
33	16.42	620.0	3,3-Dimethylpentene-1	8724	0.076	0.087	0.080	O7	0.29
34	16.77	624.6	2,2-Dimethylpentane	49513	0.440	0.525	0.453	I7	0.06
35	16.97	627.0	Methylcyclopentane	37270	0.323	0.347	0.396	N6	0.10
36	17.27	630.7	2,4-Dimethylpentane	55146	0.489	0.584	0.503	I7	0.35
37	17.59	634.4	Cyclic Diolefin or Triolefin	249	0.002	0.002	0.002	O7	0.15
38	17.75	636.2	2,2,3-Trimethylbutane	7563	0.067	0.078	0.069	I7	0.35
39	18.33	642.5	O17	443	0.004	0.004	0.004	O7	0.21
40	18.74	646.7	2,4-Dimethylpentene-1	2038	0.018	0.020	0.019	O7	0.14
41	19.08	650.2	Benzene	500525	4.034	3.692	5.329	A6	0.29
42	19.31	652.4	3-Methylhexene-1	775	0.007	0.008	0.007	O7	0.06
43	19.62	655.5	3,3-Dimethylpentane	50314	0.446	0.517	0.459	I7	0.33
44	19.77	656.9	5-Methylhexene-1	754	0.007	0.008	0.007	O7	0.13
45	19.95	658.6	Cyclohexane	3763	0.033	0.034	0.040	N6	0.44
46	20.16	660.5	2-Methyl-t-hexene-3	3037	0.026	0.031	0.028	O7	0.26
47	20.54	664.0	2-Ethyl-3-methylbutene-1	1348	0.012	0.013	0.012	O7	0.28
48	20.80	666.3	4-Methyl-t/c-hexene-2	7163	0.062	0.071	0.065	O7	0.12
49	20.99	667.9	2-Methylhexane	307650	2.726	3.231	2.808	I7	0.11
50	21.17	669.5	2,3-Dimethylpentane	117233	1.039	1.202	1.070	I7	0.05

Sample: LPCCR

Acquired on: 05-03-1994

pk#	Min.	Index	Component	Area	Wt %	Vol %	Mol %	Grp.	Shift
51	21.48	672.1	1,1-Dimethylcyclopentane	3645	0.032	0.034	0.033	N7	0.10
52	22.01	676.4	3-Methylhexane	380066	3.297	3.860	3.396	I7	0.03
53	22.39	679.5	3,4-Dimethyl-c-petnene-2	2941	0.026	0.029	0.027	O7	0.14
54	22.75	682.3	1c,3-Dimethylcyclopentane	7125	0.062	0.066	0.065	N7	0.19
55	23.10	685.0	1t,3-Dimethylcyclopentane	7458	0.065	0.070	0.068	N7	0.15
56	23.25	686.1	3-Ethylpentane	42171	0.374	0.431	0.385	I7	0.15
57	23.45	687.6	1t,2-Dimethylcyclopentane	11563	0.100	0.107	0.105	N7	0.02
58	23.58	688.5	?	1306	0.012	0.012	0.012		UNK
59	23.68	689.2	2,2,4-Trimethylpentane	3953	0.035	0.041	0.032	I7	0.24
60	24.42	694.5	3-Methyl-c-hexene-3	4067	0.035	0.040	0.037	O7	0.20
61	24.91	697.9	t-Heptene-3	6861	0.060	0.068	0.063	O7	0.25
62	25.23	700.0	n-Heptane	295632	2.620	3.082	2.698	P7	0.00
63	25.48	702.0	c-Heptene-3	16668	0.145	0.165	0.152	O7	0.16
64	25.63	703.1	2-Methyl-2-hexene	6474	0.056	0.063	0.059	O7	0.02
65	25.89	705.1	3-Methyl-t-hexene-3	5063	0.044	0.051	0.046	O7	0.40
66	26.13	706.9	3-Ethylpentene-2	3323	0.029	0.032	0.030	O7	0.21
67	26.60	710.3	c-Heptene-2	9259	0.080	0.091	0.084	O7	0.29
68	27.23	714.8	2,3-Dimethylpentene-2	7669	0.067	0.073	0.070	O7	0.03
69	28.09	720.7	1c,2-Dimethylcyclopentane	3919	0.034	0.037	0.036	N7	0.31
70	28.22	721.6	Methylcyclohexane	2377	0.021	0.022	0.022	N7	0.10
71	28.71	724.8	1,1,3-Trimethylcyclopentane	17637	0.153	0.164	0.141	N8	0.03
72	30.24	734.5	Ethylcyclopentane	3042	0.026	0.028	0.028	N7	0.14
73	30.51	736.2	2,2,3-Trimethylpentane	17101	0.151	0.170	0.137	I8	0.00
74	30.85	738.2	2,4-Dimethylhexane	31104	0.275	0.316	0.249	I8	0.01
75	31.82	743.9	1c,2t,4-Trimethylcyclopentane	3133	0.027	0.029	0.025	N8	0.10
76	32.08	745.4	3,3-Dimethylhexane	14585	0.129	0.146	0.117	I8	0.19
77	32.76	749.2	?	365	0.003	0.004	0.003		UNK
78	32.93	750.1	1t,2c,3-Trimethylcyclopentane	901	0.008	0.008	0.007	N8	0.01
79	33.14	751.3	O39	2672	0.023	0.025	0.024	O7	0.02
80	33.38	752.6	?	185	0.002	0.002	0.002		UNK
81	33.69	754.3	2,3,4-Trimethylpentane	391	0.003	0.004	0.003	I8	0.06
82	34.52	758.6	Toluene	1807049	14.652	13.592	16.410	A7	0.31
83	34.75	759.8	2,3,3-Trimethylpentane	1978	0.017	0.019	0.018	I8	0.02
84	35.27	762.4	O43	1265	0.011	0.012	0.012	O7	0.08
85	35.78	765.0	2,3-Dimethylhexane	24150	0.213	0.241	0.193	I8	0.39
86	36.00	766.1	2-Methyl-3-ethylpentane	3983	0.035	0.040	0.032	I8	0.47
87	36.20	767.1	1,1,2-Trimethylcyclopentane	2164	0.019	0.020	0.017	N8	0.15
88	36.99	770.8	2-Methylheptane	70288	0.621	0.716	0.561	I8	0.06
89	37.27	772.2	4-Methylheptane	34877	0.308	0.352	0.278	I8	0.27
90	37.43	773.0	3-Methyl-3-ethylpentane	7233	0.064	0.072	0.058	I8	0.45
91	37.53	773.4	3,4-Dimethylhexane	5956	0.053	0.059	0.048	I8	0.02
92	38.01	775.6	1,3c-Dimethylcyclohexane	523	0.005	0.005	0.004	N8	0.11
93	38.44	777.6	3-Methylheptane	84.68	0.743	0.846	0.671	I8	0.19
94	38.63	778.5	1c,2t,3-Trimethylcyclopentane	22668	0.197	0.205	0.181	N8	0.46
95	40.60	787.1	2,2,5-Trimethylhexane	2304	0.020	0.023	0.016	I9	0.03
96	40.79	787.9	3c-Ethylmethylcyclopentane	923	0.008	0.008	0.007	N8	0.01
97	41.21	789.6	3t-Ethylmethylcyclopentane	1198	0.010	0.011	0.010	N8	0.42
98	41.45	790.6	2t-Ethylmethylcyclopentane	1707	0.015	0.015	0.014	N8	0.34
99	41.64	791.4	1,1-Methylethylcyclopentane	777	0.007	0.007	0.006	N8	0.02
100	41.86	792.3	?	458	0.004	0.004	0.004		UNK

Sample: LPCCR

Acquired on: 05-03-1994

pk#	Min.	Index	Component	Area	Wt %	Vol %	Mol %	Grp.	Shift
101	42.01	793.0	2,2,4-Trimethylhexane	1495	0.013	0.014	0.011	I9	0.05
102	42.39	794.5	1t,2-Dimethylcyclohexane	1737	0.015	0.016	0.014	N8	0.46
103	42.66	795.6	t-Octene-4	1338	0.012	0.013	0.011	O8	0.16
104	43.22	797.8	1c,2c,3-Trimethylcyclopentane	4238	0.037	0.038	0.034	N8	0.02
105	43.51	798.9	1t,3-Dimethylcyclohexane	513	0.004	0.005	0.004	N8	0.00
106	43.79	800.0	n-Octane	79373	0.701	0.803	0.634	P8	0.00
107	44.53	803.8	1c,4-Dimethylcyclohexane	1256	0.011	0.011	0.010	N8	0.04
108	44.87	805.6	Octene-2	1145	0.010	0.011	0.009	O8	0.02
109	45.20	807.3	i-Propylcyclopentane	1898	0.016	0.017	0.015	N8	0.02
110	46.19	812.3	?	646	0.006	0.006	0.005		UNK
111	47.18	817.1	2,3,4-Trimethylhexane	786	0.007	0.008	0.006	I9	0.55
112	47.46	818.4	N2	415	0.004	0.004	0.003	N8	0.50
113	47.99	820.9	N3	3238	0.028	0.032	0.023	N8	0.53
114	48.93	825.3	2,3,4-Trimethylhexane	2574	0.023	0.023	0.021	I9	0.41
115	49.31	827.0	2,2-Dimethylheptane	384	0.003	0.003	0.003	I9	0.63
116	50.25	831.3	N4	691	0.006	0.007	0.005	N8	0.51
117	50.49	832.4	2,2,3-Trimethylhexane	1858	0.016	0.019	0.013	I9	0.38
118	52.08	839.3	n-Propylcyclopentane	5538	0.048	0.050	0.044	N8	0.31
119	52.43	840.8	2,6-Dimethylheptane	2651	0.023	0.026	0.019	I9	0.38
120	54.55	849.6	Ethylbenzene	483323	3.970	3.683	3.859	A8	0.44
121	57.12	859.8	m-Xylene	1118209	9.186	8.549	8.929	A8	0.08
122	57.38	860.8	p-Xylene	479767	3.941	3.682	3.831	A8	0.08
123	57.62	861.7	2,3-Dimethylheptane	2974	0.026	0.029	0.021	I9	0.04
124	58.12	863.6	3,4-Dimethylheptane	764	0.007	0.007	0.005	I9	0.24
125	58.36	864.6	3,4-Dimethylheptane	1084	0.010	0.011	0.008	I9	0.25
126	59.06	867.2	14	1763	0.016	0.017	0.013	I9	0.03
127	59.97	870.5	4-Methyloctane	8562	0.075	0.084	0.061	I9	0.01
128	60.27	871.6	2-Methyloctane	10493	0.093	0.104	0.074	I9	0.07
129	61.71	876.8	3-Ethylheptane	4120	0.036	0.040	0.029	I9	0.09
130	62.14	878.3	1,1,2-Trimethylcyclohexane	11224	0.097	0.098	0.080	N9	0.51
131	63.13	881.8	o-Xylene	764897	6.283	5.741	6.108	A8	0.06
82	68.68	900.0	n-Nonane	14631	0.129	0.145	0.104	P9	0.31
83	70.48	912.0	i-Propylbenzene	59966	0.496	0.463	0.426	A9	0.02
84	75.99	946.5	n-Propylbenzene	149718	1.238	1.155	1.063	A9	0.08
85	77.41	955.0	1-Methyl-3-ethylbenzene	471635	3.899	3.628	3.348	A9	0.39
86	77.70	956.7	1-Methyl-4-ethylbenzene	225755	1.867	1.743	1.603	A9	0.47
87	78.64	962.2	1,3,5-Trimethylbenzene	156035	1.290	1.199	1.108	A9	0.15
88	80.10	970.6	1-Methyl-2-ethylbenzene	254048	2.100	1.918	1.803	A9	0.06
89	80.41	972.3	2-Methylnonane	790	0.007	0.008	0.005	I10	0.27
90	81.44	978.1	N29	749	0.006	0.007	0.005	N10	0.45
141	81.63	979.2	I18	614	0.005	0.006	0.004	I10	0.01
142	82.03	981.4	t-Butylbenzene	1727	0.014	0.013	0.011	A9	0.60
143	82.51	984.1	1,2,4-Trimethylbenzene	796682	6.629	6.088	5.692	A9	0.02
144	84.63	995.6	i-Butylbenzene	9659	0.080	0.076	0.062	A10	0.01
145	85.00	997.6	sec-Butylbenzene	10410	0.087	0.081	0.067	A10	0.35
146	85.46	1000.0	n-Decane	1043	0.009	0.010	0.007	P10	0.00
147	86.21	1006.8	1,2,3-Trimethylbenzene	230262	1.904	1.712	1.635	A9	0.10
148	86.48	1009.2	1-Methyl-3-i-propylbenzene	30053	0.250	0.233	0.192	A10	0.19
149	86.89	1012.9	1-Methyl-4-i-propylbenzene	10426	0.087	0.081	0.067	A10	0.08
150	87.59	1019.0	2,3-Dihydroindene	33119	0.274	0.228	0.239	A9	0.06

Sample: LPCCR

Acquired on: 05-03-1994

pk#	Min.	Index	Component	Area	Wt %	Vol %	Mol %	Grp.	Shift
151	88.36	1025.8	I30	4127	0.036	0.039	0.024	I11	0.04
152	88.55	1027.5	1-Methyl-2-i-propylbenzene	3055	0.025	0.023	0.020	A10	0.37
153	89.93	1039.4	1,3-Diethylbenzene	28670	0.238	0.222	0.183	A10	0.08
154	90.26	1042.3	1-Methyl-3-n-propylbenzene	72924	0.606	0.566	0.466	A10	0.23
155	90.71	1046.1	1,4-Diethylbenzene	45076	0.375	0.350	0.288	A10	0.44
156	90.83	1047.1	1-Methyl-4-n-propylbenzene	15353	0.128	0.120	0.098	A10	0.50
157	91.09	1049.4	n-Butylbenzene	61393	0.510	0.477	0.392	A10	0.06
158	91.33	1051.3	1,3-Dimethyl-5-ethylbenzene	6489	0.054	0.049	0.041	A10	0.04
159	92.07	1057.6	1-Methyl-2-n-propylbenzene	38399	0.319	0.294	0.245	A10	0.11
160	93.29	1067.7	1,4-Dimethyl-2-ethylbenzene	63408	0.527	0.483	0.405	A10	0.30
161	93.49	1069.4	s-C5Bs / 1,3-DM-4-EtBz	58098	0.484	0.453	0.337	A11	0.05
162	93.76	1071.6	I39	506	0.004	0.005	0.003	I11	0.09
163	94.17	1075.0	1,2-Dimethyl-4-ethylbenzene	101805	0.846	0.778	0.651	A10	0.28
164	94.82	1080.2	1,3-Dimethyl-2-ethylbenzene	9568	0.080	0.072	0.061	A10	0.16
165	95.05	1082.1	?	194	0.002	0.002	0.001		UNK
166	95.27	1083.9	?	217	0.002	0.002	0.001		UNK
167	96.20	1091.4	1-Methyl-4-t-butylbenzene	4097	0.034	0.032	0.024	A11	0.15
168	96.35	1092.6	1,2-Dimethyl-3-ethylbenzene	36891	0.307	0.276	0.236	A10	0.07
169	96.89	1096.8	?	1547	0.014	0.012	0.011		UNK
170	97.10	1098.5	?	1701	0.015	0.014	0.012		UNK
171	97.55	1102.8	1-Ethyl-4-i-propylbenzene	2712	0.023	0.020	0.016	A11	0.40
172	97.69	1104.4	1,2,4,5-Tetramethylbenzene	54991	0.457	0.414	0.351	A10	0.10
173	97.86	1106.2	?	1141	0.010	0.009	0.008		UNK
174	98.06	1108.4	(2-Methylbutyl) benzene	86584	0.722	0.652	0.503	A11	0.38
175	98.36	1111.6	?	256	0.002	0.002	0.002		UNK
176	98.69	1115.2	?	1323	0.012	0.011	0.008		UNK
177	98.95	1118.0	?	465	0.004	0.004	0.003		UNK
178	99.21	1120.8	1-t-Butyl-2-Methylbenzene	352	0.003	0.003	0.002	A11	0.01
179	99.77	1126.8	5-Methylindan	18099	0.151	0.136	0.105	A11	0.51
180	100.31	1132.5	I43	5258	0.046	0.049	0.028	I12	0.55
181	100.43	1133.8	?	2338	0.021	0.022	0.013		UNK
182	100.59	1135.5	A3	9058	0.076	0.068	0.053	A11	0.52
183	100.79	1137.5	1-Ethyl-2-n-propylbenzene	17848	0.149	0.134	0.104	A11	0.02
184	101.00	1139.8	1-Methyl-3-n-butylbenzene	1602	0.013	0.012	0.009	A11	0.53
185	101.24	1142.3	1,3-Di-i-propylbenzene	44895	0.376	0.340	0.239	A12	0.52
186	101.73	1147.4	n-Pentylbenzene	1581	0.013	0.012	0.009	A11	0.46
187	101.90	1149.2	1t-M-2-(4-MP) cyclopentane	2464	0.021	0.021	0.013	N12	0.58
188	102.21	1152.4	?	2956	0.026	0.026	0.016		UNK
189	102.63	1156.8	1-Methyl-2-n-butylbenzene	5735	0.048	0.043	0.033	A11	0.72
190	102.80	1158.5	1,4-Di-i-propylbenzene	7151	0.060	0.054	0.038	A12	0.60
191	103.19	1162.6	1,2,3,4-Tetrahydronaphthalene	301	0.003	0.002	0.002	A10	0.55
192	103.47	1165.4	A1166	11170	0.093	0.073	0.072	A10	0.02
193	103.65	1167.3	Naphthalene	36309	0.302	0.237	0.243	A10	194 10
195	104.91	1180.1	?	160	0.001	0.002	0.001		UNK
196	105.15	1182.5	I47	4108	0.036	0.039	0.022	I12	0.73
197	105.54	1186.4	?	452	0.004	0.004	0.002		UNK
198	105.67	1187.7	A48	11907	0.105	0.112	0.063	A12	0.11
199	105.83	1189.2	1,3-Di-n-propylbenzene	8111	0.068	0.061	0.043	A12	0.07
200	106.65	1197.4	?	8048	0.071	0.064	0.045		UNK

Sample: LPCCR

Acquired on: 05-03-1994

pk#	Min.	Index	Component	Area	Wt %	Vol %	Mol %	Grp.	Shift
201	107.49	1207.1	?	1462	0.013	0.012	0.008		UNK
202	108.19	1215.7	?	1761	0.016	0.014	0.010		UNK
203	108.65	1221.3	?	991	0.009	0.008	0.006		UNK
204	108.89	1224.3	?	3684	0.033	0.030	0.021		UNK
205	109.10	1226.8	?	215	0.002	0.002	0.001		UNK
206	109.72	1234.3	?	253	0.002	0.002	0.001		UNK
207	109.82	1235.5	?	376	0.003	0.003	0.002		UNK
208	110.23	1240.4	?	3615	0.032	0.029	0.020		UNK
209	110.57	1244.4	1-Methyl-4-n-pentylbenzene	510	0.004	0.004	0.003	A12	0.72
210	110.77	1246.8	?	380	0.003	0.003	0.002		UNK
211	111.40	1254.3	?	2006	0.018	0.016	0.011		UNK
212	111.73	1258.3	?	762	0.007	0.006	0.004		UNK
213	112.13	1262.9	?	175	0.002	0.001	0.001		UNK
214	112.47	1267.0	?	296	0.003	0.002	0.002		UNK
215	112.97	1272.8	?	11928	0.106	0.096	0.067		UNK
216	113.69	1281.1	2-Methylnaphthalene	30612	0.256	0.201	0.184	A11	0.30
217	114.07	1285.6	?	547	0.005	0.004	0.003		UNK
218	114.99	1296.2	1-Methylnaphthalene	21214	0.177	0.140	0.128	A11	0.05
219	117.57	1400.0	C14+	262	0.002	0.002	0.001	+	0.00
220	119.05	1400.0	C14+	435	0.004	0.004	0.002	+	0.00
221	119.99	1400.0	C14+	359	0.003	0.003	0.002	+	0.00
222	121.52	1400.0	C14+	2642	0.024	0.024	0.012	+	0.00
223	121.67	1400.0	C14+	973	0.009	0.009	0.004	+	0.00
224	121.79	1400.0	C14+	741	0.007	0.007	0.003	+	0.00
225	122.38	1400.0	C14+	3450	0.030	0.032	0.016	+	0.00
226	122.52	1400.0	C14+	2730	0.024	0.025	0.012	+	0.00
227	123.47	1400.0	C14+	8524	0.075	0.079	0.039	+	0.00
228	123.75	1400.0	C14+	4270	0.037	0.039	0.019	+	0.00
229	124.95	1400.0	C14+	3360	0.029	0.031	0.015	+	0.00
230	125.11	1400.0	C14+	1132	0.010	0.010	0.005	+	0.00
231	126.01	1400.0	C14+	3530	0.031	0.033	0.016	+	0.00
82	127.71	1400.0	C14+	595	0.005	0.006	0.003	+	0.00
83	128.39	1400.0	C14+	787	0.007	0.007	0.004	+	0.00
84	129.13	1400.0	C14+	282	0.002	0.003	0.001	+	0.00
85	129.57	1400.0	C14+	1339	0.012	0.012	0.006	+	0.00
86	129.89	1400.0	C14+	262	0.002	0.002	0.001	+	0.00
87	130.23	1400.0	C14+	905	0.008	0.008	0.004	+	0.00
88	130.74	1400.0	C14+	579	0.005	0.005	0.003	+	0.00
89	131.06	1400.0	C14+	1262	0.011	0.012	0.006	+	0.00
90	131.46	1400.0	C14+	1178	0.010	0.011	0.005	+	0.00
241	132.49	1400.0	C14+	1178	0.010	0.011	0.005	+	0.00
242	132.79	1400.0	C14+	1107	0.010	0.010	0.005	+	0.00
243	133.53	1400.0	C14+	670	0.006	0.006	0.003	+	0.00
244	133.68	1400.0	C14+	554	0.005	0.005	0.003	+	0.00
245	133.79	1400.0	C14+	1259	0.011	0.012	0.006	+	0.00
246	134.74	1400.0	C14+	1433	0.013	0.013	0.007	+	0.00
247	135.23	1400.0	C14+	340	0.003	0.003	0.002	+	0.00
248	135.53	1400.0	C14+	567	0.005	0.005	0.003	+	0.00
249	135.93	1400.0	C14+	155	0.001	0.001	0.001	+	0.00
250	136.08	1400.0	C14+	267	0.002	0.002	0.001	+	0.00

Sample: LPCCR

Acquired on: 05-03-1994

pk#	Min.	Index	Component	Area	Wt %	Vol %	Mol %	Grp.	Shift
251	136.38	1400.0	C14+	309	0.003	0.003	0.001	+	0.00
252	137.28	1400.0	C14+	777	0.007	0.007	0.004	+	0.00
253	140.67	1400.0	C14+	338	0.003	0.003	0.002	+	0.00
254	141.69	1400.0	C14+	631	0.006	0.006	0.003	+	0.00

APPENDIX III.
GC-PIANO Results for the Original and Second Calibration Sets.

Sample	Vol% Total Aromatics	Benzene	Toluene	Total Xylenes	m-Xylene	p-Xylene	o-Xylene	Ethylbenzene
1	35.9	2.70	8.8	8.5	4.01	1.80	2.70	2.29
2	50.1	3.48	11.7	12.5	5.89	2.62	4.02	2.80
3	56.1	3.61	12.8	14.3	6.73	2.95	4.61	3.08
4	57.2	3.67	13.0	14.6	6.88	3.01	4.72	3.12
5	59.1	3.78	12.9	14.9	7.23	3.09	4.62	3.06
6	58.8	3.83	12.8	14.8	7.20	3.06	4.58	3.04
7	61.5	3.99	13.4	15.4	7.49	3.21	4.74	3.19
8	43.4	3.96	11.3	10.3	5.31	2.27	2.75	2.37
9	49.9	4.79	12.9	12.0	6.17	2.66	3.21	2.68
10	52.8	5.13	13.5	12.8	6.60	2.81	3.42	2.79
11	60.6	5.73	15.5	15.4	7.92	3.38	4.12	3.17
12	59.8	5.50	15.1	15.3	7.83	3.33	4.09	3.12
13	52.8	3.65	12.4	13.3	6.67	2.85	3.82	2.87
14	51.6	3.72	12.1	12.9	6.45	2.77	3.71	2.83
15	49.2	3.60	11.4	12.3	6.09	2.62	3.55	2.74
16	50.9	3.85	11.6	12.4	6.13	2.63	3.62	2.71
17	58.8	4.39	12.6	13.9	6.71	2.86	4.29	2.80
18	59.0	4.43	12.7	13.9	6.74	2.85	4.31	2.80
19	58.6	4.75	12.4	13.4	6.33	2.65	4.38	2.96
20	60.4	4.71	12.8	14.3	6.71	2.86	4.70	3.06
21	62.7	5.01	13.2	14.5	6.84	2.85	4.77	3.17
22	60.4	4.95	12.6	13.7	6.47	2.72	4.49	3.06
23	59.2	4.88	12.5	13.3	6.28	2.63	4.34	3.02
24	58.3	4.90	12.2	13.1	6.20	2.59	4.28	2.99
25	57.2	3.61	12.2	14.6	6.92	2.97	4.70	2.96
26	63.8	4.38	14.1	16.5	7.86	3.39	5.24	3.59
27	63.8	4.59	14.6	16.5	7.85	3.37	5.29	3.59
28	64.0	4.69	14.5	16.8	7.97	3.41	5.43	3.55
29	65.6	4.54	14.4	17.2	8.15	3.45	5.60	3.64
30	63.8	4.25	13.6	16.9	7.92	3.43	5.55	3.60
31	67.9	4.26	15.2	19.0	9.09	3.84	6.11	3.78
32	67.6	4.19	15.0	18.9	8.99	3.83	6.09	3.79
33	67.2	4.46	15.5	18.8	8.90	3.80	6.06	3.72
34	68.0	4.62	15.7	19.2	9.15	3.88	6.18	3.74
35	66.0	4.51	15.0	18.4	8.74	3.69	5.93	3.57
36	66.7	4.14	14.6	18.7	8.72	3.73	5.93	3.73
37	66.1	4.20	14.2	18.4	8.86	3.77	6.08	3.69
38	67.3	4.34	15.1	18.7	8.94	3.78	6.02	3.69
39	66.5	4.98	16.2	18.6	8.99	3.80	5.80	3.64
40	55.9	4.13	12.9	15.0	7.42	3.20	4.39	3.14
41	68.0	5.39	15.4	17.1	8.16	3.41	5.53	3.58
42	67.7	5.41	15.9	17.5	8.42	3.45	5.67	3.64
43	66.5	5.67	15.5	17.0	8.06	3.36	5.55	3.73
44	66.8	5.41	15.8	18.1	8.64	3.61	5.82	3.74
45	67.3	5.41	15.9	18.3	8.74	3.69	5.85	3.78
46	66.9	5.00	15.2	18.6	8.33	3.78	6.00	3.86
47	67.6	4.67	15.8	19.3	9.24	3.89	6.20	3.90
48	66.2	4.65	15.5	19.4	8.27	3.94	6.23	3.89
49	66.5	4.46	15.5	19.5	9.29	3.96	6.26	3.91
50	66.7	4.67	15.7	19.6	9.32	3.97	6.26	3.90
51	66.9	4.45	15.8	20.0	9.57	4.03	6.39	3.96
52	67.3	4.54	15.7	19.5	9.29	3.93	6.29	3.84
53	59.5	4.23	12.6	14.0	6.80	2.86	4.34	2.82
54	68.3	4.40	14.2	16.7	7.92	3.42	5.36	3.63
55	65.2	3.57	13.4	17.3	8.25	3.57	5.50	3.41
56	65.8	3.38	13.4	17.6	8.36	3.60	5.60	3.52
57	64.5	3.69	13.6	18.0	8.55	3.68	5.74	3.68
58	67.6	1.79	11.5	17.2	8.09	3.56	5.55	3.69
59	65.7	3.44	13.4	18.0	8.52	3.71	5.81	3.71
60	62.1	3.03	11.5	15.5	7.26	3.24	5.00	3.27
61	62.2	3.03	12.4	15.6	7.43	3.25	4.91	3.39
62	64.1	3.42	12.4	15.3	7.22	3.18	4.95	3.24

Original Calibration Set

Range 35.9 - 68.0 2.70 - 5.73 8.77 - 16.2 8.51 - 20.0 4.01 - 9.57 1.80 - 4.03 2.70 - 6.39 2.29 - 3.96

Second Calibration Set

Range 35.9 - 68.3 1.79 - 5.73 8.77 - 16.2 8.51 - 20.0 4.01 - 9.57 1.80 - 4.03 2.70 - 6.39 2.29 - 3.96

Sample	Vol% Total								
	Olefins	Paraffins	n-Hexane	n-Heptane	Iso-paraffins	Isopentane	2-Methylhexane	Naphthenes	Methylcyclopentane
1	0.46	22.19	5.19	7.48	34.2	1.06	4.12	6.51	1.49
2	1.07	15.44	4.08	3.55	30.5	8.25	2.82	2.09	0.62
3	1.17	12.23	3.70	2.95	26.9	7.97	2.49	1.50	0.47
4	1.22	12.90	3.65	2.80	26.2	7.92	2.43	1.35	0.43
5	1.04	13.73	2.98	2.52	24.0	3.63	2.68	0.91	0.17
6	1.07	12.79	3.17	2.65	25.0	3.62	2.81	1.01	0.19
7	1.02	10.70	3.31	2.84	24.3	3.29	3.00	1.13	0.24
8	0.51	14.77	4.50	3.92	34.6	3.60	3.64	6.03	1.88
9	0.67	13.63	4.27	3.12	31.1	4.28	3.18	3.92	1.19
10	0.80	14.51	4.01	2.60	28.6	4.77	2.77	2.75	0.85
11	1.06	13.37	3.52	1.66	22.7	4.81	1.94	1.33	0.38
12	1.10	14.67	3.38	1.61	22.3	4.38	1.88	1.16	0.36
13	1.44	13.96	3.61	3.36	27.3	3.05	2.90	3.58	0.77
14	1.60	14.14	3.98	3.62	27.2	2.91	2.92	4.38	0.95
15	1.70	15.10	4.21	3.85	28.3	2.65	2.95	4.65	1.02
16	1.29	14.72	4.17	3.58	27.7	2.70	2.86	4.21	0.95
17	1.05	11.84	3.59	2.54	24.6	3.15	2.45	1.99	0.40
18	1.05	11.77	3.60	2.54	24.5	3.17	2.45	2.00	0.40
19	0.87	11.75	3.77	2.98	25.6	2.52	2.98	1.63	0.36
20	0.90	10.76	3.65	2.80	25.2	2.49	2.84	1.40	0.30
21	0.84	10.34	3.54	2.72	23.1	2.44	2.77	1.36	0.31
22	0.81	10.58	3.82	3.06	25.0	1.98	3.01	1.70	0.42
23	0.79	10.62	3.86	3.34	25.7	1.85	3.16	1.96	0.49
24	0.82	11.09	4.16	3.34	26.2	1.91	3.15	1.99	0.49
25	0.92	11.85	3.78	3.41	27.4	2.70	3.31	1.67	0.39
26	1.33	9.56	3.27	2.85	21.9	1.92	2.89	1.58	0.37
27	1.24	9.46	3.41	2.99	22.3	1.81	3.02	1.53	0.40
28	1.19	9.40	3.48	2.81	22.5	2.08	2.99	1.18	0.30
29	1.13	8.82	3.36	2.87	21.9	1.72	3.03	1.33	0.29
30	1.11	9.24	3.55	3.00	23.6	2.13	3.20	1.33	0.28
31	1.29	8.94	3.17	2.19	20.3	2.45	2.47	0.81	0.20
32	1.33	8.70	3.26	2.33	20.6	2.30	2.58	1.00	0.22
33	1.28	8.93	3.24	2.47	20.8	2.22	2.71	1.07	0.24
34	1.30	8.50	3.34	2.34	20.6	2.32	2.62	0.96	0.23
35	1.34	9.50	3.55	2.36	21.4	2.34	2.63	0.95	0.24
36	1.35	9.05	3.83	2.35	21.6	2.36	2.60	1.13	0.26
37	1.41	9.24	3.38	2.32	21.1	2.37	2.60	0.97	0.21
38	1.36	9.16	3.39	2.21	20.6	2.43	2.48	0.89	0.22
39	1.18	8.55	3.62	2.40	22.2	2.96	2.67	1.04	0.23
40	0.97	12.90	3.35	3.17	28.1	3.46	3.49	1.64	0.37
41	0.85	8.90	2.98	2.44	20.0	1.91	2.66	1.05	0.26
42	0.93	8.41	2.67	2.61	20.9	2.06	2.87	1.06	0.25
43	0.94	8.92	3.25	2.79	21.6	1.97	2.99	1.24	0.32
44	1.15	8.69	3.25	2.66	21.6	2.27	2.93	1.09	0.26
45	1.18	8.85	3.15	2.56	21.1	2.27	2.83	0.90	0.26
46	1.17	8.72	3.28	2.61	21.5	2.33	2.89	1.07	0.25
47	1.17	8.56	2.96	2.65	20.9	2.28	2.92	1.04	0.23
48	1.25	9.02	3.24	2.67	21.8	2.36	2.95	1.03	0.24
49	1.20	9.15	2.99	2.72	21.3	2.24	2.97	1.06	0.23
50	1.23	8.80	3.13	2.67	21.6	2.42	2.97	1.02	0.23
51	1.15	9.03	2.81	2.71	21.4	2.40	3.00	1.01	0.21
52	1.20	8.98	3.01	2.60	21.0	2.24	2.87	0.98	0.22
53	1.04	11.67	3.57	2.53	24.5	3.16	2.43	1.90	0.40
54	1.45	8.73	3.20	2.35	19.2	1.81	2.45	1.34	0.37
55	1.34	8.76	2.86	2.88	21.5	1.93	3.00	1.54	0.32
56	1.30	8.67	2.57	2.98	21.3	1.92	3.08	1.60	0.31
57	1.44	8.83	3.46	3.08	22.8	1.66	3.23	1.58	0.35
58	1.04	6.65	1.28	2.72	20.6	1.34	2.68	1.67	0.18
59	1.39	9.11	3.39	2.70	21.8	2.08	2.89	1.29	0.28
60	1.36	9.14	3.09	2.98	24.6	1.88	2.98	1.79	0.35
61	1.40	9.04	2.65	3.14	24.0	2.03	3.04	2.07	0.40
62	1.40	8.93	3.55	3.17	22.6	1.30	3.17	1.76	0.41

Original Calibration Set

Range 0.46 - 1.70 8.36 - 22.2 2.67 - 5.19 1.61 - 7.48 20.0 - 34.6 1.06 - 8.25 1.88 - 4.12 0.81 - 6.51 0.17 - 1.88

Second Calibration Set

Range 0.46 - 1.70 6.65 - 22.2 1.28 - 5.19 1.61 - 7.48 19.2 - 34.6 1.06 - 8.25 1.88 - 4.12 0.81 - 6.51 0.17 - 1.88

APPENDIX IV.

Bandwidth Test Results.

Scan	Peak 1	Peak 2	Peak 3	Bandwidth
1	1143.53	1681.08	2166.63	10.45
2	1143.52	1681.08	2166.62	10.46
3	1143.53	1681.08	2166.62	10.45
4	1143.53	1681.08	2166.62	10.45
5	1143.53	1681.08	2166.62	10.45
6	1143.53	1681.08	2166.62	10.45
7	1143.52	1681.08	2166.62	10.45
8	1143.53	1681.08	2166.62	10.46
9	1143.53	1681.08	2166.62	10.45
10	1143.53	1681.08	2166.62	10.45

Summary of Accuracy and Bandwidth

Average	1143.53	1681.08	2166.62	10.45
Delta	-0.10	0.18	-0.10	0.45
Std. Dev.	0.005	0.002	0.003	0.002
Maximum	1143.53	1681.08	2166.63	10.46
Minimum	1143.52	1681.08	2166.62	10.45
Max - Min	0.0157	0.0063	0.0095	0.0067

APPENDIX V.

Noise Test Results

Scan	EOC	Peak-to-Peak	Maximum	Lambda	Minimum	Lambda	Bias	RMS
1	0	0.309	0.098	1368	-0.212	1542	-0.045	0.052
2	0	0.048	0.023	1558	-0.025	1610	-0.002	0.010
3	0	0.077	0.038	1500	-0.040	1540	-0.007	0.011
4	0	0.123	0.059	1146	-0.064	1184	-0.010	0.020
5	0	0.064	0.025	1144	-0.039	1228	-0.010	0.012
6	0	0.112	0.086	1182	-0.026	1200	0.040	0.020
7	0	0.065	0.021	1224	-0.045	1142	-0.009	0.012
8	0	0.067	0.046	1134	-0.021	1496	0.010	0.012
9	0	0.061	0.021	1136	-0.041	1172	-0.010	0.012
10	0	0.052	0.041	1500	-0.010	1488	0.012	0.010

Summary of Noise

Average		0.098					-0.003	0.017
Maximum		0.309					0.040	0.052
Minimum		0.048					-0.045	0.010